





TABLE OF CONTENTS

SUMMARY	1
1. INTRODUCTION	4
2. AIRSPACE DESCRIPTION	4
2.1. ATS SERVICES AND PROCEDURES	12
2.2. DATA SOURCES AND SOFTWARE	13
2.2.1. Software.....	16
2.3. AIRCRAFT POPULATION	17
2.4. TEMPORAL DISTRIBUTION OF FLIGHTS	19
2.5. TRAFFIC DISTRIBUTION PER FLIGHT LEVEL.....	22
2.6. LOCATIONS FOR RISK ASSESSMENTS	24
3. LATERAL COLLISION RISK ASSESSMENT	26
3.1. REICH COLLISION RISK MODEL	26
3.2. AVERAGE AIRCRAFT DIMENSIONS: $\lambda_x, \lambda_y, \lambda_z$	30
3.3. PROBABILITY OF VERTICAL OVERLAP: $P_z(0)$	30
3.4. AVERAGE GROUND SPEED: V	32
3.5. AVERAGE RELATIVE LONGITUDINAL SPEED: ΔV	35
3.6. AVERAGE RELATIVE LATERAL SPEED: \bar{y}	36
3.7. AVERAGE RELATIVE VERTICAL SPEED: \bar{z}	37
3.8. LATERAL OVERLAP PROBABILITY: $P_Y(S_Y)$	37
3.9. LATERAL OCCUPANCY	44
3.9.1. Traffic growth hypothesis.....	46
3.9.2. Lateral occupancy values obtained.....	47
3.9.2.1. Canaries.....	47
3.9.2.2. SAL1	49
3.9.2.3. SAL2	50
3.9.2.4. Dakar1	51
3.9.2.5. Dakar2	53
3.9.2.6. Recife	54
3.10. LATERAL COLLISION RISK	55
3.10.1. Lateral collision risk values obtained	55
3.10.1.1. Canaries.....	56
3.10.1.2. SAL1	57
3.10.1.3. SAL2	58
3.10.1.4. Dakar1	59
3.10.1.5. Dakar2.....	60
3.10.1.6. Recife.....	61
3.10.2. Considerations on the results	62
3.10.3.1. Parallel routes.....	62
3.10.3.2. RANDOM route.....	62
4. VERTICAL COLLISION RISK ASSESSMENT	64
4.1. INTRODUCTION	64



4.2. TECHNICAL VERTICAL COLLISION RISK ASSESSMENT	65
4.2.1. Collision Risk Model.....	65
4.2.2. Average aircraft dimensions: $\lambda_x, \lambda_y, \lambda_z, \lambda_h$	70
4.2.3. Probability of lateral overlap: $P_y(0)$	71
4.2.4. Probability of horizontal overlap: $P_h(\theta)$	73
4.2.4.1. Application to the EUR/SAM Airspace	76
4.2.5. Relative velocities	78
4.2.6. Vertical overlap probability: $P_z(S_z)$	81
4.2.6.1. ASE Distribution Modelling.....	84
4.2.6.2. AAD Distribution Modelling.....	86
4.2.6.3. TVE Distribution Modelling	87
4.2.7. Vertical occupancy	89
4.2.7.1. Vertical occupancy values obtained	91
4.2.7.1.1 Canaries.....	92
4.2.7.1.2 SAL1	97
4.2.7.1.3 SAL2	103
4.2.7.1.4 Dakar1	106
4.2.7.1.5 Dakar2.....	107
4.2.7.1.6 Recife.....	108
4.2.8. Technical vertical collision risk.....	111
4.2.8.1 Canaries.....	111
4.2.8.2 SAL1	113
4.2.8.3 SAL2	115
4.2.8.4 Dakar1	117
4.2.8.5 Dakar2	119
4.2.8.6 Recife	121
4.2.9. Considerations on the results.....	123
4.2.10.1. Parallel and crossing routes.....	123
4.2.10.2. RANDOM route.....	124
4.3. TOTAL VERTICAL COLLISION RISK ASSESSMENT.....	124
4.3.1. Vertical Collision Risk Models for large height deviations	127
4.3.1.1. Aircraft levelling off at a wrong level	127
4.3.1.2. Aircraft climbing or descending through a flight level.....	129
4.3.1.3. Large height deviations not involving whole numbers of flight levels.....	131
4.3.2. Data on EUR/SAM large height deviations	132
4.3.3. Total vertical collision risk	134
4.3.3.1. Considerations on the results.....	136
5. CONCLUSIONS	137
6. ACRONYMS	142
7. REFERENCES.....	142
ANNEX 1: METHODS FOR OCCUPANCY ESTIMATE.....	144
A1.1. DEFINITION	145
A1.2. METHODS FOR OCCUPANCY ESTIMATE.....	146
A1.2.1. STEADY STATE FLOW MODEL.....	146
A1.2.1.1. Number of flight hours H.....	147
A1.2.1.2. Total proximity time T_y	148
A1.2.1.3. Occupancy	149



A1.2.2.DIRECT ESTIMATION FROM TIME AT WAYPOINT PASSING 150

A1.3. CROSSING OCCUPANCY.....151

ANNEX 2: ASE DISTRIBUTIONS FOR EUR/SAM CORRIDOR.....153

A2.1. ASE DISTRIBUTIONS FOR EUR/SAM CORRIDOR.....154



TABLE OF FIGURES

Figure 1 Existing route network	5
Figure 2 EUR/SAM Corridor	6
Figure 3 Route network	7
Figure 4 Direct routes (RANDOM)	8
Figure 5 Direct-to trajectories in SAL Oceanic UIR.....	9
Figure 6 Crossing traffic in non published routes analysed (more than 50 aircraft/year).....	11
Figure 7 Number of flights per day in the Canaries	19
Figure 8 Number of flights per day of the week in the Canaries.....	20
Figure 9 Number of flights per half-hour crossing EDUMO, TENPA, IPERA and GUNET	21
Figure 10 Number of flights per half-hour crossing DIKEB, OBKUT, ORARO and NOISE.	22
Figure 11 Number of aircraft on routes UN-741, UN-866, UN-873 and UN-857 in the Canaries	23
Figure 12 Number of Southbound aircraft on routes UN-741, UN-866, UN-873 and UN-857 in the Canaries	23
Figure 13 Number of Northbound aircraft on routes UN-741, UN-866, UN-873 and UN-857 in the Canaries	24
Figure 14 Locations for risk assessments	25
Figure 15 Speeds obtained from Palestra	32
Figure 16 Speeds limited to 575kts in the current scenario in the Canaries.....	34
Figure 17 Lateral collision risk for the period 2008-2018 in Canaries	56
Figure 18 Lateral collision risk for the period 2008-2018 in SAL1	57
Figure 19 Lateral collision risk for the period 2008-2018 in SAL2	58
Figure 20 Lateral collision risk for the period 2008-2018 in Dakar1	59
Figure 21 Lateral collision risk for the period 2008-2018 in Dakar2.....	60
Figure 22 Lateral collision risk for the period 2008-2018 in Recife.....	61
Figure 23 Number of Southbound flights on routes RANDOM, UN-741 and UN-866	63
Figure 24 Number of Northbound flights on routes RANDOM, UN-741 and UN-866	63



Figure 25 Geometry of the crossing routes	73
Figure 26 Breakdown of height-keeping errors.....	84
Figure 27 Technical vertical collision risk for the period 2008-2018 in the Canaries	112
Figure 28 Technical vertical collision risk for the period 2008-2018 in the Canaries - Enlarged.....	113
Figure 29 Technical vertical collision risk for the period 2008-2018 in SAL1	114
Figure 30 Technical vertical collision risk for the period 2008-2018 in SAL1 - Enlarged...	115
Figure 31 Technical vertical collision risk for the period 2008-2018 in SAL2	116
Figure 32 Technical vertical collision risk for the period 2008-2018 in SAL2 - Enlarged...	117
Figure 33 Technical vertical collision risk for the period 2008-2018 in Dakar1	118
Figure 34 Technical vertical collision risk for the period 2008-2018 in Dakar1 - Enlarged	119
Figure 35 Technical vertical collision risk for the period 2008-2018 in Dakar2	120
Figure 36 Technical vertical collision risk for the period 2008-2018 in Dakar2 - Enlarged	121
Figure 37 Technical vertical collision risk for the period 2008-2018 in Recife.....	122
Figure 38 Technical vertical collision risk for the period 2008-2018 in Recife - Enlarged..	123
Figure 39 Illustration of the three basic deviation paths	126



TABLE OF TABLES

Table 1 Aircraft population and number of flights per type in the Canarias UIR.....	17
Table 2 Average aircraft dimensions.....	30
Table 3 Average speeds.....	35
Table 4 Average relative longitudinal speed.....	36
Table 5 Lateral navigation error types.....	39
Table 6 Lateral overlap probability for different separations between routes with RNP10....	43
Table 7 Lateral occupancy parameters in the Canarias UIR.....	47
Table 8 Lateral occupancies in the Canarias UIR, in 2008.....	48
Table 9 Lateral occupancy estimate for the Canarias until 2018 with an annual traffic growth rate of 8%.....	48
Table 10 Lateral occupancy parameters in SAL1.....	49
Table 11 Lateral occupancy estimate for SAL1 until 2018 with an 8% annual traffic growth rate.....	50
Table 12 Lateral occupancy parameters in SAL2.....	50
Table 13 Lateral occupancy estimate for SAL2 until 2018 with an 8% annual traffic growth rate.....	51
Table 14 Lateral occupancy parameters in Dakar1.....	52
Table 15 Lateral occupancy estimate for Dakar1 until 2018 with an 8% annual traffic growth rate.....	52
Table 16 Lateral occupancy parameters in Dakar2.....	53
Table 17 Lateral occupancy estimate for Dakar2 until 2018 with an 8% annual traffic growth rate.....	54
Table 18 Lateral occupancy parameters in Recife.....	54
Table 19 Lateral occupancy estimate for Recife until 2018 with an 8% annual traffic growth rate.....	55
Table 20 Lateral collision risk for the period 2008-2018 in Canarias.....	56
Table 21 Lateral collision risk for the period 2008-2018 in SAL1.....	57
Table 22 Lateral collision risk for the period 2008-2018 in SAL2.....	58
Table 23 Lateral collision risk for the period 2008-2018 in Dakar1.....	59



Table 24 Lateral collision risk for the period 2008-2018 in Dakar2	60
Table 25 Lateral collision risk for the period 2008-2018 in Recife	61
Table 26 Average aircraft dimensions for the vertical collision risk model	70
Table 27 Horizontal overlap probabilities for Canaries	77
Table 28 Horizontal overlap probabilities for SAL1	77
Table 29 Horizontal overlap probabilities for SAL2	78
Table 30 Horizontal overlap probabilities for Dakar1	78
Table 31 Horizontal overlap probabilities for Recife	78
Table 32 Relative speeds in crossings (Canaries and SAL1)	80
Table 33 Relative speeds in crossings (SAL2 and Recife)	81
Table 34 Estimates of Proportions of Height-Keeping Errors	88
Table 35 Vertical occupancy due to same and opposite direction traffic in Canaries location with current traffic levels	92
Table 36 Number of aircraft in the Canaries airspace	93
Table 37 Time windows for crossing occupancies in the Canaries	94
Table 38 Number of proximate events due to crossing traffic in the Canaries	95
Table 39 Vertical occupancy estimate for the Canaries until 2018 with an annual traffic growth rate of 8%	97
Table 40 Vertical occupancy due to same and opposite direction traffic in SAL1 with current traffic levels	98
Table 41 Number of flights in SAL1	98
Table 42 Time windows for crossing occupancies in SAL1	99
Table 43 Number of proximate events due to crossing traffic in SAL1	100
Table 44 Vertical occupancy estimate for SAL1 until 2018 with an 8% annual traffic growth rate	102
Table 45 Vertical occupancy due to same and opposite direction traffic in SAL2 with current traffic levels	103
Table 46 Number of flights in SAL2	104
Table 47 Time windows for crossing occupancies in SAL2	104
Table 48 Number of proximate events due to crossing traffic in SAL2	105



Table 49 Vertical occupancy estimate for SAL2 until 2018 with an 8% annual traffic growth rate	106
Table 50 Vertical occupancy due to same and opposite direction traffic in Dakar1 with current traffic levels	106
Table 51 Vertical occupancy estimate for Dakar1 until 2018 with an 8% annual traffic growth rate	107
Table 52 Vertical occupancy due to same and opposite direction traffic in Dakar2 with current traffic levels	108
Table 53 Vertical occupancy estimate for Dakar2 until 2018 with an 8% annual traffic growth rate	108
Table 54 Vertical occupancy due to same and opposite direction traffic in Recife with current traffic levels	109
Table 55 Number of flights in Recife	109
Table 56 Time windows for crossing occupancy in Recife	110
Table 57 Number of proximate events due to crossing traffic in Recife	110
Table 58 Vertical occupancy estimate for Recife until 2018 with an 8% annual traffic growth rate	111
Table 59 Technical vertical collision risk for the period 2008-2018 in the Canaries	112
Table 60 Technical vertical collision risk for the period 2008-2018 in SAL1	114
Table 61 Technical vertical collision risk for the period 2008-2018 in SAL2	116
Table 62 Technical vertical collision risk for the period 2008-2018 in Dakar1	118
Table 63 Technical vertical collision risk for the period 2008-2018 in Dakar2	120
Table 64 Technical vertical collision risk for the period 2008-2018 in Recife	122
Table 65 Received data from July 2007 to July 2008	¡Error! Marcador no definido.
Table 66 Large height deviations reported by SAL	133
Table 67 Large height deviations reported by Dakar	133
Table 68 Large height deviations reported by Atlantic-Recife	134
 Table A1. 1 Proportion of flight time and ASE distributions per aircraft type in the Canaries	 159

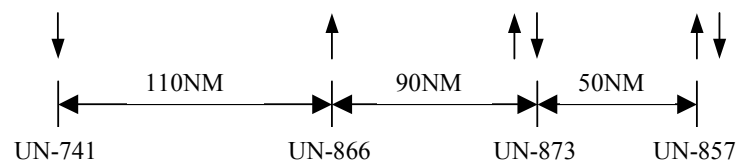


SUMMARY

This document includes the collision risk assessment that has been made for the EUR/SAM Corridor, in the South Atlantic, for flight levels between FL290 and FL410. It is a post-implementation safety assessment in order to evaluate collision risk after the change in the routing structure, which took place 5th July 2007 (routes UN-741 and UN-866, previously bidirectional, became unidirectional).

Two quantitative risk assessments, based on suitable versions of the Reich Collision Risk Model, have been carried out. The first assessment concerns the lateral collision risk whilst the second one concerns the vertical collision risk. The vertical collision risk assessment has been split into two parts. The first part considers the risk due to technical causes, whilst the second one considers the risk due to all causes.

The scenario analysed is the current route network, composed of four nearly parallel north-south routes, being the two easternmost bidirectional and the other two, unidirectional. Traffic on the RANDOM route, placed about 100NM to the west of the current UN-741 and used mainly by IBERIA and LAN-CHILE has not been considered in the analysis. Nevertheless, it is assumed that its contribution would not change the results dramatically. RNP10 and RVSM are implemented within this airspace.



Current route network

As far as crossing traffic is concerned, apart from the traffic on the published routes that crosses the Corridor in SAL, Dakar and Recife (UR-976/UA-602, UL-435 and UL-695/UL-375), traffic that crosses the Corridor using non published routes that carry more than 50 aircraft per year, has also been considered.



The software tool CRM, used in previous studies, has been updated and used to obtain the different parameters of the Reich Collision Risk Model in each one of the UIRs crossed by the Corridor.

The CRM program uses flight plan data obtained from Palestra, Aena’s database, for the Canaries and traffic data from the samples provided by SAL and Atlantic-Recife. For this study, flight plan data from 10th July 2007 to 10th July 2008 have been examined to determine the type of aircraft in the airspace, the average flight characteristics of the typical aircraft and the passing frequencies of these aircraft in the Canaries. For the rest of UIRs, the period analysed has been from 1st November 2007 to 31st January 2008 and from 1st April 2008 to 30th June 2008. No traffic data from Dakar has been received.

Extrapolation of traffic data has been necessary in some cases in order to obtain the traffic distribution along the Corridor and on crossing routes. Therefore, trajectories and information at required waypoints (i.e., time and FL) have been assumed, considering the most logical routes and speeds. This may have an influence in the results, as several assumptions have had to be made due to the incompleteness of the data provided.

Considering a number of parameters such as probabilities of lateral and vertical overlaps, lateral, vertical and crossing occupancies, average speed, average relative velocities and aircraft dimensions, the lateral, technical vertical collision risk and total vertical risk have been assessed and compared with the maximum values allowed, ¹ $TLS = 5 \times 10^{-9}$, $TLS = 2.5 \times 10^{-9}$ and $TLS = 5 \times 10^{-9}$, respectively.

The risk has been evaluated in 6 different locations along the Corridor and an estimation of the collision risk for the next 10 years has been calculated, assuming a traffic growth rate of 8% per year.

¹ TLS: Target Level of Safety

The results obtained are very similar in all the locations and the risk associated to the Corridor is the largest of all the values obtained.

For current traffic levels, the calculated lateral collision risk is 2.451×10^{-9} , whilst the lateral collision risk estimated for 2018 with an annual traffic growth rate of 8% is 5.2915×10^{-9} . These values do not take into account traffic on the RANDOM route. Nevertheless, since traffic on this route only represents 2.5% of the traffic in the Corridor, it is considered that the collision risk due to this route will not make the collision risk go above the TLS and the system is considered to be laterally safe until 2017.

As far as the technical vertical risk is concerned, the value of the collision risk for the current traffic levels is estimated to be 0.2725×10^{-9} and the technical vertical collision risk estimated for 2018 with an annual traffic growth rate of 8%, 0.5883×10^{-9} . Both values are below the TLS.

The vertical risk due to large height deviations has been calculated using the deviations reported by Atlantic-Recife, which included all the required information. As the contribution of these deviations to the total vertical risk in the Corridor, (4.7000×10^{-8} if the value 0.059 is taken for $P_y(0)$), greatly exceed the TLS, the contribution to the risk of SAL and Dakar deviations has not been calculated.

Nevertheless, it is important to remark that **all the deviations received were due to a coordination error**, and they are not related to RVSM operations. If these coordination errors were not taken into account, the total vertical risk would comply with the TLS, since it would be equal to the technical vertical risk. In any case, as the problem is clearly identified, the use of adequate corrective actions to reduce coordination errors in the Corridor will reduce the risk. These measures should be applied as soon as possible.

1. INTRODUCTION

This report presents the post-implementation collision risk assessment made for the EUR/SAM Corridor in order to analyse safety after the change in the routing structure, which took place 5th July 2007 (routes UN-741 and UN-866, previously bidirectional, became unidirectional).

It assesses the current and projected lateral and vertical collision risk in the Corridor, where RNP10 and RVSM are implemented, with data of traffic between FL290 and FL410 collected during the first year of operation, from 10th July 2007 to 10th July 2008.

For this study, the program CRM has been updated and used to obtain the different parameters of the Reich Collision Risk Model in each one of the UIRs crossed by the Corridor.

The values given by the CRM correspond to the time period analysed, July 07-July 08 in this case. Taking these values into account and the traffic forecast for the future, it has been possible to estimate the collision risk for the following years.

2. AIRSPACE DESCRIPTION

As it has already been said, the airspace analysed in this report is the EUR/SAM Corridor, where RNP10 and RVSM are implemented. This Corridor lies in the South Atlantic airspace between the Canary Islands and Brazil.

The scenario analysed is the current tracks system. Figure 1 shows the existing route network together with the horizontal boundaries of the area to be considered in the risk assessment.



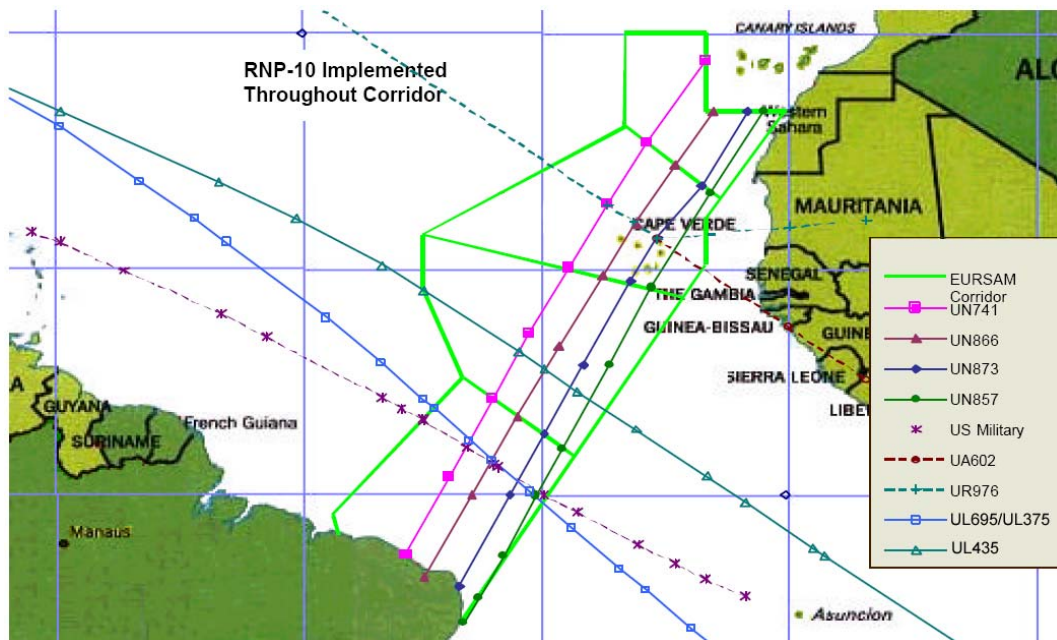


Figure 1
Existing route network

The existing route network is composed of four nearly parallel north-south routes situated within the Canaries UIR, SAL Oceanic UIR/UTA, Dakar Oceanic UIR and Recife FIR.

The denomination of the routes is, from west to east, UN-741, UN-866, UN-873 and UN-857, and their magnetic direction varies around 45° for northbound traffic and 225° for southbound traffic.

Minimum lateral separation between routes is 110NM for routes UN-741/UN-866, 90NM for routes UN-866/UN-873 and 50NM for routes UN-873/UN-857.

Routes UN-741 and UN-866 are unidirectional, with traffic in odd and even flight levels, (Southbound traffic on route UN-741 and Northbound traffic on route UN-866). On the other hand, routes UN-873 and UN-857 are bidirectional. The flight level allocation scheme in these last two routes is the following:

- Southbound flight levels: FL300, FL320, FL340, FL360, FL380 and FL400.
- Northbound flight levels: FL290, FL310, FL330, FL350, FL370, FL390 and FL410.

The following figure shows a detailed image of the tracks system, with all the fixes or Waypoint Position Reporting Points that define it:

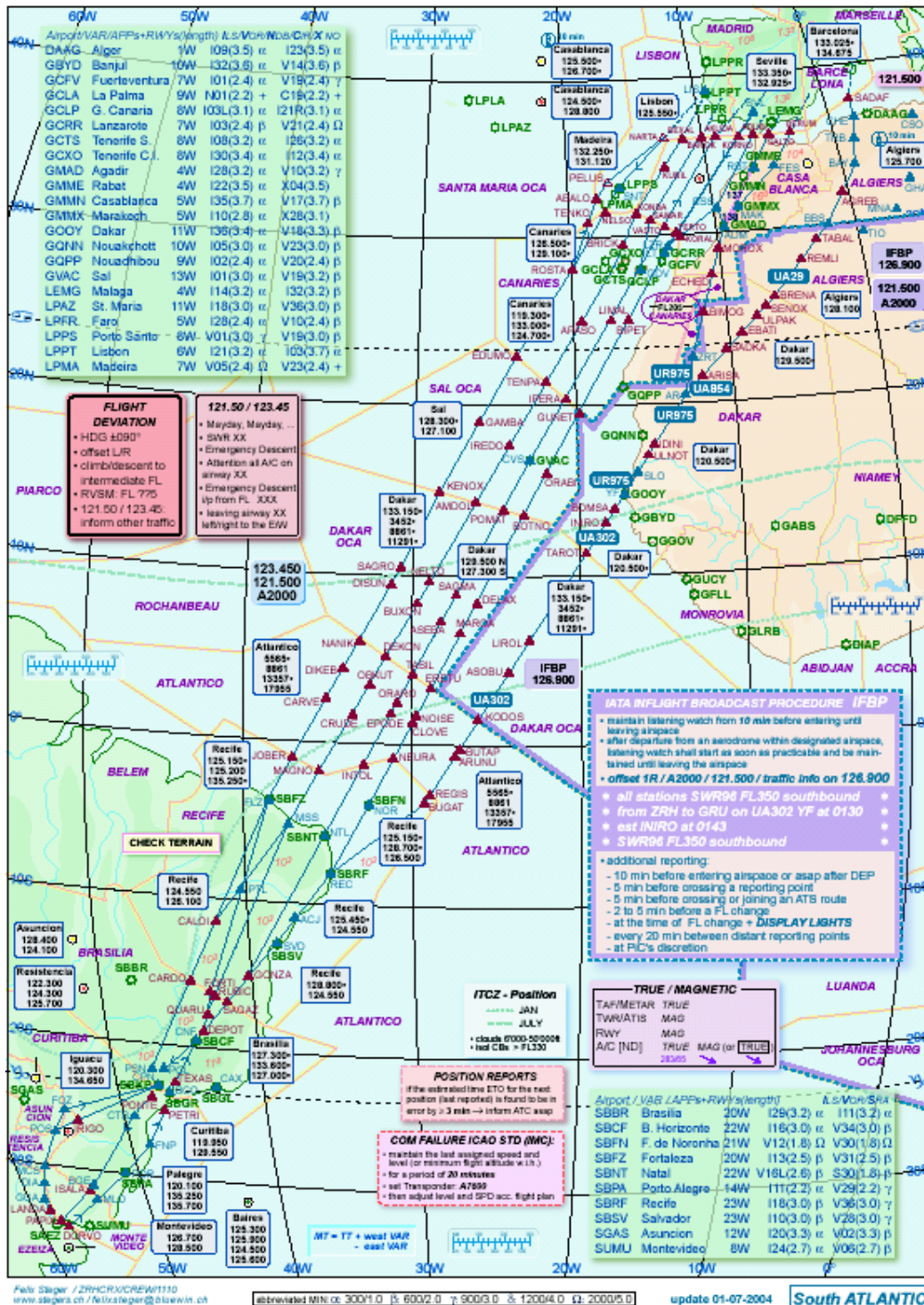


Figure 2
EUR/SAM Corridor



A scheme of the current route network is shown in Figure 3.

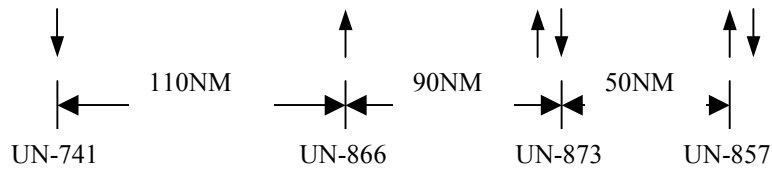


Figure 3
Route network

Besides these four routes, there is also traffic on the direct routes ROSTA-NADIR and NADIR-ABALO (RANDOM), placed about 100NM to the west of the current UN-741 and used mainly by IBERIA and LAN-CHILE. Although this traffic is random and there is certain dispersion in the trajectories, most of the traffic on this route within the Canaries UIR crosses the following points:

- Northbound traffic:
 - 25 00 03N, 24 59 59W
 - 30 00 01N, 20 59 59W
- Southbound traffic:
 - Nelso
 - Rosta
 - 24 59 57N, 23 00 02W
 - 23 26 58N, 24 19 03W

An image of these routes along the Corridor can be seen in the following figure.

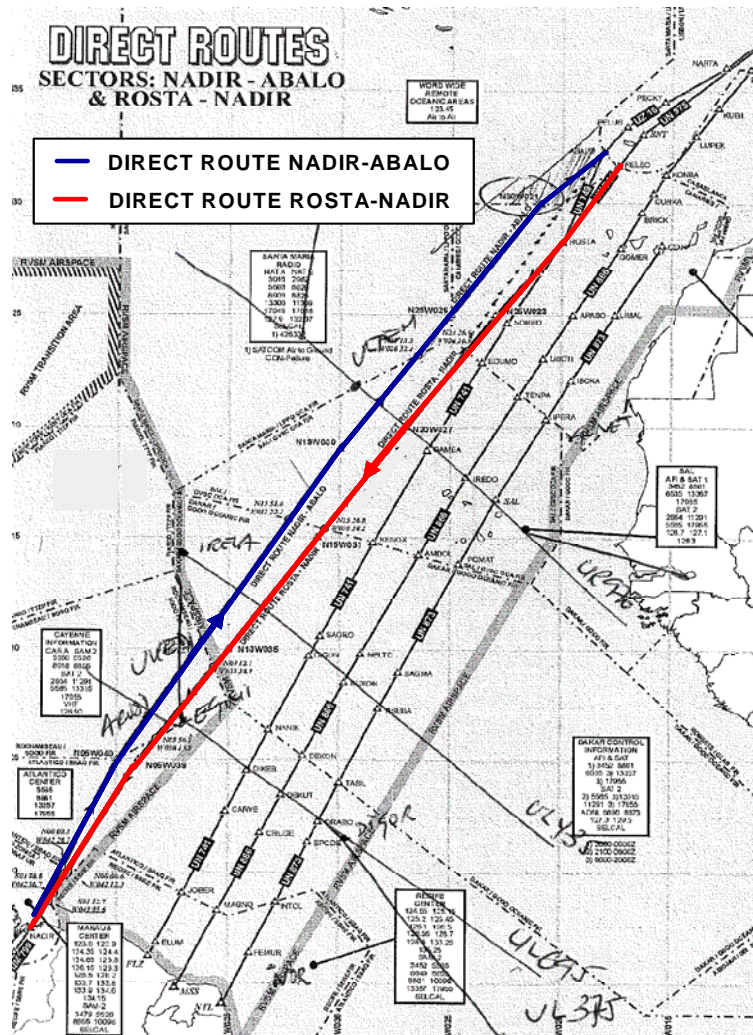


Figure 4
Direct routes (RANDOM)

Although the number of aircraft on these routes will be indicated later, they have not been considered in the collision risk assessment.

There is also some traffic crossing the Corridor in published routes in SAL UIR (UR-976/UA-602), in Dakar UIR (UL-435) and in Recife UIR (UL-695/UL-375).

In the analysis of the traffic data provided by SAL, it has been noticed that, apart from traffic on crossing route UR-976, there is also traffic in the proximity of this route that has been cleared with a “Direct to” between LUMPO and ULTEM waypoints. The number of aircraft



on these direct-to trajectories is comparable to the number of aircraft that fly exactly on route UR-976/UA-602. Therefore, this crossing traffic cannot be considered negligible.

Figure 5 shows, highlighted in green, the direct routes indicated in the data provided by SAL for November 2007. Although there is certain dispersion around the line that joins LUMPO and ULTEM, it will be considered that all these flights follow that line, as it is not possible to analyze each of them independently. This crossing trajectory will be referred to as ULTEM-LUMPO in the rest of the document.

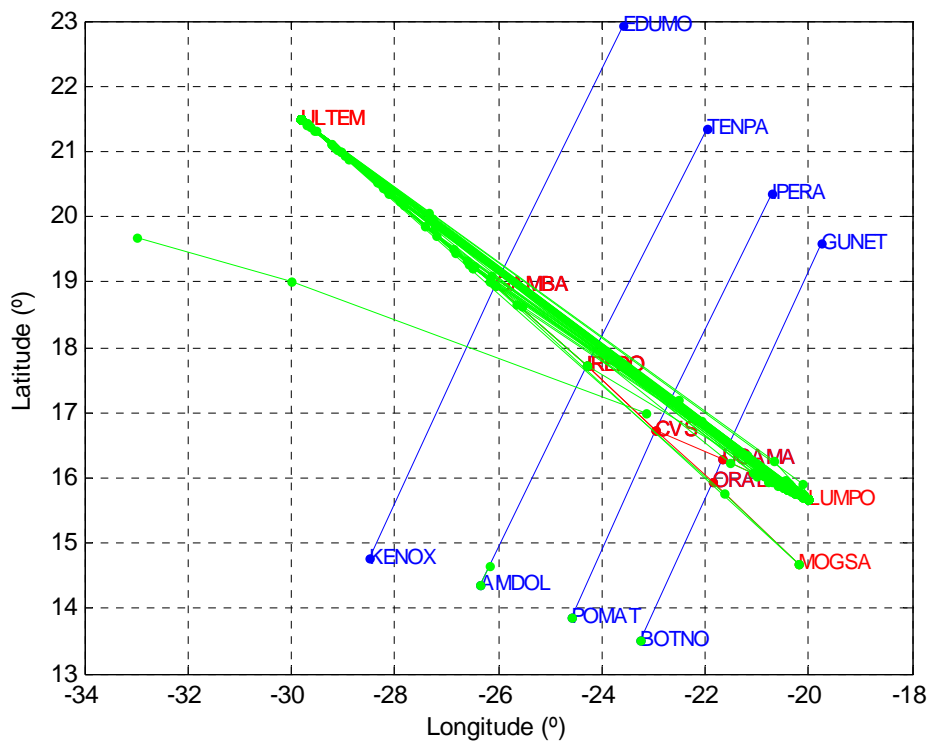


Figure 5
Direct-to trajectories in SAL Oceanic UIR

Apart from the published crossing routes, some crossing traffic in non published routes was also detected in the pre-implementation study, ([Ref. 11], [Ref. 15]). Given that not all the trajectories could be analysed, some hypotheses had to be made and only those trajectories with more than 50 aircraft per annum were analysed.



In this study, besides the trajectories already considered in the pre-implementation collision risk assessment, current traffic data has also been examined in order to identify whether there are new trajectories with more than 50 aircraft per annum that should be included in the assessment.

41 crossing trajectories (real crossings or changes between routes) have been identified in the Canaries UIR, 33 in SAL UIR, 9 in Dakar UIR and 4 in Recife UIR. From these, the trajectories with more than 50 aircraft per year to be considered in this study are the ones shown in Figure 6, i.e:

- CVS-GUNET
- LIMAL-ETIBA
- EDUMO-APASO
- EDUMO-COOR3²
- ULTEM-KENOX
- GUNET-LUMPO
- KENOX-COOR2³
- GAMBA-COOR1⁴
- GAMBA-TENPA
- EDUMO-COOR1⁴
- CVS-AMDOL
- BOTNO-CVS
- TENPA-CVS
- ULTEM-LUMPO

² COOR3 is not a published name for any waypoint. It will be used in this document to refer to the point given in the traffic data samples by the coordinates (0200000N, 0322500W).

³ COOR2 is not a published name for any waypoint. It will be used in this document to refer to the point given in the traffic data samples by the coordinates (0100000N, 0350000W).

⁴ COOR1 is not a published name for any waypoint. It will be used in this document to refer to the point given in the traffic data samples by the coordinates (0153000N, 0270000W).



Analysing these trajectories, only 0.87% of the traffic is not being considered in the Canaries UIR, 1.32% in SAL, 0.18% in Dakar and 0.08% in Recife. Therefore, this hypothesis seems reasonable, at least in a first approach, specially considering that these crossings or changes between routes only occur when there is not any traffic around.

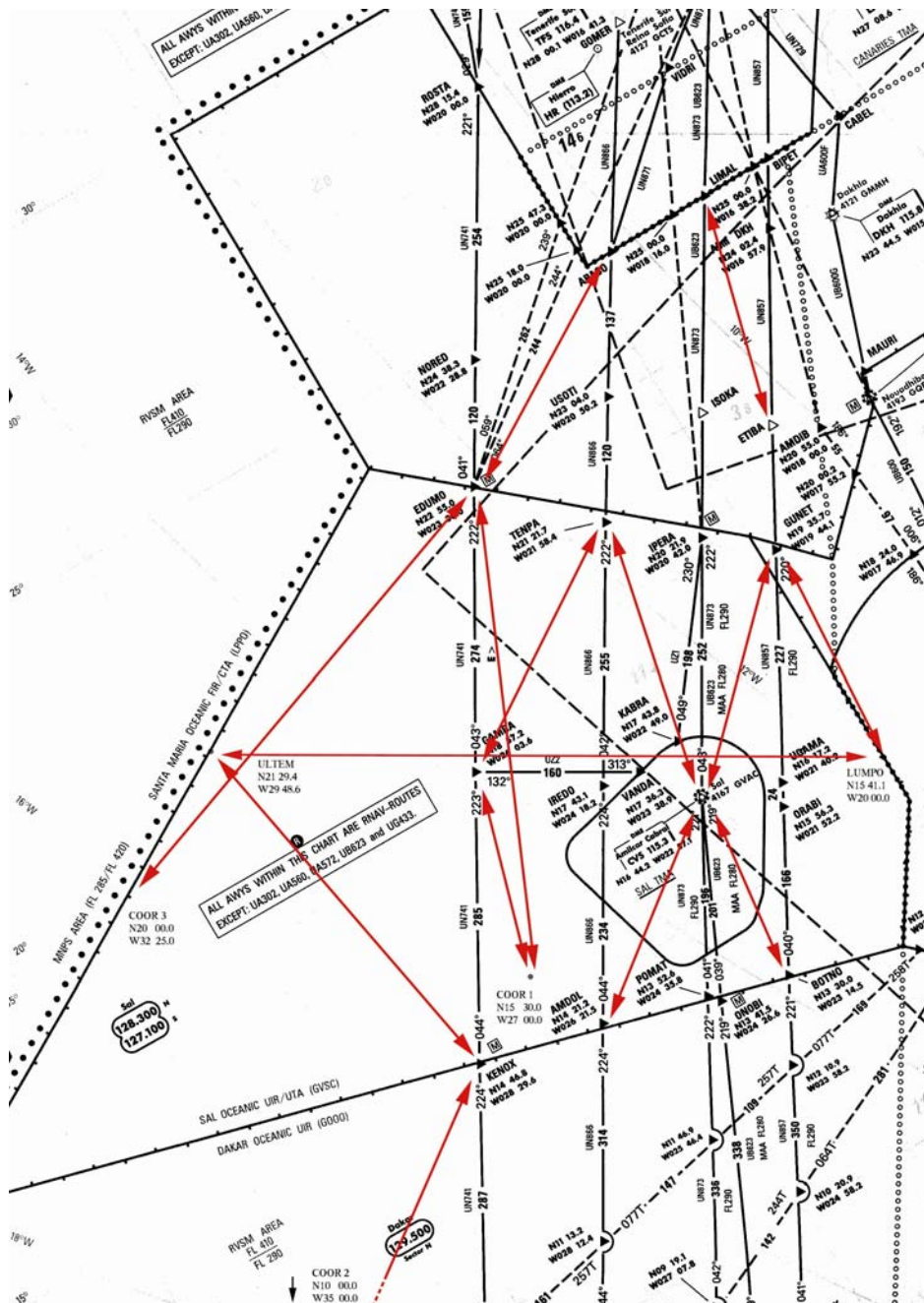


Figure 6
Crossing traffic in non published routes analysed (more than 50 aircraft/year)



2.1. ATS SERVICES AND PROCEDURES

The airspace in the area of the South Atlantic EUR/SAM Corridor is subject to procedural control with pilot voice waypoint position reporting. While VHF voice communications are available over approximately the same areas where DME coverage is available, the primary means of communications is HF voice. Appropriately equipped aircraft can also use SATCOM and HF Data Link (HF DL) throughout the South Atlantic EUR/SAM Corridor.

There are two DME stations inside the RNP10 airspace, namely CVS, Almilcar Cabral, and NOR, Noronha. Their ranges are limited by the RF horizon to about 200NM. There are also some DME stations to the north and south of the RNP10 airspace, in the Canary Islands and in Recife.

Although radar surveillance is not available for the parallel route system in the four FIR/UIRs, it is available in the adjacent Canaries TMA, on the coast of Brazil and in Cape Verde. Radar range is also limited by the RF horizon.

These radars do provide an opportunity to monitor the lateral and the vertical deviations of aircraft flying in the Corridor. However, information from these radars was not available for this study.

The system called SACCAN (ADS-CPDLC in the Canaries FIR/UIR) is also installed in the Canary Islands. The main purpose of SACCAN is to provide air traffic control services to FANS 1/A aircraft operating in the Canary airspace.

FANS 1/A equipped aircraft use the SITA and ARINC networks and can communicate with SACCAN by means of the Aeronautical Mobile Satellite Service (AMSS) provided by INMARSAT, or by VHF when within the range of any of the multiple SITA or ARINC VHF data link stations, like the ones of SITA located in the Canary Islands.



The technical coverage of SACCAN is the coverage provided by the constellation of geostationary satellites INMARSAT, i.e. global coverage (except for the poles). Nevertheless, operationally, the area of interest is the oceanic area of the Canary FIR where there is not radar coverage.

SACCAN uses FANS-1/A technology. The system improves surveillance (with ADS) and communications (with CPDLC) of the FANS-1 or FANS-A equipped aircraft, when flying over the oceanic area of the Canary FIR. The system is in pre-operational phase since 5th July 2007.

According to the AIC NR 13/A/08GO of 30th October 2008, the pre-operational implementation of ADS and CPDLC in Dakar Oceanic is also effective from November 1st 2008.

This study does not consider the reduction of the collision risk that would be obtained with the use of ADS.

2.2. DATA SOURCES AND SOFTWARE

For this study, flight progress data from the Canary, SAL and Recife ACCs, between FL290 and FL410, have been made available.

Data from the Canary is the flight progress data stored in Palestra, Aena’s database. It consists of initial flight plan data updated by the controllers with pilot position reports.

Occasionally, it can happen that due to workload constraints controllers, although obviously updating their personal flight progress information, do not enter the information into the database system. As a consequence, the altitude information obtained from Palestra is not always correct. In the same way, it is possible that typographical errors have been introduced



while inputting the information or that some of this information has been omitted. Some of these errors have been detected and corrected by software.

In the collision risk assessment made by ARINC in 2001,[Ref. 2], that was the base for RNP10 implementation in the South Atlantic Corridor and for the introduction of the current route UN-873, it was mentioned that several errors regarding flight level were identified in the flight plans because a high proportion of flights did not match the vertical route structure. This has been verified analysing some flight plans from Palestra, chosen by chance. The used software takes this into account and corrects altitudes assuming that:

- All aircraft conform to the vertical route structure.
- No aircraft entered or left the vertical route structure.
- The reported altitudes are close to the actual altitudes.
- The reported altitudes are less than the actual altitudes.

The analysed Palestra flight plans are those which cover the time period 10th July 2007 to 10th July 2008. They include reports for all waypoints in the Canaries UIR.

Besides data from Palestra, a traffic sample from SAL (01/11/07-31/01/08 and 01/04/08-10/07/08) and a traffic sample from Atlantic-Recife (01/09/2007-30/06/08) were also available for this assessment. No traffic data from Dakar has been received for this study.

Data from SAL include information on all aircraft overflying the airspace, including traffic on the four main routes of the Corridor and traffic on the crossing routes UR-976/UA-602. Data from Recife include traffic on the main routes overflying the airspace with origin/destination Cape Verde that do not overfly the Canaries and traffic on the crossing routes UL-375/UL-695.

Nevertheless, analysing these traffic samples, it has been noticed that not all the flights on the main routes detected in Palestra that, according to their origin/destiny were supposed to have flown in SAL, appear in the data provided by SAL. Likewise, for the aircraft that do not



overfly the Canaries, there are some flights in the sample provided by SAL that do not appear in the sample of Recife, when they should. The same happens with some aircraft from Recife data sample that should also be found in the sample of SAL. Therefore, in this study only data from those months for which there is traffic information from both UIRs, SAL and Recife, has been used, combining the data in order to get a complete sample and extrapolating to other UIRs when necessary.

Thus, data from 10th July 2007 to 10th July 2008 has been used to obtain the different parameters of the collision risk assessment in the Canaries UIR and data from 1st November 2007 to 31st January 2008 and from 1st April 2008 to 30th June 2008 for the rest of the UIRs. Although a larger sample would have been desirable, this 6 months sample can be considered representative of the traffic pattern in the Corridor.

Given that the formats in which data from SAL and Recife was provided were different from each other and different from the one used by Palestra, a transformation of formats was necessary to get all the data in the same format (the one used by Palestra).

Another issue to take into account is the fact that, in the data provided by SAL and Recife, sometimes there was not information of all the needed waypoints and, in some other cases, the information was incoherent. As a result, trajectories and information at required waypoints (i.e., time and FL) were assumed, considering the most logical routes and speeds for the extrapolation. This may have an influence on the results, as it will be explained later on.

An example of the inconsistencies derived from the incompleteness of the data provided is that, apparently, several air collisions would have occurred on route UR-976, owing to the existence of “kamikazes”. As, obviously, this has not actually happened, it is assumed that it is due to the lack of data provided in the traffic sample, that does not include flight changes in some cases. These particular events have been identified and corrected. Nevertheless, in general, some other assumptions will be necessary due to this incompleteness, and final results may not be reliable.



As it has already been said, extrapolation has been necessary for the main routes of the Corridor, in order to obtain the traffic distribution along the Corridor. It has also been necessary to extrapolate crossing traffic on published routes when information of all the required waypoints was not available. Specially, for the ULTEM-LUMPO direct-to trajectory, it has been necessary to extrapolate all the flights of the crossing route and all the flights of the main routes to the points where the line ULTEM-LUMPO intersects each of the main routes, i.e. (19.3339N, 25.8696W), (18.2838N, 239765W), (17.4741N, 22.5246W) and (16.5673N, 20.9063W).

Apart from traffic data, some data on large height deviations has also been received, as it will be explained in 4.3.

2.2.1. Software

The software tool CRM, created by Aena, has been used to obtain the different parameters of the lateral and vertical Reich Collision Risk Model in each one of the UIRs crossed by the Corridor, in the current route network.

The CRM program uses flight plan data obtained from Palestra, Aena’s database, for the Canaries and traffic data from the samples provided by SAL and Atlantic-Recife. For this study, flight plan data from 10th July 2007 to 10th July 2008 have been examined to determine the type of aircraft in the airspace, the average flight characteristics of the typical aircraft and the passing frequencies of these aircraft.

The values given by the CRM correspond to the time period analysed, July 2007-July 2008 in this case. Taking these values into account and the traffic forecast for the future, it is possible to estimate the collision risk for the following years.



2.3. AIRCRAFT POPULATION

The most common aircraft types, the number of flights per type and the proportion of these types over the total of flights detected during the time period considered between FL290 and FL410 have been analysed.

Table 1 shows the values obtained for the Canarias UIR together with the geometric dimensions of these aircraft types. Similar results have been obtained for the rest of UIRs.

Aircraft type	Count	% AC	Length (m)	Wingspan (m)	Height (m)
A330-200	9447	27,8705452	63,7	60,03	16,74
A340-300	4220	12,4498466	63,7	60,3	16,74
B767-300	3315	9,77991503	47,6	54,9	15,9
B747-400	2941	8,67654	70,7	64,4	19,4
A340-600	2078	6,13051688	74,37	63,6	17,8
B777-200	2052	6,05381166	63,7	60,9	18,5
MD11	1603	4,72917158	61,2	51,7	17,6
A310	1422	4,19518527	46,4	43,89	15,8
B757-200	1352	3,98867123	47,32	38,05	13,6
B737-800	1238	3,65234836	39,47	34,31	12,5
A320	746	2,20084966	37,57	34,1	11,76
A320-100	516	1,52230352	37,57	34,1	11,76
A340-500	428	1,26268586	67,9	63,45	17,1
A319	314	0,92636299	33,84	34,1	11,76
B777-300	304	0,89686099	73,9	60,9	19,3
B767-200	234	0,69034694	48,5	47,6	15,8
A340-200	227	0,66969554	59,39	60,3	16,74
F900	150	0,44253009	20,2	19,3	7,6
B747-200	123	0,36287468	70,7	59,6	19,3
PRM1	100	0,29502006	---	---	---
E135	94	0,27731886	26,33	20,04	6,76
A330-300	89	0,26256785	63,7	60,03	16,74
B737-700	75	0,22126505	33,6	34,3	12,5
B77W	68	0,20061364	73,9	60,9	18,5
GLF4	55	0,16226103	26,9	23,79	7,64
F2TH	54	0,15931083	20,21	19,33	7,55

Table 1
Aircraft population and number of flights per type in the Canarias UIR

Aircraft type	Count	% AC	Length (m)	Wingspan (m)	Height (m)
CL60	50	0,14751003	20,86	19,35	6,28
GLF5	42	0,12390843	29,42	28,5	7,87
C17	40	0,11800802	53	51,8	16,8
L101	38	0,11210762	50,05	50,09	16,8
B747-300	33	0,09735662	70,7	59,6	19,3
H25B	31	0,09145622	15,6	15,7	5,4
B737-200	26	0,07670522	30,54	28,34	11,28
DC10	25	0,07375502	55,2	50,4	17,9
L101	38	0,11210762	50,05	50,09	16,8
B747-300	33	0,09735662	70,7	59,6	19,3
H25B	31	0,09145622	15,6	15,7	5,4
B737-200	26	0,07670522	30,54	28,34	11,28
DC10	25	0,07375502	55,2	50,4	17,9
E190	25	0,07375502	36,24	28,72	10,57
B707-300	22	0,06490441	46,6	44,42	12,93
B777	21	0,06195421	67,78	61,68	18,5
GALX	21	0,06195421	18,99	17,71	6,52
GLEK	21	0,06195421	30,3	28,65	7,57
C750	18	0,05310361	22,05	19,38	5,84
CL30	16	0,04720321	---	---	---
LJ35	16	0,04720321	14,71	11,97	3,71
FA50	14	0,04130281	18,52	18,96	6,97
B737-300	12	0,03540241	33,4	28,9	11,1
Otros	180	0,53103611	---	---	---

Table 1 (cont)
Aircraft population and number of flights per type in the Canaries UIR

The data sample in the Canaries UIR includes 33896 flights of 102 different aircraft types. The population is dominated by large airframes such as A330-200, A340-300, B767-300, B747-400, A340-600 and B777-200. These six types make up about 71% of the total number of flights. The next 11 types, that also belong to the Airbus and Boeing families, make up another 24.73% and the rest, 4.3% is distributed among the other 85 aircraft types.

2.4. TEMPORAL DISTRIBUTION OF FLIGHTS

Several graphs, showing the temporal distribution of flights, will be displayed in this section. The first one, Figure 7, shows the distribution of the number of flights per day in EDUMO, TENPA, IPERA and GUNET from 10th July 2007 to 10th July 2008, differentiating between Northbound (NB) and Southbound (SB) traffic.

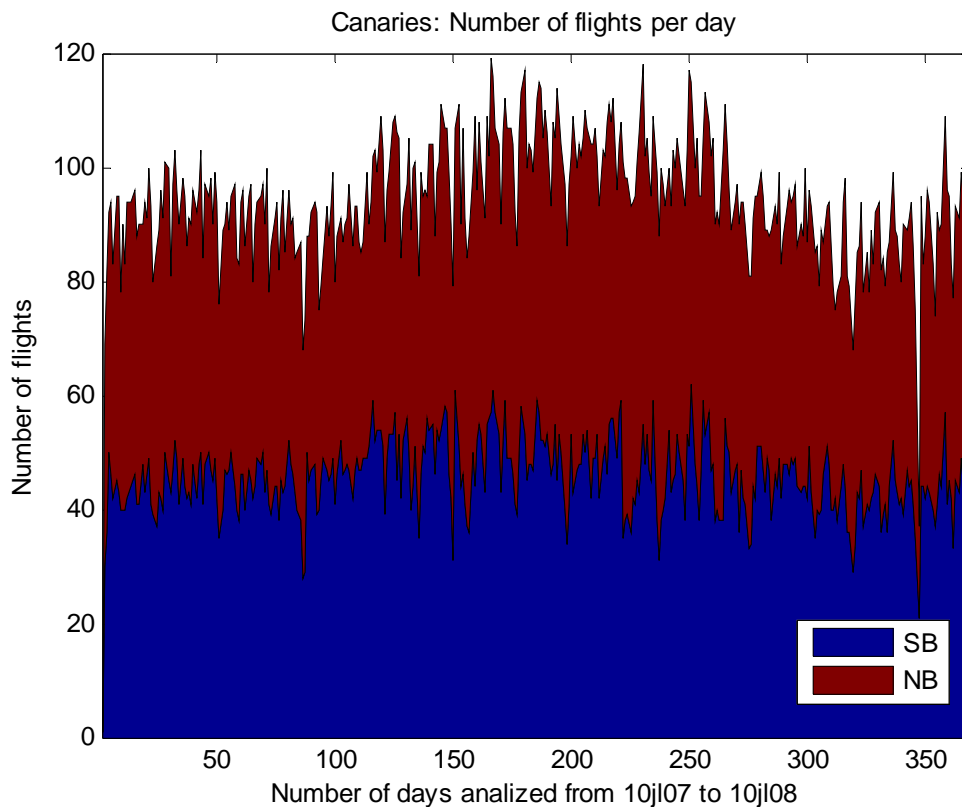


Figure 7
Number of flights per day in the Canaries

The overall average traffic is 91.9 flights per day with a standard deviation of 12.05 flights per day.

Figure 8 shows the distribution of the same traffic over the days of the week

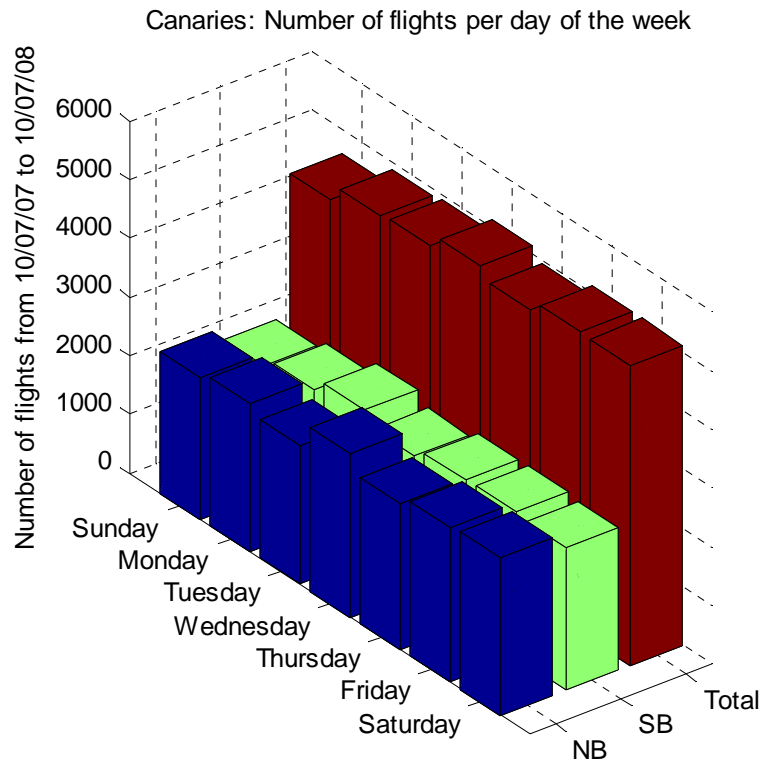


Figure 8
Number of flights per day of the week in the Canaries

In the following two figures what is shown is the distribution of flights per half-hour. The first one shows the distribution of flights obtained with the time of waypoint crossing in EDUMO, TENPA, IPERA and GUNET (Canaries), distributing the 33896 aircraft detected over the studied period according to the time of day at which they crossed those waypoints. The second one shows the distribution of flights obtained with the time of waypoint crossing in DIKEB, OBKUT, ORARO and NOISE (Recife). They also distinguish between Northbound (NB) and Southbound (SB) traffic.

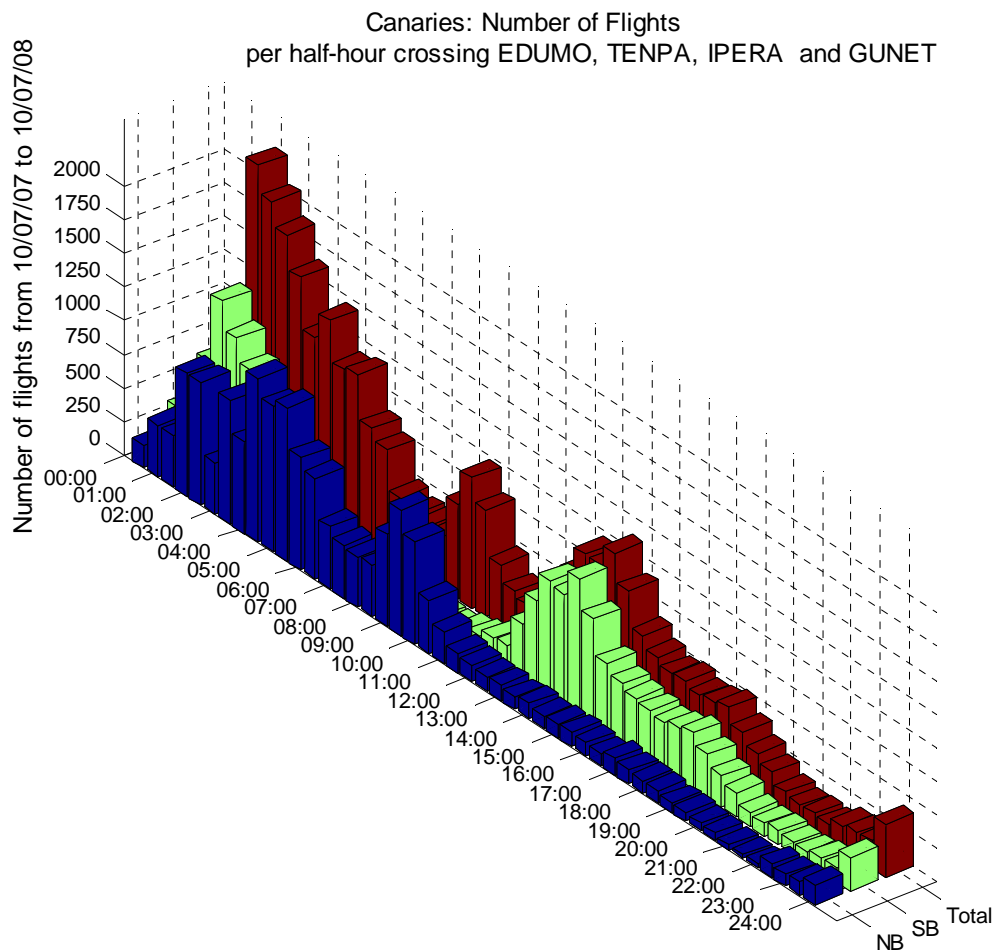


Figure 9
Number of flights per half-hour crossing EDUMO, TENPA, IPERA and GUNET

It can be seen that, in Canaries, it is from 00:00h to 3:00h and from 13:00 to 20:00h when the highest concentration of southbound flights occurs, whilst most of the northbound aircraft concentrate between from 00:00h to 10:00h.

The temporal distribution of the 29491 aircraft detected over the same period in Recife, according to the time of day at which they crossed DIKEB, OBKUT, ORARO and NOISE waypoints is shown in Figure 10.

In this figure, it can be seen that the highest traffic concentration occurs between 00:00h and 8:00h and, in a lower extent, from 15:00h to 24:00h.



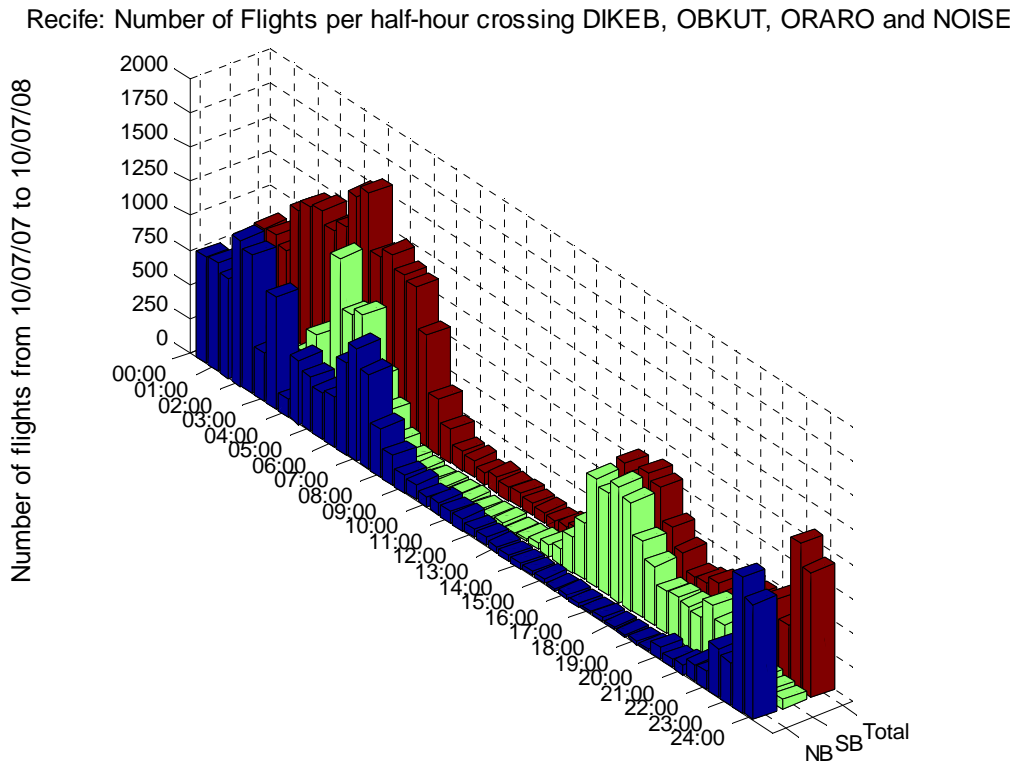


Figure 10
Number of flights per half-hour crossing DIKEB, OBKUT, ORARO and NOISE.

2.5. TRAFFIC DISTRIBUTION PER FLIGHT LEVEL

Traffic distribution per flight level will be depicted in the graphics of this section. Figure 11 shows the total amount of traffic for the main routes in Canarias, distributed by route and flight level. Figure 12 and Figure 13 are similar, but they only include the Southbound and the Northbound traffic, respectively.

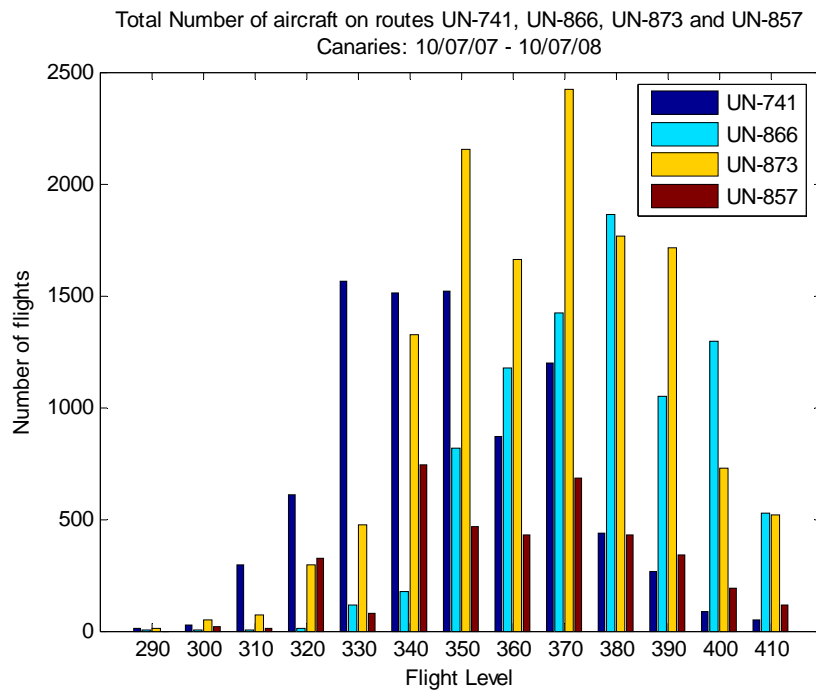


Figure 11
Number of aircraft on routes UN-741, UN-866, UN-873 and UN-857 in the Canary Islands

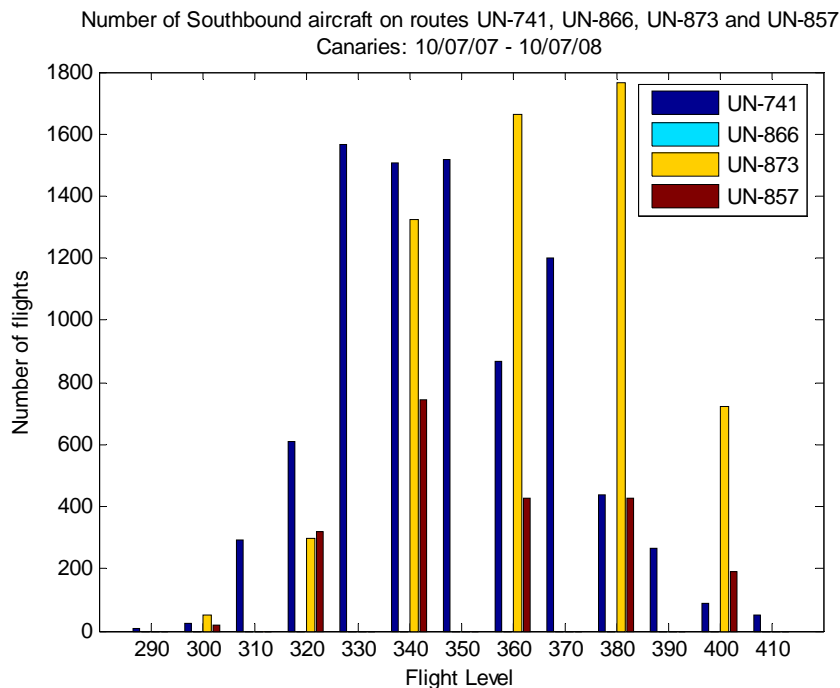


Figure 12
Number of Southbound aircraft on routes UN-741, UN-866, UN-873 and UN-857 in the Canary Islands



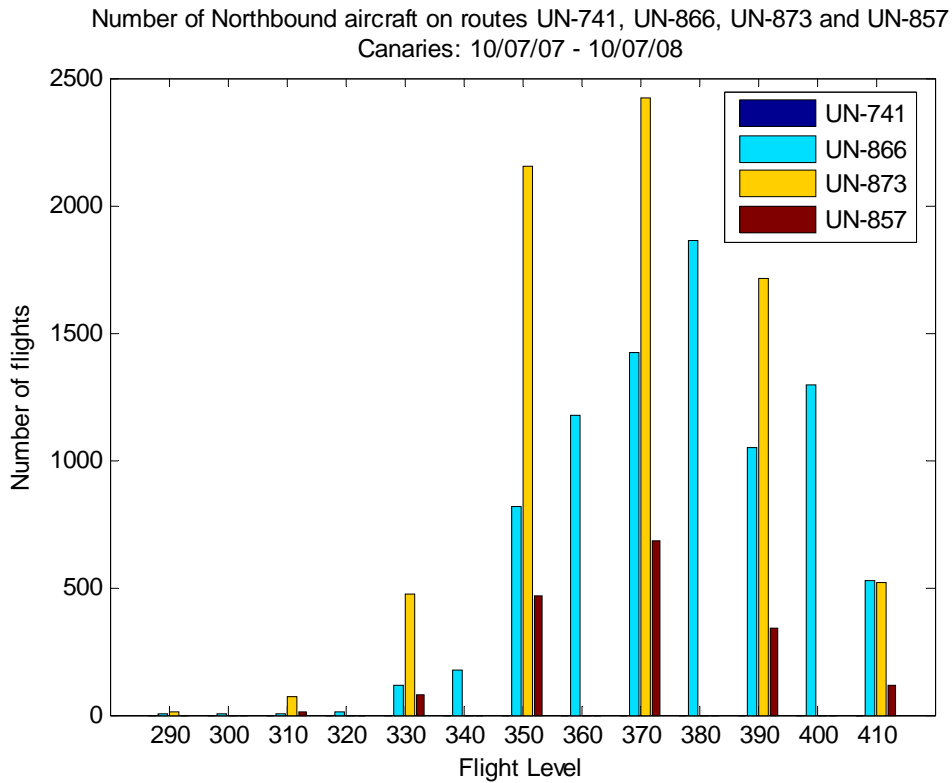


Figure 13
Number of Northbound aircraft on routes UN-741, UN-866, UN-873 and UN-857 in the Canaries

2.6. LOCATIONS FOR RISK ASSESSMENTS

For the studied scenario, lateral and vertical collision risks are assessed. This assessment is made in six different locations along the Corridor, covering the four UIRs. These locations are shown in Figure 14:

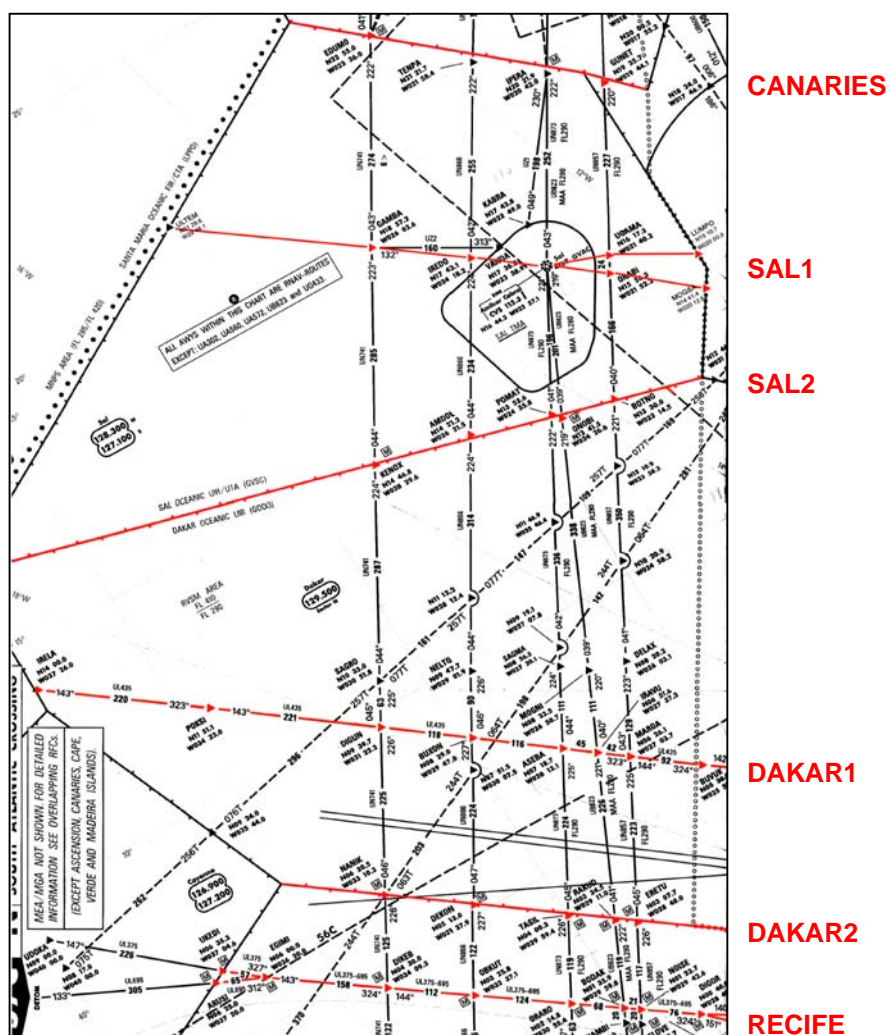


Figure 14
Locations for risk assessments

The locations are:

- Canaries: boundary between the Canaries UIR and the SAL OCEANIC UIR
- SAL1: Route UR-976/UA-602
- SAL2: Boundary between SAL OCEANIC UIR and DAKAR OCEANIC UIR
- DAKAR1: Route UL-435



- DAKAR2: Boundary between DAKAR OCEANIC UIR and ATLANTIC FIR
- RECIFE: Route UL-375/UL-695

Traffic data from 10th July 2007 to 10th July 2008 has been used to obtain collision risk in Canaries; whereas traffic data from 01st November 2007 to 31st January 2008 and 01st April 2008 to 30th June 2008 has been used for the rest of locations.

The risk associated to the Corridor will be the largest of the values obtained in all the locations.

3. LATERAL COLLISION RISK ASSESSMENT

3.1. REICH COLLISION RISK MODEL

As the four routes in the EUR/SAM Corridor are nearly parallel, it is possible to use the Reich Collision Risk Model to calculate lateral collision risk.

It models the lateral collision risk due to the loss of lateral separation between aircraft on adjacent parallel tracks flying at the same flight level.

The model reads as follows:

$$N_{ay} = P_y(S_y) \cdot P_z(0) \cdot \frac{\lambda_x}{S_x} \cdot \left\{ E_{y\text{ same}} \cdot \left[\frac{|\Delta \bar{v}|}{2 \cdot \lambda_x} + \frac{|\bar{y}|}{2 \cdot \lambda_y} + \frac{|\bar{z}|}{2 \cdot \lambda_z} \right] + E_{y\text{ opposite}} \cdot \left[\frac{2 \cdot |\bar{v}|}{2 \cdot \lambda_x} + \frac{|\bar{y}|}{2 \cdot \lambda_y} + \frac{|\bar{z}|}{2 \cdot \lambda_z} \right] \right\}$$

Equation 1



Where:

- N_{ay} is the expected number of accidents (two per each aircraft collision) per flight hour due to the loss of lateral separation between aircraft flying on tracks with nominal spacing S_y .
- S_y is the minimum standard lateral separation.
- $P_y(S_y)$ is the probability of lateral overlap of aircraft nominally flying on laterally adjacent paths at the same flight level.
- $P_z(0)$ is the probability of vertical overlap of aircraft nominally flying at the same flight level.
- E_{ysame} is the same direction lateral occupancy, i.e. the average number of same direction aircraft flying on laterally adjacent tracks at the same flight level within segments of length $2S_x$ centred on the typical aircraft.
- $E_{yopposite}$ is the opposite direction lateral occupancy, i.e. the average number of opposite direction aircraft flying on laterally adjacent tracks at the same flight level within segments of length $2S_x$ centred on the typical aircraft.
- S_x is the length of the longitudinal window used in the calculation of occupancies.
- λ_x is the average length of an aircraft.
- λ_y is the average width of an aircraft.
- λ_z is the average height of an aircraft.



- $|\overline{\Delta v}|$ is the average relative along-track speed of two aircraft flying at the same flight level in the same direction.
- $|\overline{v}|$ is the average ground speed of an aircraft.
- $|\overline{y}|$ is the average lateral cross-track speed between aircraft that have lost their lateral separation.
- $|\overline{z}|$ is the average relative vertical speed of aircraft flying at the same flight level.

A collision, and consequently two accidents, can only occur if there is overlap between two aircraft in all three dimensions simultaneously. Equation 1 gathers the product of the probabilities of losing separation in each one of the three dimensions.

As it has already been said, $P_z(0)$ is the probability of vertical overlap; $P_y(S_y)$, the probability of lateral overlap and the combinations $\frac{\lambda_x}{S_x} E_{ysame}$ and $\frac{\lambda_x}{S_x} E_{yopposite}$ relate to the probability of longitudinal overlap of aircraft on adjacent parallel tracks and at the same altitude.

All the probabilities can be interpreted as proportions of flight time in the airspace during which overlap in the pertinent dimension occurs.

As the collision risk is expressed as the expected number of accidents per flight hour, the joint overlap probability must be converted into number of events involving joint overlap in the three dimensions, relating overlap probability with passing frequency⁵. This is achieved by means of the expressions within square brackets in Equation 1. Each of the terms within square brackets represents the reciprocal of the average duration of an overlap in one of the

⁵ Passing frequency between two adjacent routes is the average number of events, per flight hour, in which two aircraft are in longitudinal overlap when travelling in the opposite or same direction at the same flight level

dimensions. For example, $\frac{|\Delta \bar{v}|}{2\lambda_x}$ is the reciprocal of the average duration of an overlap in the longitudinal direction for same direction traffic. In the case of longitudinal direction too, but for opposite direction, the average relative speed is $2v$ and the average overlap time is $\frac{2|\bar{v}|}{2\lambda_x}$.

The model is based on the following hypothesis:

- All tracks are parallel
- All collisions normally occur between aircraft on adjacent routes, although, if the probability of overlap is significantly large, they may also occur on non-adjacent routes.
- The entry times into the track system are uncorrelated.
- The lateral deviations of aircraft on adjacent tracks are uncorrelated.
- The lateral speed of an aircraft is not correlated with its lateral deviation.
- The aircraft are replaced by rectangular boxes.
- There is no corrective action by pilots or ATC when aircraft are about to collide.

The model also assumes that the nature of the events making up the lateral collision risk is completely random. This implies that any location within the system can be used to collect a representative data sample on the performance of the system.

In the following sections all the parameters that appear in Equation 1 will be analysed.

3.2. AVERAGE AIRCRAFT DIMENSIONS: $\lambda_x, \lambda_y, \lambda_z$

Table 1 shows the dimensions of the various aircraft types found in the Canarias UIR during the studied period of time. The average aircraft dimensions have been calculated using the dimensions of each aircraft type and the proportions of flights by type as weighting factors.

The results obtained in this way for the different locations are the ones shown in Table 2:

Location	Length (λ_x)		Wingspan (λ_y)		Height (λ_z)	
	Value (ft)	Value (NM)	Value (ft)	Value (NM)	Value (ft)	Value (NM)
Canaries	192.18	0.0316	180.13	0.0296	53.49	0.0088
SAL1	205.03	0.0337	192.82	0.0317	55.98	0.0092
SAL2	202.08	0.0333	189.45	0.0312	55.29	0.0091
Dakar1	202.10	0.0333	189.44	0.0312	55.30	0.0091
Dakar2	202.06	0.0332	189.41	0.0312	55.29	0.0091
Recife	202.10	0.0333	189.45	0.0312	55.30	0.0091

Table 2
Average aircraft dimensions

3.3. PROBABILITY OF VERTICAL OVERLAP: $P_z(0)$

The probability of vertical overlap of aircraft nominally flying at the same flight level of laterally adjacent flight paths is denoted by $P_z(0)$. It is defined by:

$$P_z(0) = \int_{-\lambda_z}^{\lambda_z} f^{z_{12}}(z) dz$$

Equation 2

where $f^{z_{12}}$ denotes the probability density of the vertical distance z_{12} between two aircraft with height deviations z_1 and z_2 nominally at the same flight level, i.e.

$$z_{12} = z_1 - z_2$$

Equation 3



and

$$f^{z_{12}} = \int_{-\infty}^{\infty} f^{TVE}(z_1) f^{TVE}(z_1 - z) dz_1$$

Equation 4

Equation 4 assumes that deviations of the two aircraft are independent and have the same probability density, $f^{TVE}(z_1)$. λ_z denotes the average aircraft height. Substitution of Equation 4 into Equation 2 gives:

$$P_z(0) = \int_{-\lambda_z}^{\lambda_z} \int_{-\infty}^{\infty} f^{TVE}(z_1) f^{TVE}(z_1 - z) dz_1 dz$$

Equation 5

This expression can be approximated by:

$$P_z(0) = 2\lambda_z \int_{-\infty}^{\infty} f^{TVE}(z_1) f^{TVE}(z_1) dz_1$$

Equation 6

Thus, the probability density $f^{TVE}(z_1)$ is needed to calculate $P_z(0)$. It should be taken from section 4.2.6.3 and $P_z(0)$ should be calculated by means of Equation 5. Nevertheless, the Eurocontrol RVSM Tool with which the value of $P_z(1000)$ has been obtained, (see 4.2.6) does not calculate this value.

However, as the $P_z(1000)$ obtained for this study ($P_z(1000)_{POST} = 4 \times 10^{-9}$) is similar, but slightly higher than the one obtained in the pre-implementation collision risk assessment ($P_z(1000)_{PRE} = 3.12 \times 10^{-9}$), the value of $P_z(0)$ will also be similar to the one calculated in the previous study ($P_z(0)_{PRE} = 0.4642$) and slightly smaller, as the average aircraft height is also the same. This number will also be smaller than the one obtained by ARINC in [Ref. 2]. Therefore, in order to be more conservative, the value used in this study has also been the one obtained by ARINC, $P_z(0) = 0.57$, as in the pre-implementation case.



3.4. AVERAGE GROUND SPEED: V

As data on cleared speeds were not provided, speeds and relative velocities have been estimated by comparing waypoint report times. To do this, the CRM program compares the time of waypoint crossing in two waypoints of the track, it calculates the difference between them and multiplies the inverse of this value by the distance that separates those waypoints. The result of this operation is the speed of each aircraft. The average speed, v , is then obtained as the mean value of the speeds of all the aircraft that flew on the four routes during the considered period of time.

As it was previously mentioned, Palestra database contains several errors. Some errors have been detected in some waypoint crossing times, what leads to extremely high speeds, even impossible in some cases.

As an example, Figure 15 shows speeds of the southbound aircraft that flew in the Canaries UIR, in the studied period of time, on route UN-873 and on route UN-857.

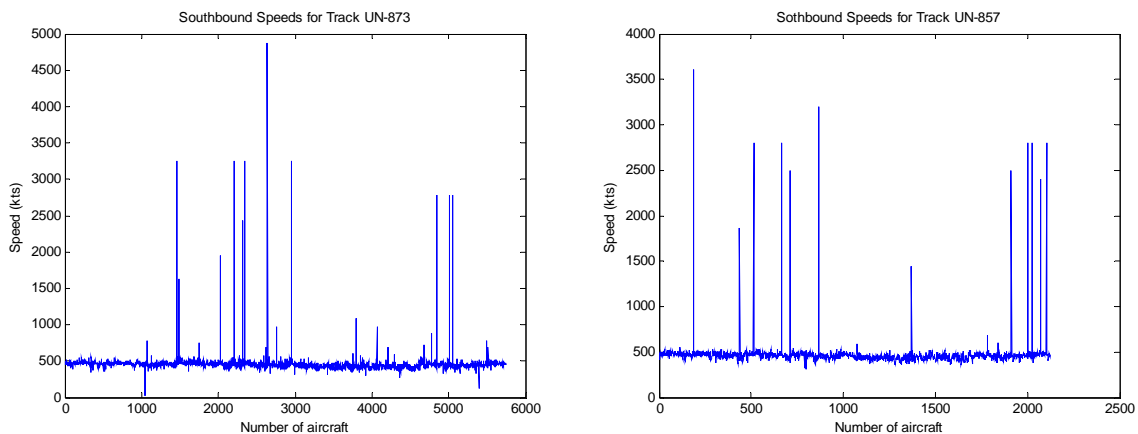


Figure 15
Speeds obtained from Palestra

For example, data from one of the flight plans corresponding to 6th July 2008, identified as the one corresponding to one of the peaks for southbound speeds on route UN-857, is shown here:



```

Indicativo Origen Destino HoraSacta HoraDespegue HoraArribada
IBE6843 LEMD SAEZ 06-07-08,01:43:09 - 06-07-08,10:59:09
TipoAeronave ReglasVuelo TipoVuelo Nacionalidad Estela VelCrucero NivelCrucero
Matricula
A346 I S I H 486 310
ECJLE
ActivadoTdr EquipoNCA ProcDesp ProcArr TrazaRadar
N RWYPDSSHIZ - - S
Hora Preactiv. ATOT IOBT UOBT CTOT
- - 05-07-08,23:25:00 05-07-08,23:45:00 -
TipoCreacionPV N°Aeronaves EstadoRVSM EstadoFrec833 EquipoSSR
FPL 1 Equipado Equipado S
Codigos SSR utilizados: 1
CodigoSSR Fecha
4522 06-07-08,00:48:08
Sectores atravesados : 2
Sector NivelEntrada HoraEntrada HoraSalida NivelEntrada
NivelSalida
NE S 06-07-08,01:43:09 06-07-08,02:07:00 330 340
SE S 06-07-08,02:07:00 06-07-08,02:37:09 340 340
Fijos sobrevolados : 6
Clase Fijo Cx Cy HoraETO NivelPaso TipoETO
1 TERTO 01243040 0300614N 06-07-08,01:43:09 330 TDR
1 LZR 01330360 0290958N 06-07-08,01:52:04 340 TDR
1 DEREV 01512410 0264323N 06-07-08,02:13:59 340 TDR
1 BIPET 01621290 0250002N 06-07-08,02:29:04 340 TDR
1 ETIBA 01840420 0212019N 06-07-08,02:36:39 340 TDR
1 GUNET 01944030 0193544N 06-07-08,02:37:09 340 TDR
Ruta Calculada:
** TERTO/N0486F330 LZR/N0486F340 DEREV BIPET ETIBA GUNET/N0486F340 **
Segmentos atravesados : 1
EstadoTLPV Centro HoraEntrada HoraSalida
PrimerSector UltimoSector PrimerFijo UltimoFijo
Espera terminado ACC_CANARIAS 06-07-08,01:43:09 06-07-08,02:37:09 NE
SE TERTO GUNET
Firs atravesados : 3
Fir HoraEntrada HoraSalida
ACC_CANARIAS 06-07-08,01:43:09 06-07-08,02:37:09
FIR_CANARIAS 06-07-08,01:43:09 06-07-08,02:37:09
FIR_ESPAÑA 06-07-08,01:43:09 06-07-08,02:37:09
    
```

According to the flight plan, the distance between BIPET and GUNET has been flown in just 8'05'', what leads to such a high speed (2800kts).

The CRM software tries to correct this problem, limiting the maximum speed. This maximum speed has been fixed in 575 kts. This value is still too high, but it has been taken since it corrects those values that were excessively high and it considers possible anomalous cases in which, because of the characteristics of the aircraft and the existing wind, speeds higher than the habitual ones could be reached. Nevertheless, in this case, a lower limitation has been used, since the maximum speed considered in the creation of the extrapolated flight plans, which are the input for CRM, was 520 kts.



With this limitation, the speed of each aircraft that flew during the analysed period of time on each route in the Canarias UIR is shown in the following graphs:

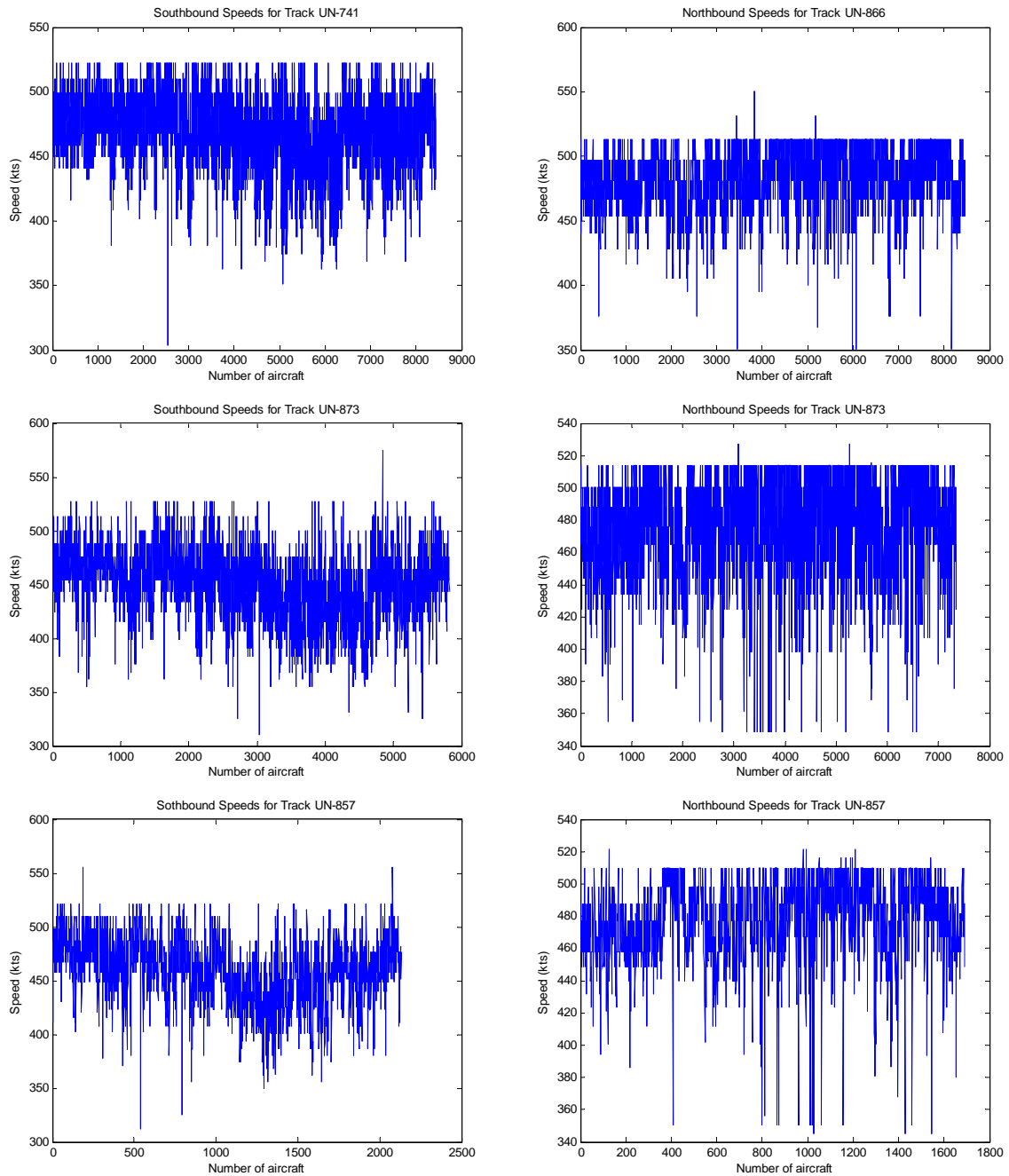


Figure 16
Speeds limited to 575kts in the current scenario in the Canarias

Similar graphs can be obtained for the rest of locations.



From these speeds, the average ground speed obtained in the different locations is shown in Table 3:

Location	Average Speeds		
	Southbound (kts)	Northbound (kts)	Average (kts)
Canaries	457	480	469
SAL1	459	474	466
SAL2	451	491	471
Dakar1	457	482	470
Dakar2	462	494	478
Recife	456	497	476

Table 3
Average speeds

3.5. AVERAGE RELATIVE LONGITUDINAL SPEED: Δv

Δv denotes the average relative longitudinal speed between aircraft flying in the same direction, since it has already been pointed out that in the case of aircraft flying in opposite directions, the average relative longitudinal speed is $2v$.

The relative longitudinal speed has been obtained from the differences between the speeds of all the pairs of aircraft that constitute a proximate pair⁶ in the same direction. The average relative speed is the mean value of all the calculated differences.

The results obtained for the current scenario can be seen in Table 4. The value considered in the collision risk assessment is the one shown in the last column of the tables, slightly higher than the value obtained, in order to be conservative:

⁶ Lateral proximate pair.- It is defined as an event in which one aircraft on one track passes another aircraft on an adjacent track at the same level and within a longitudinal distance $2S_x$ ($2T_0$ if it is expressed in time).

Location	Average relative longitudinal speeds			
	Southbound (kts)	Northbound (kts)	Average (kts)	Conservative value considered (kts)
Canaries	20.9	19.1	20.0	21
SAL1	42.1	42.0	42.0	42
SAL2	18.8	20.6	19.7	21
Dakar1	14.8	24.5	19.7	21
Dakar2	15.5	35.9	25.7	26
Recife	23.7	37.1	30.4	31

Table 4
Average relative longitudinal speed

3.6. AVERAGE RELATIVE LATERAL SPEED: $\overline{|\dot{y}|}$

$|\dot{y}|$ is the average relative lateral cross-track speed between aircraft, flying on adjacent routes at the same flight level, that have lost their lateral separation.

The estimation of this parameter generally involves the extrapolation of radar data, speeds and lateral deviations, but such radar data were not available for the current report.

In the study made by ARINC ([Ref. 2]) this value was considered to be $|\overline{\dot{y}}| = 42kts$, which corresponds to a deviation angle of approximately 5° at an average ground speed of 475-480kts. Although, for example in the North Atlantic (NAT) the value considered was $|\overline{\dot{y}}| = 80kts$, ARINC thought that this value was too conservative for the SAT. Occurrence of waypoint insertion errors and other types of operational errors in the SAT is quite limited, because routes are defined by predetermined fixes, not being necessary to tell their coordinates, which can be misunderstood, but simply its name. ARINC took this into consideration to reduce the value of $|\overline{\dot{y}}|$.

In this study, the value considered has also been $|\overline{\dot{y}}| = 42kts$.



3.7. AVERAGE RELATIVE VERTICAL SPEED: \bar{z}

$|\bar{z}|$ denotes the average modulus of the relative vertical speed between a pair of aircraft on the same flight level of adjacent tracks that has lost lateral separation. It is generally assumed that $|\bar{z}|$ is independent of the size of the lateral separation between the aircraft and, for aircraft in level flight, it can also be considered that there is no dependency of $|\bar{z}|$ with the vertical separation between the aircraft.

Data about $|\bar{z}|$ are relatively scarce. Nevertheless, in the study made by ARINC ([Ref. 2]), it was mentioned that data from the NAT showed that $|\bar{z}|$ was of the order of 1kt. From that, ARINC took $|\bar{z}| = 1.5kts$, slightly more conservative. This value has also been considered in this case.

3.8. LATERAL OVERLAP PROBABILITY: $P_Y(S_Y)$

The probability of lateral overlap of aircraft nominally flying on adjacent flight paths, separated by S_y , is denoted by $P_y(S_y)$ and it is defined by:

$$P_y(S_y) = \int_{-\lambda_y}^{\lambda_y} f^{y_{12}}(y) dy$$

Equation 7

Where $f^{y_{12}}$ denotes the probability density of the lateral distance y_{12} between two aircraft with lateral deviations y_1 and y_2 , nominally separated by S_y , i.e.

$$y_{12} = S_y + y_1 - y_2$$

Equation 8



and

$$f^{y_{12}}(y) = \int_{-\infty}^{\infty} f^y(y_1) f^y(S_y + y_1 - y) dy_1$$

Equation 9

Equation 9 assumes that the lateral deviations of the two aircraft are independent and have the same probability density, $f^y(y_1)$. λ_y denotes the average aircraft width. Substitution of Equation 9 into Equation 7 gives:

$$P_y(S_y) = \int_{-\lambda_y}^{\lambda_y} \int_{-\infty}^{\infty} f^y(y_1) f^y(S_y + y_1 - y) dy_1 dy$$

Equation 10

This last equation can be approximated by:

$$P_y(S_y) \approx 2\lambda_y \int_{-\infty}^{\infty} f^y(y_1) f^y(S_y + y_1) dy_1$$

Equation 11

The probability density function $f^y(y_1)$ depends on the nominal and non-nominal navigation capabilities of the aircraft. Nominal navigation performance takes into account typical lateral deviations that arise from ordinary navigational uncertainties when systems are working properly, whilst non-nominal performance represents atypical errors that occur infrequently and that would likely arise from pilot or controller mistakes, or from equipment malfunctions. These atypical errors play an important role in the collision risk, since they may cause large deviations.

The different types of lateral navigation errors are classified as follows according to [Ref. 3]:



Type of error	Description
A	Committed by aircraft not certified for operation in the RNP airspace
B	ATC system loop error
C1	Equipment control error including inadvertent waypoint error
C2	Waypoint insertion error due to the correct entry of incorrect position
D	Other with failure notified to ATC in time for action
E	Other with failure notified to ATC too late for action
F	Other with failure notified/receive by ATC
G	Lateral deviations due to weather when unable to obtain prior ATC clearance

Table 5
Lateral navigation error types

If data of the occurrence of each of these types of errors were available, it would be possible to model the probability density function of the lateral deviations associated to each individual type and to obtain a global distribution by taking a weighted mixture of the individual deviation distributions. The weighting factors would be determined by the frequencies with which the different types of errors occur.

This information was not available for this study. Therefore, to model the probability density function of Equation 11 it is assumed that all lateral errors or deviations follow the same probability distribution. This distribution may then be determined on the basis of a sample of data describing lateral deviations of aircraft from their tracks. It is usually modelled as a mixture of two distributions. These two distributions are:

- The core distribution, which represents errors that derive from standard navigation system deviations. These errors are always present, as navigation systems are not perfect and they have a certain precision.
- The tail distribution, which represents gross navigation errors (GNE), that corresponds to what has been denominated before as non-nominal performance.

It should also be noted that not all atypical errors are large in magnitude and that in most cases it is impossible to determine with certainty if a given observed lateral error arose from the core or from the tail term of the distribution.

Therefore, the overall probability density of lateral navigation errors can be written as:

$$f_y(y_1) = (1 - \alpha) \times f_1(y_1) + \alpha \times f_2(y_1)$$

Equation 12

where:

- $f_1(y_1)$ represents the probability density function that models navigation errors arising from typical deviations of the aircraft navigation systems.
- $f_2(y_1)$ represents the probability density function that models lateral navigation errors due to equipment failures, human errors and other atypical errors.
- α represents the percentage of aircraft that experience such anomalies, whose distribution of lateral deviations is $f_2(y_1)$.
- $(1-\alpha)$ represents the percentage of aircraft that do not experience such anomalies in their lateral deviations.

To make the tail distribution conservative, the tail distribution is often taken as a double exponential distribution, because of its thick tail.

ARINC, [Ref. 2], also considered a zero mean double exponential distribution for the core term as in the North Pacific collision risk analysis.

The same distribution is used in this study. So,



$$f_1(y_1) = \frac{1}{2a_1} \exp\left(-\frac{|y_1|}{a_1}\right)$$

Equation 13

$$f_2(y_1) = \frac{1}{2a_2} \exp\left(-\frac{|y_1|}{a_2}\right)$$

Equation 14

Substituting Equation 13 and Equation 14 in Equation 12:

$$f_y(y_1) = (1 - \alpha) \frac{1}{2a_1} \exp\left(-\frac{|y_1|}{a_1}\right) + \alpha \frac{1}{2a_2} \exp\left(-\frac{|y_1|}{a_2}\right)$$

Equation 15

The parameter a_1 is determined by the RNP value, since this value indicates that 95% of the deviations are under that value. So, a_1 is obtained solving the following integral:

$$\int_{-RNP}^{RNP} f_1(y_1) dy_1 = 0.95$$

Equation 16

The value for a_1 is then:

$$a_1 = -\frac{RNP}{\log 0.05}$$

Equation 17

Using Equation 17:

$$a_1 = 3.338 \text{ NM} \quad (RNP10)$$

As far as the value of a_2 is concerned, in [Ref. 4] it is pointed out that, for a given value of α , $P_y(S_y)$ is maximized taking $a_2 = S_y$. In this case, the minimum separation between tracks is $S_y = 50\text{NM}$, and therefore, $a_2 = 50\text{NM}$.



Knowing a_2 , it is possible to obtain the lateral deviations interval within which the aircraft would be with a 95% probability. To do it, the integral of the probability density function is calculated in the unknown interval. The result is a relation between the known parameter a_2 and the maximum unknown lateral deviation that define the 95% interval.

$$\int_{-x}^x f_2(y_1) dy_1 = 0.95 \quad \Rightarrow \quad a_2 = -\frac{x}{\log 0.05}$$

Equation 18

Thus, taking $a_2 = 50NM$, 95% of the lateral deviations will be within the interval $[-150,150]$ NM.

The remaining parameter to be fixed in order to define the probability density function completely is α .

This parameter may be interpreted as the probability of an individual aircraft experiencing an anomaly resulting in its distribution of lateral deviations having the scale factor a_2 , instead of a_1 , or as the proportion of aircraft experiencing anomalies in their lateral navigation performance.

A derivation for the estimate of the weighting factor α used in the study made by ARINC can be found in Appendix A of the cited study ([Ref. 2]). Assuming that one aircraft experiencing a lateral navigation anomaly has been observed, ARINC obtained the value of α from:

$$\alpha = 1 - 0.05^{1/n}$$

Equation 19

where n is the annual number of flights, being $n = 22255$ in that study.

With all that, the obtained value was $\alpha = 1.346 \times 10^{-4}$. The above mentioned Appendix can be consulted for a detailed explanation of its derivation.



In this case, there is no evidence either of any anomalies leading to large navigation errors. Therefore, the same hypothesis of having one large error in the analysed period could be used and the parameter α is obtained using Equation 19, being n the number of aircraft detected in the studied period of time.

Of the six different locations where risk is computed, the least number of aircraft in the time period studied (July 07-July 08), 28475, is obtained in SAL1. This value will be used to obtain the parameter α in all the UIRs, what will be conservative. Thus, $n = 28475$ and $\alpha = 1.0520 \times 10^{-4}$.

Once the parameters a_1 , a_2 and α are defined, the probability density function of the lateral navigation errors is completely modelled.

Using Equation 11, the lateral overlap probability obtained for the different lateral separations between routes existing in the Corridor are the following ones:

RNP10 S_{ymin}=50NM $\alpha=1.0520*10^{-4}$	Py(50)	Py(90)	Py(110)	Py(140)
Canaries	$6.8262*10^{-8}$	$2.0712*10^{-8}$	$1.3884*10^{-8}$	$7.6197*10^{-9}$
SAL1	$7.3074*10^{-8}$	$2.2172*10^{-8}$	$1.4862*10^{-8}$	$8.1568*10^{-9}$
SAL2	$7.1796*10^{-8}$	$2.1785*10^{-8}$	$1.4603*10^{-8}$	$8.0142*10^{-9}$
Dakar1	$7.1792*10^{-8}$	$2.1783*10^{-8}$	$1.4602*10^{-8}$	$8.0138*10^{-9}$
Dakar2	$7.1781*10^{-8}$	$2.1780*10^{-8}$	$1.4599*10^{-8}$	$8.0124*10^{-9}$
Recife	$7.1795*10^{-8}$	$2.1784*10^{-8}$	$1.4602*10^{-8}$	$8.0140*10^{-9}$

Table 6
Lateral overlap probability for different separations between routes with RNP10

The probability increases when the spacing between the routes decreases, as it was expected.

3.9. LATERAL OCCUPANCY

In Equation 1 there are two occupancy terms, one for same direction occupancy and another one for opposite direction occupancy.

Same direction occupancy is defined as the average number of aircraft that are, in relation to the typical aircraft:

- flying in the same direction as it;
- nominally flying on tracks one lateral separation standard away;
- nominally at the same flight level as it; and
- within a longitudinal segment centred on it.

The above definition has been expanded to include tracks that are separated by more than one lateral separation standard because there is a significant collision risk arising from the probability of overlap between non adjacent tracks.

The length of the longitudinal segment, $2S_x$, is usually considered to be the length equivalent to 20 minutes of flight at 480kts. It has been verified that the relationship between S_x and the occupancy is quite linear.

A similar set of criteria can be used to define opposite direction occupancy, just replacing “flying in the same direction as it” by “flying in the opposite direction”.

Occupancy, in general, relates to the longitudinal overlap probability and can be obtained from:

$$E_y = \frac{2T_y}{H}$$

Equation 20



Where:

- T_y represents the total proximity time generated in the system.
- H represents the total number of flight hours generated in the system during the considered period of time.

In Equation 20, the factor 2 allows the conversion of number of collisions into number of accidents.

Two methods can be used to calculate occupancies: “steady state flow model” and “direct estimation from time at waypoint passing”. In this study the method used has been the second one.

This method calculates the number of proximate pairs comparing the time at which aircraft on one route pass a waypoint with the time at which aircraft on a parallel route pass the homologous waypoint. When the difference between passing times is less than certain value, 10 minutes in this case, it is considered that there is a proximate pair in that pair of routes.

Then, occupancy can be calculated using the following expression:

$$E_y = \frac{2n_y}{n}$$

Equation 21

Where n_y is the number of proximate pairs and n is the total number of aircraft.

A more detailed explanation of each method can be found in Annex 1.

As lateral overlap probability depends on lateral spacing between routes and, as it has been said in section 2, routes in the EUR/SAM Corridor are not equally spaced, the terms $P_y(S_y)E_{y\text{same}}$ and $P_y(S_y)E_{y\text{opposite}}$ in Equation 1 must be split into several terms.



It can be seen in Table 6 that $P_y(90)$ is about 30% of $P_y(50)$, $P_y(110)$ is about 20% of $P_y(50)$ and $P_y(140)$ is about 11% of $P_y(50)$. So, their contributions to the lateral collision risk cannot be ignored and Equation 1, should be written as follows:

$$N_{ay} = \left\{ P_y(50) \cdot E_{y_{same}} + P_y(90) \cdot E_{y_{same}}^* + P_y(140) \cdot E_{y_{same}}^{**} \right\} \cdot P_z(0) \cdot \frac{\lambda_x}{S_x} \left\{ \frac{|\Delta \bar{v}|}{2\lambda_x} + \frac{|\bar{y}|}{2\lambda_y} + \frac{|\bar{z}|}{2\lambda_z} \right\} +$$

$$\left\{ P_y(90) \cdot E_{y_{opposite}} + P_y(110) \cdot E_{y_{opposite}}^* + P_y(140) \cdot E_{y_{opposite}}^{**} \right\} \cdot P_z(0) \cdot \frac{\lambda_x}{S_x} \left\{ \frac{2|\bar{v}|}{2\lambda_x} + \frac{|\bar{y}|}{2\lambda_y} + \frac{|\bar{z}|}{2\lambda_z} \right\}$$

Equation 22

Where $E_{y_{same}}$ denotes same direction occupancy for routes UN-873/UN-857; $E_{y_{same}}^*$, same direction occupancy for routes UN-866/UN-873 and $E_{y_{same}}^{**}$, same direction occupancy for routes UN-866/UN-857; $E_{y_{opposite}}$, opposite direction occupancy for routes UN-866/UN-873; $E_{y_{opposite}}^*$, opposite direction occupancy for routes UN-741/UN-866 and $E_{y_{opposite}}^{**}$, opposite direction occupancy for routes UN-866/UN-857.

Therefore, three same occupancy values and three opposite direction occupancy values must be computed.

3.9.1. Traffic growth hypothesis

This study presents the collision risk calculated from data corresponding from July 2007 to July 2008, but it also presents an estimate of the collision risk over a 10 years horizon.

To do that, it is necessary to know which is the traffic forecast for that period of time in the studied airspace. Taking into account the data given by STATFOR-EUROCONTROL for the high-growth scenario, [Ref. 14], the annual traffic growth rate for the traffic flows in the South Atlantic airspace would be 7.7%. Thus, an annual traffic growth rate of 8% is considered in this analysis.



3.9.2. Lateral occupancy values obtained

This section presents the same direction and opposite direction lateral occupancy values provided by the CRM programme for the current time and an estimate of the occupancy until 2018, with the annual traffic growth rate indicated before, 8%.

3.9.2.1. Canaries

Table 7 shows the number of aircraft and the number of same and opposite direction proximate pairs detected on the four routes from 10th July 2007 till 10th July 2008, in the Canaries UIR.

The number of aircraft detected on route RANDOM is also indicated in this table, although they have not been considered in the collision risk estimation.

Number of flights on UN-741	8439
Number of flights on UN-866	8461
Number of flights on UN-873	13174
Number of flights on UN-857	3822
Total number of flights (excluding flights on route RANDOM)	33896
Number of flights on route RANDOM (South-North)	64
Number of aircraft on route RANDOM (North-South)	860
Number of same direction proximate pairs for tracks UN-866/UN-873	587
Number of same direction proximate pairs for tracks UN-873/UN-857	421
Number of same direction proximate pairs for tracks UN-866/UN-857	115
Number of opposite direction proximate pairs for tracks UN-741/UN-866	294
Number of opposite direction proximate pairs for tracks UN-866/UN-873	131
Number of opposite direction proximate pairs for tracks UN-866/UN-857	59

Table 7
Lateral occupancy parameters in the Canaries UIR

From these data, the occupancies obtained, based on traffic levels representative of 2008, are the ones shown in Table 8:



Lateral occupancies in 2008	
Same direction lateral occupancy for tracks UN-873/UN-857 (E_{ysame})	0.0248
Same direction lateral occupancy for tracks UN-866/UN-873 (E_{ysame}^*)	0.0346
Same direction lateral occupancy for tracks UN-866/UN-857 (E_{ysame}^{**})	0.0068
Opposite direction lateral occupancy for tracks UN-866/UN-873 ($E_{yopposite}$)	0.0077
Opposite direction lateral occupancy for tracks UN-741/UN-866 ($E_{yopposite}^*$)	0.0173
Opposite direction lateral occupancy for tracks UN-866/UN-857 ($E_{yopposite}^{**}$)	0.0035

Table 8
Lateral occupancies in the Canaries UIR, in 2008

Assuming an annual traffic growth rate of 8%, the occupancies for the next 10 years are summarized in Table 9. It holds that occupancy is approximately proportional to traffic flow rate:

8% annual traffic growth		2008	2010	2012	2014	2016	2018
Same direction lateral occupancy	UN-873/UN-857 (E_{ysame})	0.0248	0.0290	0.0338	0.0394	0.0460	0.0536
	UN-866/UN-873 (E_{ysame}^*)	0.0346	0.0404	0.0471	0.0550	0.0641	0.0748
	UN-866/UN-857 (E_{ysame}^{**})	0.0068	0.0079	0.0092	0.0108	0.0126	0.0146
Opposite direction lateral occupancy	UN-866/UN-873 ($E_{yopposite}$)	0.0077	0.0090	0.0105	0.0123	0.0143	0.0167
	UN-741/UN-866 ($E_{yopposite}^*$)	0.0173	0.0202	0.0236	0.0275	0.0321	0.0375
	UN-866/UN-857 ($E_{yopposite}^{**}$)	0.0035	0.0041	0.0047	0.0055	0.0064	0.0075

Table 9
Lateral occupancy estimate for the Canaries until 2018 with an annual traffic growth rate of 8%



3.9.2.2. SAL1

Table 10 shows the number of aircraft and the number of same and opposite direction proximate pairs detected on the four routes from 1st November 2007 till 31st January 2008 and from 1st April till 30th June 2008. Occupancies obtained from these data will be representative for year 2008.

Number of flights on UN-741	4144
Number of flights on UN-866	4155
Number of flights on UN-873	4179
Number of flights on UN-857	1727
Total number of flights (excluding flights on route RANDOM)	14205
Number of same direction proximate pairs for tracks UN-866/UN-873	304
Number of same direction proximate pairs for tracks UN-873/UN-857	68
Number of same direction proximate pairs for tracks UN-866/UN-857	33
Number of opposite direction proximate pairs for tracks UN-741/UN-866	158
Number of opposite direction proximate pairs for tracks UN-866/UN-873	21
Number of opposite direction proximate pairs for tracks UN-866/UN-857	16

Table 10
Lateral occupancy parameters in SAL1

From these data, and assuming an annual traffic growth rate of 8%, the occupancies for the next 10 years are summarized in Table 11. It holds that occupancy is approximately proportional to traffic flow rate:



8% annual traffic growth		2008	2010	2012	2014	2016	2018
Same direction lateral occupancy	UN-873/UN-857 (E_{ysame})	0.0096	0.0112	0.0130	0.0152	0.0177	0.0207
	UN-866/UN-873 (E_{ysame}^*)	0.0428	0.0499	0.0582	0.0679	0.0792	0.0924
	UN-866/UN-857 (E_{ysame}^{**})	0.0046	0.0054	0.0063	0.0074	0.0086	0.0100
Opposite direction lateral occupancy	UN-866/UN-873 ($E_{yopposite}$)	0.0030	0.0034	0.0040	0.0047	0.0055	0.0064
	UN-741/UN-866 ($E_{yopposite}^*$)	0.0222	0.0259	0.0303	0.0353	0.0412	0.0480
	UN-866/UN-857 ($E_{yopposite}^{**}$)	0.0023	0.0026	0.0031	0.0036	0.0042	0.0049

Table 11
Lateral occupancy estimate for SAL1 until 2018 with an 8% annual traffic growth rate

3.9.2.3. SAL2

Table 12 presents the number of aircraft and the number of same and opposite direction proximate pairs detected on the four routes from 1st November 2007 till 31st January 2008 and from 1st April till 30th June 2008.

Number of flights on UN-741	4319
Number of flights on UN-866	4169
Number of flights on UN-873	4654
Number of flights on UN-857	1757
Total number of flights (excluding flights on route RANDOM)	14899
Number of same direction proximate pairs for tracks UN-866/UN-873	288
Number of same direction proximate pairs for tracks UN-873/UN-857	119
Number of same direction proximate pairs for tracks UN-866/UN-857	56
Number of opposite direction proximate pairs for tracks UN-741/UN-866	228
Number of opposite direction proximate pairs for tracks UN-866/UN-873	26
Number of opposite direction proximate pairs for tracks UN-866/UN-857	24

Table 12
Lateral occupancy parameters in SAL2



From these data, and assuming an annual traffic growth rate of 8%, the occupancies for the next 10 years are shown in Table 13. It holds that occupancy is approximately proportional to traffic flow rate:

8% annual traffic growth		2008	2010	2012	2014	2016	2018
Same direction lateral occupancy	UN-873/UN-857 (E_{ysame})	0.0160	0.0186	0.0217	0.0253	0.0296	0.0345
	UN-866/UN-873 (E_{ysame}^*)	0.0387	0.0451	0.0526	0.0613	0.0716	0.0835
	UN-866/UN-857 (E_{ysame}^{**})	0.0075	0.0088	0.0102	0.0119	0.0139	0.0162
Opposite direction lateral occupancy	UN-866/UN-873 ($E_{yopposite}$)	0.0035	0.0041	0.0047	0.0055	0.0065	0.0075
	UN-741/UN-866 ($E_{yopposite}^*$)	0.0306	0.0357	0.0416	0.0486	0.0567	0.0661
	UN-866/UN-857 ($E_{yopposite}^{**}$)	0.0032	0.0038	0.0044	0.0051	0.0060	0.0070

Table 13
Lateral occupancy estimate for SAL2 until 2018 with an 8% annual traffic growth rate

3.9.2.4. Dakar1

Table 14 shows the number of aircraft and the number of same and opposite direction proximate pairs detected on the four routes from 1st November 2007 till 31st January 2008 and from 1st April till 30th June 2008 in Dakar1 location.

Number of flights on UN-741	4302
Number of flights on UN-866	4171
Number of flights on UN-873	4650
Number of flights on UN-857	1759
Total number of flights (excluding flights on route RANDOM)	14882
Number of same direction proximate pairs for tracks UN-866/UN-873	326
Number of same direction proximate pairs for tracks UN-873/UN-857	135
Number of same direction proximate pairs for tracks UN-866/UN-857	63
Number of opposite direction proximate pairs for tracks UN-741/UN-866	127
Number of opposite direction proximate pairs for tracks UN-866/UN-873	27
Number of opposite direction proximate pairs for tracks UN-866/UN-857	42

Table 14
Lateral occupancy parameters in Dakar1

Assuming an annual traffic growth rate of 8%, the occupancies for the next 10 years are summarized in Table 15. It holds that occupancy is approximately proportional to traffic flow rate:

8% annual traffic growth		2008	2010	2012	2014	2016	2018
Same direction lateral occupancy	UN-873/UN-857 (E_{ysame})	0.0181	0.0212	0.0247	0.0288	0.0336	0.03917
	UN-866/UN-873 (E_{ysame}^*)	0.0438	0.0511	0.0596	0.0695	0.0811	0.0946
	UN-866/UN-857 (E_{ysame}^{**})	0.0085	0.0099	0.0115	0.0134	0.0157	0.0183
Opposite direction lateral occupancy	UN-866/UN-873 ($E_{yopposite}$)	0.0036	0.0042	0.0049	0.0056	0.0067	0.0078
	UN-741/UN-866 ($E_{yopposite}^*$)	0.0171	0.0199	0.0232	0.0271	0.0316	0.0368
	UN-866/UN-857 ($E_{yopposite}^{**}$)	0.0056	0.0066	0.0077	0.0090	0.0104	0.0122

Table 15
Lateral occupancy estimate for Dakar1 until 2018 with an 8% annual traffic growth rate



3.9.2.5. Dakar2

Table 16 shows the number of aircraft and the number of same and opposite direction proximate pairs detected on the four routes from 1st November 2007 till 31st January 2008 and from 1st April till 30th June 2008.

Number of flights on UN-741	4302
Number of flights on UN-866	4178
Number of flights on UN-873	4645
Number of flights on UN-857	1760
Total number of flights (excluding flights on route RANDOM)	14885
Number of same direction proximate pairs for tracks UN-866/UN-873	328
Number of same direction proximate pairs for tracks UN-873/UN-857	138
Number of same direction proximate pairs for tracks UN-866/UN-857	61
Number of opposite direction proximate pairs for tracks UN-741/UN-866	103
Number of opposite direction proximate pairs for tracks UN-866/UN-873	17
Number of opposite direction proximate pairs for tracks UN-866/UN-857	34

Table 16
Lateral occupancy parameters in Dakar2

Considering an annual traffic growth rate of 8%, the occupancies for the next 10 years are can be seen in Table 17. It holds that occupancy is approximately proportional to traffic flow rate:



8% annual traffic growth		2008	2010	2012	2014	2016	2018
Same direction lateral occupancy	UN-873/UN-857 (E_{ysame})	0.0185	0.0216	0.0252	0.0294	0.0343	0.0400
	UN-866/UN-873 (E_{ysame}^*)	0.0441	0.0514	0.0600	0.0699	0.0816	0.0951
	UN-866/UN-857 (E_{ysame}^{**})	0.0082	0.0096	0.0112	0.0130	0.0152	0.0177
Opposite direction lateral occupancy	UN-866/UN-873 ($E_{yopposite}$)	0.0023	0.0027	0.0031	0.0036	0.0042	0.0049
	UN-741/UN-866 ($E_{yopposite}^*$)	0.0138	0.0161	0.0188	0.0220	0.0256	0.0299
	UN-866/UN-857 ($E_{yopposite}^{**}$)	0.0046	0.0053	0.0062	0.0072	0.0085	0.0099

Table 17
Lateral occupancy estimate for Dakar2 until 2018 with an 8% annual traffic growth rate

3.9.2.6. Recife

Table 18 shows the number of aircraft and the number of same and opposite direction proximate pairs detected on the four routes from 1st November 2007 till 31st January 2008 and from 1st April till 30th June 2008.

Number of flights on UN-741	4302
Number of flights on UN-866	4178
Number of flights on UN-873	4640
Number of flights on UN-857	1759
Total number of flights (excluding flights on route RANDOM)	14879
Number of same direction proximate pairs for tracks UN-866/UN-873	331
Number of same direction proximate pairs for tracks UN-873/UN-857	138
Number of same direction proximate pairs for tracks UN-866/UN-857	61
Number of opposite direction proximate pairs for tracks UN-741/UN-866	105
Number of opposite direction proximate pairs for tracks UN-866/UN-873	18
Number of opposite direction proximate pairs for tracks UN-866/UN-857	24

Table 18
Lateral occupancy parameters in Recife



From these data, and assuming an annual traffic growth rate of 8%, the occupancies for the next 10 years are presented in Table 19. It holds that occupancy is approximately proportional to traffic flow rate:

8% annual traffic growth		2008	2010	2012	2014	2016	2018
Same direction lateral occupancy	UN-873/UN-857 (E_{ysame})	0.0186	0.0216	0.0252	0.0294	0.0343	0.0400
	UN-866/UN-873 (E_{ysame}^*)	0.0445	0.05190	0.0605	0.0706	0.0824	0.0961
	UN-866/UN-857 (E_{ysame}^{**})	0.0082	0.0096	0.0112	0.0130	0.0152	0.0177
Opposite direction lateral occupancy	UN-866/UN-873 ($E_{yopposite}$)	0.0024	0.0028	0.0033	0.0038	0.0045	0.0052
	UN-741/UN-866 ($E_{yopposite}^*$)	0.0141	0.0165	0.0192	0.0224	0.0261	0.0305
	UN-866/UN-857 ($E_{yopposite}^{**}$)	0.0032	0.00376	0.0044	0.0051	0.0060	0.0070

Table 19
Lateral occupancy estimate for Recife until 2018 with an 8% annual traffic growth rate

3.10. LATERAL COLLISION RISK

Once all the parameters of Equation 22 are obtained, it is possible to calculate the lateral collision risk for the current scenario. This value must not exceed the maximum allowed, for which the system is considered to be safe. This threshold, denominated TLS (Target Level of Safety), has been set to $TLS = 5 \times 10^{-9}$. It means that 5×10^{-9} accidents per flight hour are accepted.

3.10.1. Lateral collision risk values obtained

In the current system, with RNP10, two routes unidirectional and two routes bidirectional, the collision risk values obtained until 2018 in the different locations are the ones shown in the following sections.



3.10.1.1. Canaries

Lateral collision risk in Canaries location, assuming an annual traffic growth rate of 8%, is shown in Table 20 and Figure 17:

Lateral Collision Risk	8% annual traffic growth
2008	2.1289×10^{-9}
2009	2.2992×10^{-9}
2010	2.4831×10^{-9}
2011	2.6818×10^{-9}
2012	2.8963×10^{-9}
2013	3.1280×10^{-9}
2014	3.3782×10^{-9}
2015	3.6485×10^{-9}
2016	3.9404×10^{-9}
2017	4.2556×10^{-9}
2018	4.5961×10^{-9}

Table 20
Lateral collision risk for the period 2008-2018 in Canaries

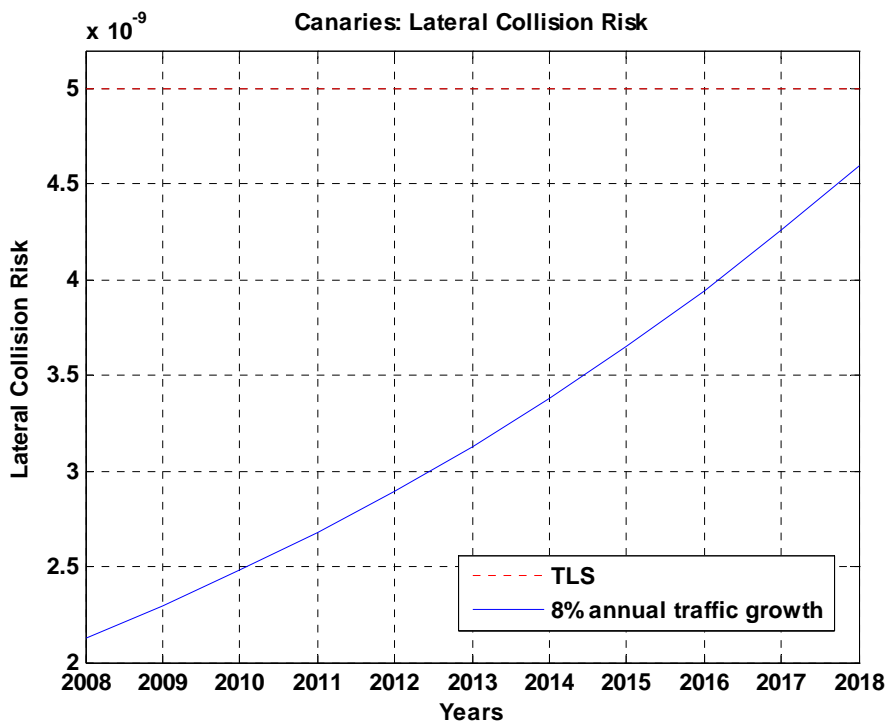


Figure 17
Lateral collision risk for the period 2008-2018 in Canaries



3.10.1.2. SAL1

Lateral collision risk in SAL1 location, assuming an annual traffic growth rate of 8%, is shown in Table 21 and Figure 18:

Lateral Collision Risk	8% annual traffic growth
2008	$2.0055 \cdot 10^{-9}$
2009	$2.1659 \cdot 10^{-9}$
2010	$2.3392 \cdot 10^{-9}$
2011	$2.5263 \cdot 10^{-9}$
2012	$2.7284 \cdot 10^{-9}$
2013	$2.9467 \cdot 10^{-9}$
2014	$3.1824 \cdot 10^{-9}$
2015	$3.4370 \cdot 10^{-9}$
2016	$3.7120 \cdot 10^{-9}$
2017	$4.0089 \cdot 10^{-9}$
2018	$4.3296 \cdot 10^{-9}$

Table 21
Lateral collision risk for the period 2008-2018 in SAL1

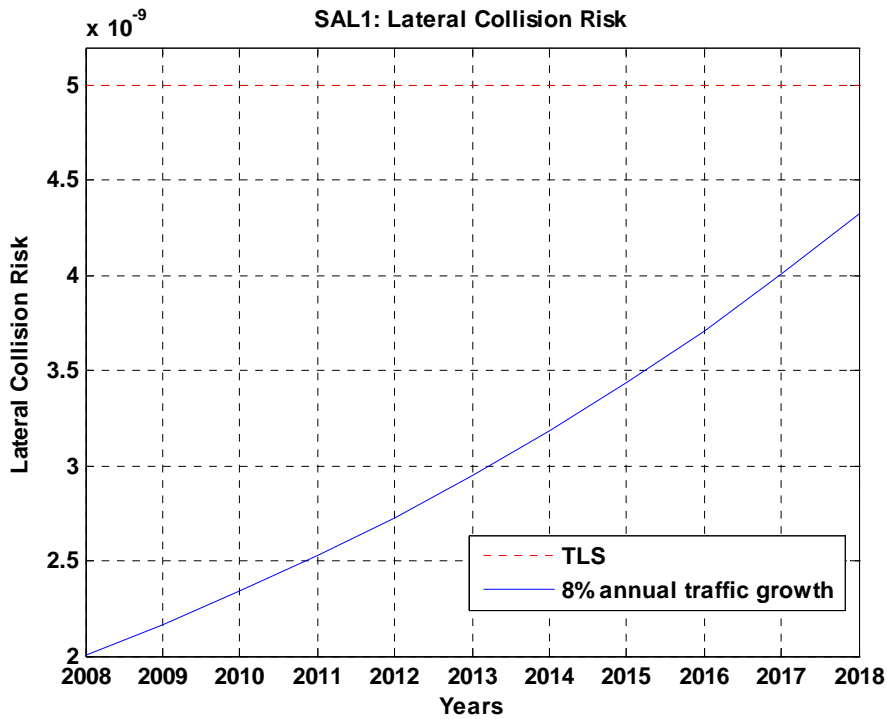


Figure 18
Lateral collision risk for the period 2008-2018 in SAL1

3.10.1.3. SAL2

Lateral collision risk in SAL2 location, assuming an annual traffic growth rate of 8%, is shown in Table 22 and Figure 19:

Lateral Collision Risk	8% annual traffic growth
2008	$2.4510 \cdot 10^{-9}$
2009	$2.6471 \cdot 10^{-9}$
2010	$2.8589 \cdot 10^{-9}$
2011	$3.0876 \cdot 10^{-9}$
2012	$3.3346 \cdot 10^{-9}$
2013	$3.6013 \cdot 10^{-9}$
2014	$3.8894 \cdot 10^{-9}$
2015	$4.2006 \cdot 10^{-9}$
2016	$4.5367 \cdot 10^{-9}$
2017	$4.8996 \cdot 10^{-9}$
2018	$5.2915 \cdot 10^{-9}$

Table 22
Lateral collision risk for the period 2008-2018 in SAL2

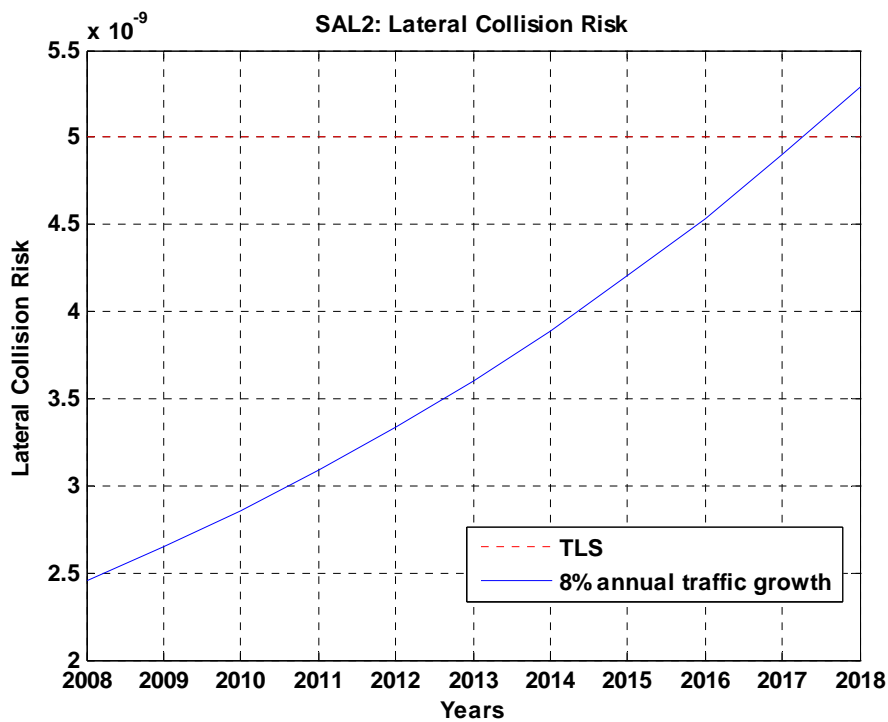


Figure 19
Lateral collision risk for the period 2008-2018 in SAL2



3.10.1.4. Dakar1

Lateral collision risk in Dakar1 location, considering an annual traffic growth rate of 8%, is shown in Table 23 and Figure 20:

Lateral Collision Risk	8% annual traffic growth
2008	1.9075×10^{-9}
2009	2.0601×10^{-9}
2010	2.2249×10^{-9}
2011	2.4029×10^{-9}
2012	2.5951×10^{-9}
2013	2.8028×10^{-9}
2014	3.0270×10^{-9}
2015	3.2691×10^{-9}
2016	3.5307×10^{-9}
2017	3.8131×10^{-9}
2018	4.1182×10^{-9}

Table 23
Lateral collision risk for the period 2008-2018 in Dakar1

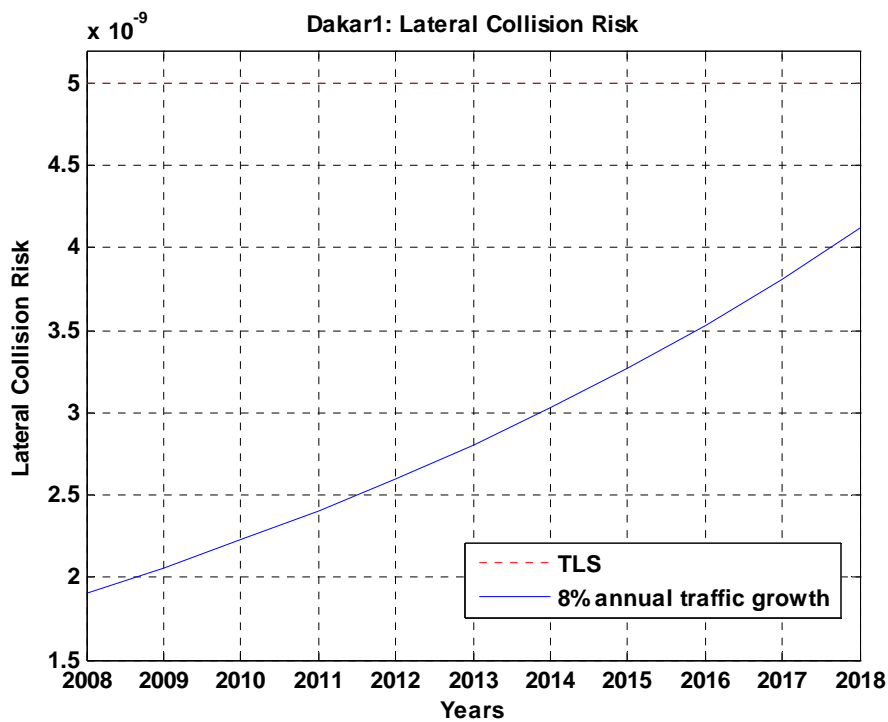


Figure 20
Lateral collision risk for the period 2008-2018 in Dakar1

3.10.1.5. Dakar2

Lateral collision risk in Dakar2 location, considering an annual traffic growth rate of 8%, is shown in Table 24 and Figure 21:

Lateral Collision Risk	8% annual traffic growth
2008	1.6749×10^{-9}
2009	1.8089×10^{-9}
2010	1.9536×10^{-9}
2011	2.1099×10^{-9}
2012	2.2787×10^{-9}
2013	2.461×10^{-9}
2014	2.6579×10^{-9}
2015	2.8705×10^{-9}
2016	3.1002×10^{-9}
2017	3.3482×10^{-9}
2018	3.6160×10^{-9}

Table 24
Lateral collision risk for the period 2008-2018 in Dakar2

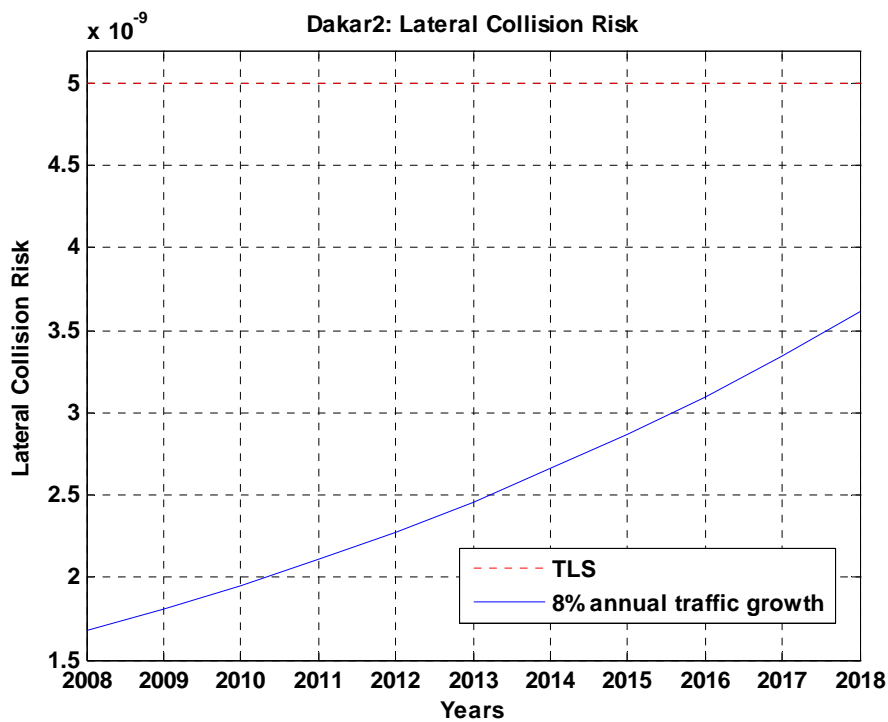


Figure 21
Lateral collision risk for the period 2008-2018 in Dakar2



3.10.1.6. Recife

Lateral collision risk in Recife location, considering an annual traffic growth rate of 8%, is shown in Table 25 and Figure 22:

Lateral Collision Risk	8% annual traffic growth
2008	1.7024*10 ⁻⁹
2009	1.8385*10 ⁻⁹
2010	1.9856*10 ⁻⁹
2011	2.1445*10 ⁻⁹
2012	2.3160*10 ⁻⁹
2013	2.5013*10 ⁻⁹
2014	2.7014*10 ⁻⁹
2015	2.9175*10 ⁻⁹
2016	3.1509*10 ⁻⁹
2017	3.4030*10 ⁻⁹
2018	3.6752*10 ⁻⁹

Table 25
Lateral collision risk for the period 2008-2018 in Recife

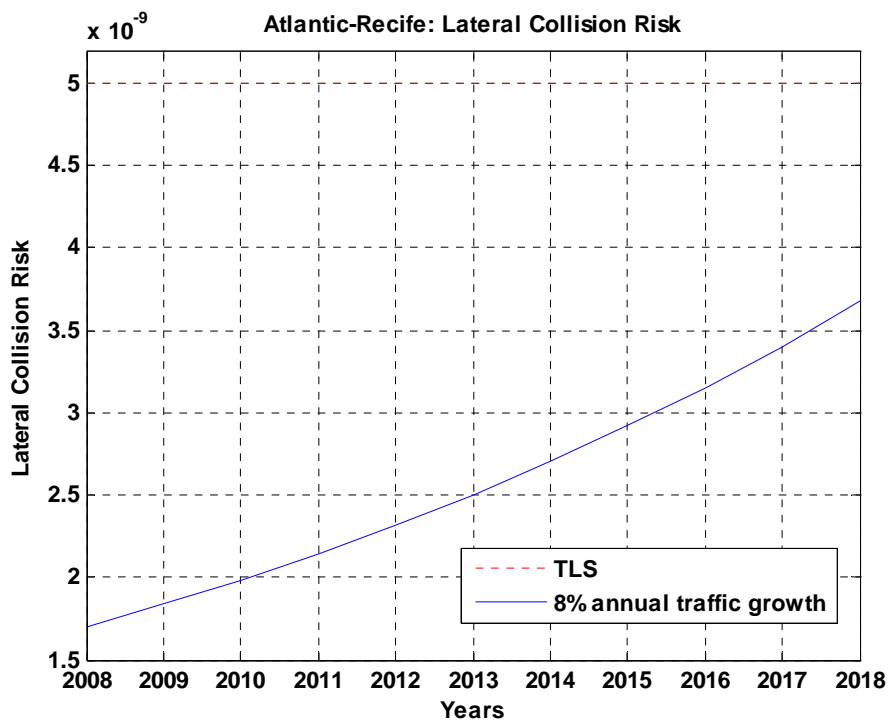


Figure 22
Lateral collision risk for the period 2008-2018 in Recife



3.10.2. Considerations on the results

3.10.3.1. Parallel routes

Lateral collision risk is below the $TLS = 5 \times 10^{-9}$ with the current traffic flow and it is estimated that, considering 8% as the annual traffic growth rate, it will continue to be laterally safe until 2017. According to these results, the TLS would be exceeded in 2018. Nevertheless, it must be taken into account that conservative assumptions have been made.

Comparing these results with those obtained for the pre-implementation safety assessment, [Ref. 15], it can be seen that the new values are higher. This is due to the traffic growth in the Corridor (higher than expected) and the different distribution of traffic on the flight levels of unidirectional routes.

It has also been confirmed that the results are similar in all the locations analysed.

3.10.3.2. RANDOM route

Although traffic on the direct routes (RANDOM) has not been considered, it is assumed that risk due to this route will not dramatically change the results obtained. The reasoning for this assumption is based on the following points:

- Traffic on these two routes only represents 2.5% of the total traffic
- Traffic on the route ROSTA-NADIR is southbound traffic and mainly even levels are used.
- Traffic on the route NADIR-ABALO is northbound traffic. It is scarce and only odd levels are used.

Figure 23 and Figure 24 show the traffic distribution, per flight level, of the westernmost routes, including the RANDOM routes.



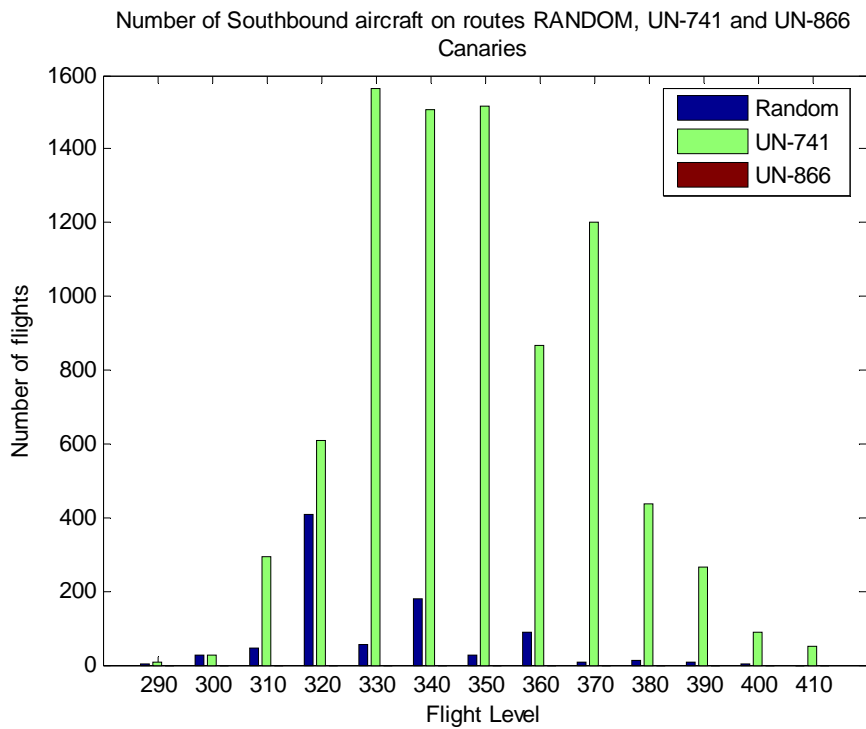


Figure 23
Number of Southbound flights on routes RANDOM, UN-741 and UN-866

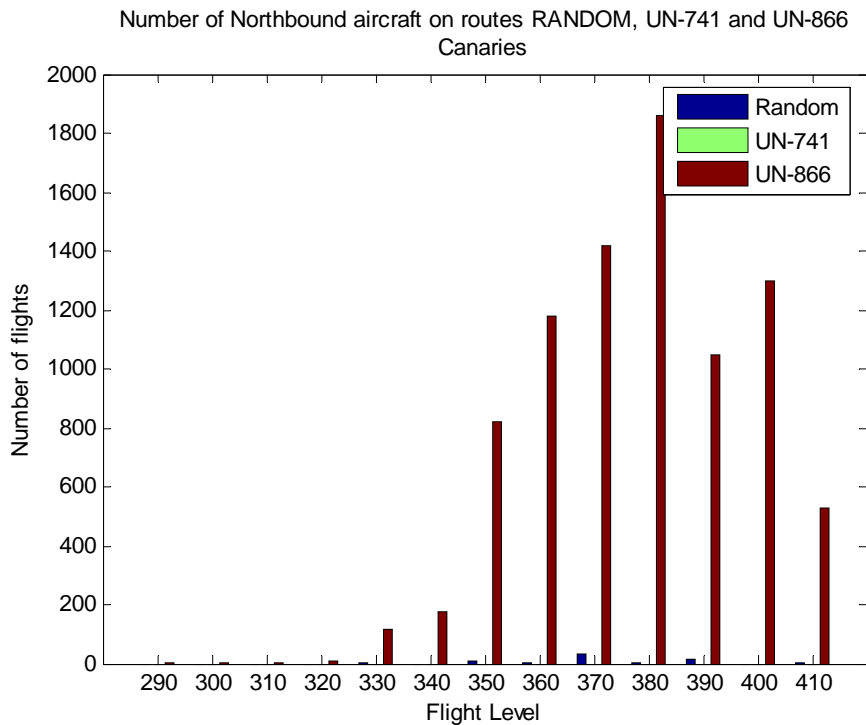


Figure 24
Number of Northbound flights on routes RANDOM, UN-741 and UN-866

Taking all this into account,

- There will be no proximate pairs at the same FL between the two direct routes.
- As traffic on the route ROSTA-NADIR is separated longitudinally at the Canarias as if it was UN-741 traffic, there is a scarce probability of having proximate pairs between this route and route UN-741.
- The contribution to risk of routes ROSTA-NADIR/UN-866 and NADIR-ABALO/UN-741 is considered to be small due to:
 - The reduced number of aircraft on RANDOM route, what implies a low probability of having proximate pairs between these pairs of routes
 - The large separation between routes: 110NM and 90NM minimum in the Canarias, which increases along the Corridor till NADIR

4. VERTICAL COLLISION RISK ASSESSMENT

4.1. INTRODUCTION

Vertical collision risk, i.e. the risk due to the loss of vertical separation between aircraft on adjacent flight levels is generally made up of three traffic components, namely same direction traffic, opposite direction traffic and crossing traffic.

Vertical collision risk models for same and opposite direction traffic are similar to those for lateral collision risk presented before. They apply to aircraft in straight and level flight. This condition can be assumed to be satisfied within the EUR/SAM Corridor. Nevertheless, some operational causes of height deviations may lead to an aircraft climbing or descending through other flight levels, requiring a different type of modelling.



There are two requirements that must be achieved to consider the airspace vertically safe. They are the following ones:

- In accordance with ICAO Guidance Material, [Ref. 7], the risk of mid-air collision in the vertical dimension within RVSM airspace, due to technical height keeping performance, shall meet a Target Level of Safety of $2.5 \cdot 10^{-9}$ fatal accidents per flight hour.
- In accordance with ICAO Guidance Material, [Ref. 7], the management of the overall vertical collision risk within RVSM airspace shall meet a Target Level of Safety of $5.0 \cdot 10^{-9}$ fatal accidents per flight hour.

In the following sections, the technical vertical risk and the overall vertical risk are assessed.

4.2. TECHNICAL VERTICAL COLLISION RISK ASSESSMENT

Technical vertical risk represents the risk of a collision between aircraft on adjacent flight levels due to normal or typical height deviations of RVSM approved aircraft. It is attributable to the height-keeping errors that result from the combination of altimetry system errors (ASE) and autopilot performance in the vertical dimension.

4.2.1. Collision Risk Model

The Reich model used for lateral collision risk can also be applied to calculate vertical collision risk between aircraft on adjacent flight levels of the same track, flying in either the same or the opposite direction. In this case the model is expressed by this equation:



$$N_{az} = P_z(S_z) \cdot P_y(0) \cdot \frac{\lambda_x}{S_x} \cdot E_{z\text{same}} \left[\frac{|\Delta\bar{v}|}{2 \cdot \lambda_x} + \frac{|\dot{\bar{y}}|}{2 \cdot \lambda_y} + \frac{|\dot{\bar{z}}|}{2 \cdot \lambda_z} \right] +$$

$$+ P_z(S_z) \cdot P_y(0) \cdot \frac{\lambda_x}{S_x} \cdot E_{z\text{opposite}} \cdot \left[\frac{2 \cdot |\bar{v}|}{2\lambda_x} + \frac{|\dot{\bar{y}}|}{2\lambda_y} + \frac{|\dot{\bar{z}}|}{2\lambda_z} \right]$$

Equation 23

Where:

- N_{az} is the expected number of accidents (two per each aircraft collision) per flight hour due to the loss of vertical separation.
- S_z is the vertical separation minimum.
- $P_z(S_z)$ is the probability of vertical overlap of aircraft nominally flying on adjacent flight levels of the same track.
- $P_y(0)$ is the probability of lateral overlap of aircraft nominally flying on the same track.
- $E_{z\text{same}}$ is the same direction vertical occupancy, i.e. the average number of same direction aircraft flying on adjacent flight levels of the same track within segments of length $2S_x$ centred on the typical aircraft.
- $E_{z\text{opposite}}$ is the opposite direction vertical occupancy, i.e. the average number of opposite direction aircraft flying on adjacent flight levels of the same track within segments of length $2S_x$ centred on the typical aircraft.
- S_x is the length of the longitudinal window used in the calculation of occupancies.
- λ_x is the average length of an aircraft.

- λ_y is the average width of an aircraft.
- λ_z is the average height of an aircraft.
- $|\Delta \bar{v}|$ is the average relative along-track speed of two aircraft flying on the same track in the same direction.
- $|\bar{v}|$ is the average ground speed of an aircraft.
- $|\bar{y}|$ is the average lateral cross-track speed between aircraft flying on the same track.
- $|\bar{z}|$ is the average relative vertical speed of aircraft flying on the same track.

As can be seen from Equation 23, the elements of the collision risk model for same and opposite direction traffic are the probabilities of overlap and the average durations of overlaps in the different co-ordinate directions. In the model for same and opposite direction traffic, overlap of two aircraft is defined as overlap of rectangular boxes enveloping the aircraft. It is also assumed that during a situation of overlap, the sides of the boxes remain parallel.

Similar elements play a part in a model of vertical collision risk on crossing routes, but in a more complicated way. Due to the geometry of a crossing, the sides of the rectangular boxes enveloping the aircraft will not be parallel during a situation of horizontal overlap. As a result, the estimation of the average duration of an overlap becomes more complicated. This problem has been addressed by modelling the aircraft by cylinders and calculating the average duration of an overlap from the

overlap of the circular cross sections of the cylinders. The diameter of the cylinders is taken as the largest of the length and the wingspan of the aircraft.

Another difference to take into account is that, for a pair of crossing routes, the probability of horizontal overlap cannot be factored into the probabilities of overlap in the longitudinal and lateral directions.

The vertical collision risk model for crossing routes on the basis of the cylindrical aircraft model can be expressed as:

$$N_{az}(cross) = P_z(S_z)P_h(\theta)E_z(\theta) \left\{ \frac{v_{rel}(\theta)}{\frac{\pi\lambda_h}{2}} + \frac{|\bar{z}|}{2\lambda_z} \right\}$$

Equation 24

Where the relative velocity $v_{rel}(\theta)$ is given by:

$$v_{rel}(\theta) = \sqrt{v_1^2 + v_2^2 - 2v_1v_2 \cos(\theta)}$$

Equation 25

The new parameters are:

- θ , the angle between two crossing routes, i.e. the angle between the aircraft headings.
- λ_h , the average diameter of a cylinder representing an aircraft. It is the largest of the average aircraft wingspan or fuselage length.
- S_h , horizontal separation among aircraft on crossing routes. It is used for the calculation of $E_z(\theta)$ values.



- $E_z(\theta)$, twice the probability of horizontal overlap of circles representing horizontal cross sections of aircraft on crossing routes.
- $V_{rel}(\theta)$, the average relative horizontal speed between aircraft flying on crossing routes.
- $P_h(\theta)$, the probability of horizontal overlap for two aircraft at adjacent flight levels on routes crossing at angle θ .

When there are several pairs of crossing routes with different crossing angles θ_i , $i=1, \dots, n$, the model can be applied to each pair of routes and combined subsequently to give:

$$N_{az}(cross) = P_z(S_z) \sum_1^n P_h(\theta_i) E_z(\theta_i) \left\{ \frac{v_{rel}(\theta_i)}{\frac{\pi \lambda_h}{2}} + \frac{|\bar{z}|}{2 \lambda_z} \right\}$$

Equation 26

where n is the number of groups made from crossing routes with similar angles of intersection.

When the number of crossing angles is relatively large, Equation 26 can be approximated by the model of Equation 24 by taking conservative estimates of $E_z(\theta_i)$ and $v_{rel}(\theta_i)$ valid for each value of i , $i=1, \dots, n$.

The vertical collision risk model for crossing tracks can be combined with the model for same and opposite direction traffic to give the complete technical vertical collision risk model for the RVSM safety assessment for the EUR/SAM Corridor in the SAT, i.e.

$$\begin{aligned}
 N_{az} = & P_z(S_z) \cdot P_y(0) \cdot \frac{\lambda_x}{S_x} \cdot E_{zsame} \left[\frac{|\Delta \bar{v}|}{2 \cdot \lambda_x} + \frac{|\bar{y}|}{2 \cdot \lambda_y} + \frac{|\bar{z}|}{2 \cdot \lambda_z} \right] + \\
 & + P_z(S_z) \cdot P_y(0) \cdot \frac{\lambda_x}{S_x} \cdot E_{zopposite} \left[\frac{2 \cdot |\bar{v}|}{2 \cdot \lambda_x} + \frac{|\bar{y}|}{2 \cdot \lambda_y} + \frac{|\bar{z}|}{2 \cdot \lambda_z} \right] + \\
 & + P_z(S_z) \sum_1^n P_h(\theta_i) E_z(\theta_i) \left[\frac{v_{rel}(\theta_i)}{\frac{\pi \lambda_h}{2}} + \frac{|\bar{z}|}{2 \cdot \lambda_z} \right]
 \end{aligned}$$

Equation 27

4.2.2. Average aircraft dimensions: $\lambda_x, \lambda_y, \lambda_z, \lambda_h$

Table 2 showed the average aircraft dimensions for the lateral collision risk model. Clearly, the same dimensions apply to the vertical model. In addition, the vertical model for crossing traffic needs the average diameter of a cylinder enveloping the aircraft. Table 26 shows the pertinent average aircraft dimensions.

Location	Length (λ_x)		Wingspan (λ_y)		Height (λ_z)		Diameter (λ_h)	
	Value (ft)	Value (NM)	Value (ft)	Value (NM)	Value (ft)	Value (NM)	Value (ft)	Value (NM)
Canaries	192.18	0.0316	180.13	0.0296	53.49	0.0088	192.18	0.0316
SAL1	205.03	0.0337	192.82	0.0317	55.98	0.0092	205.03	0.0337
SAL2	202.08	0.0333	189.45	0.0312	55.29	0.0091	202.08	0.0333
Dakar1	202.10	0.0333	189.44	0.0312	55.30	0.0091	202.10	0.0333
Dakar2	202.06	0.0332	189.41	0.0312	55.29	0.0091	202.06	0.0332
Recife	202.10	0.0333	189.45	0.0312	55.30	0.0091	202.10	0.0333

Table 26
Average aircraft dimensions for the vertical collision risk model



4.2.3. Probability of lateral overlap: $P_y(0)$

The probability of lateral overlap for aircraft nominally flying at adjacent flight levels of the same path is denoted by $P_y(0)$. It is defined by:

$$P_y(0) = \int_{-\lambda_y}^{\lambda_y} f^{y_{12}}(y) dy$$

Equation 28

Where $f^{y_{12}}(y)$ denotes the probability density of the lateral distance y_{12} between two aircraft with lateral deviations y_1 and y_2 , nominally at the same track, i.e.

$$y_{12} = y_1 - y_2$$

Equation 29

and

$$f^{y_{12}}(y) = \int_{-\infty}^{\infty} f^y(y_1) f^y(y_1 - y) dy_1$$

Equation 30

Equation 30 assumes that the deviations of the two aircraft are independent and have the same probability density. λ_y denotes the average aircraft width.

Substitution of Equation 30 into Equation 28 gives:

$$P_y(0) = \int_{-\lambda_y}^{\lambda_y} \int_{-\infty}^{\infty} f^y(y_1) f^y(y_1 - y) dy_1 dy$$

Equation 31

This last equation can be approximated by:



$$P_y(0) \approx 2\lambda_y \int_{-\infty}^{\infty} f^y(y_1) f^y(y_1) dy_1$$

Equation 32

The probability density $f^y(y_1)$ was described in 3.8. Using that function in Equation 32, the resulting estimate based on $\lambda_y = 190 \text{ ft}$ is $P_y(0) = 0.0048$.

This factor has a significant effect on the risk estimate. Therefore, it should not be underestimated. $P_y(0)$ will increase as the lateral navigational performance of typical aircraft improves, causing a corresponding increase in the collision risk estimate. The RGCSP was aware of this problem and attempted to account for improvements in navigation systems when defining the RVSM global system performance specification. Based on the performance of highly accurate area navigation systems observed in European airspace, which demonstrated lateral path-keeping errors with a standard deviation of 0.3NM, the RGCSP adopted a value of 0.059 as the value of $P_y(0)$ for the global system performance. This was the value used in the pre-implementation assessment.

Nevertheless, in some recent collision risk studies, [Ref. 16],[Ref. 17], the approach followed was to assume that some aircraft would have a better lateral performance and considered that a proportion α , $0 \leq \alpha \leq 1$, of the airspace users would be using GNSS navigation, with standard deviation 0.06123NM. The most conservative assumption consists in assuming that the full aircraft population are using GNSS, $\alpha=1$. Thus, taking the probability density as Gaussian⁷, with 0 mean and 0.06123NM standard deviation, the value obtained with Equation 32 for the lateral overlap probability is: $P_y(0) = 0.2881$. This value will be considered in this study, although it may be overly conservative for the EUR/SAM Corridor.

⁷ As the calculation of $P_y(0)$ is dominated by the core of the densities, the choice of the type of the probability density is less critical than for the calculation of $P_y(S_y)$.



4.2.4. Probability of horizontal overlap: $P_h(\theta)$

$P_h(\theta)$ denotes the horizontal overlap probability for crossing routes. The method used in [Ref. 12] for the CAR/SAM region to obtain $P_h(\theta)$ is literally described below:

Lets consider two aircraft, A and B, flying in crossing routes with angle θ , in adjacent levels i and $i-1$, vertically separated by S_z . The origin of the system of coordinates (x,y) , in the horizontal plane, is the crossing point. The axle x coincides with the aircraft route A, that is in the origin $(0,0)$, flying in the positive direction. The angle θ is measured since the axle x in the counter-clockwise direction. The aircraft B is in the position (U_x,U_y) , flying to the origin. Consider U the variable that designates the horizontal distance between two aircraft, so that the distance U_h is inside the proximity area given by $S_h = \sqrt{S_x^2 + S_y^2}$. The geometry described can be seen in Figure 25.

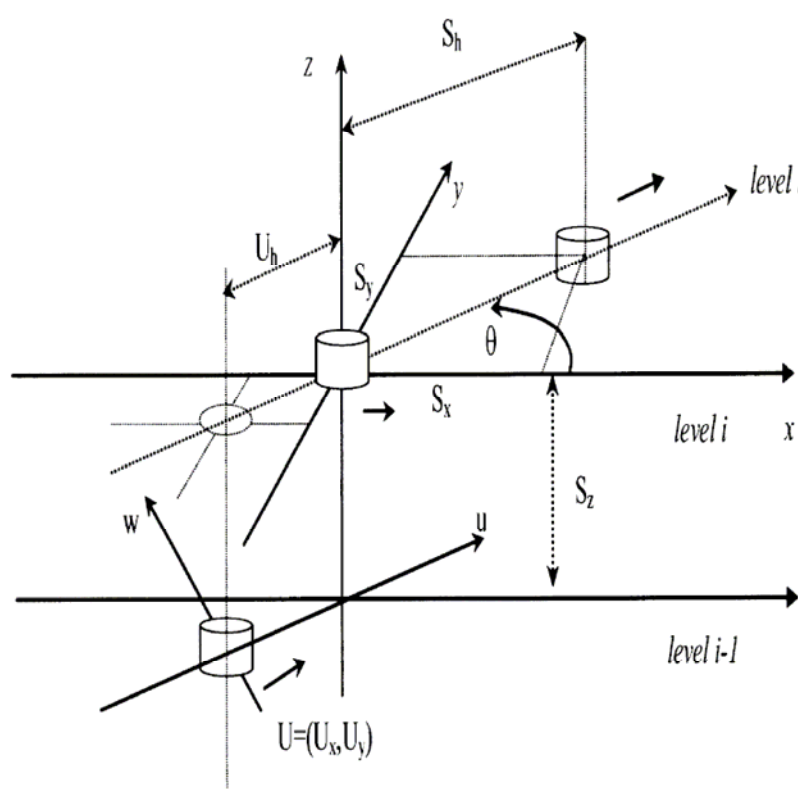


Figure 25
Geometry of the crossing routes

Considering that the variables that represent the longitudinal and lateral positions are independent and random, then, mathematically, $P_h(\theta)$ can be expressed by:

$$P_h(\theta) = \frac{h(U)\pi\lambda_h^2}{\int_{-S_h}^{S_h} \int_{-\sqrt{S_h^2-x^2}}^{\sqrt{S_h^2-x^2}} h(U) dx dy}$$

Equation 33

Where $h(U)$ is a density function of horizontal overlap, bi-dimensional, for the aircraft in adjacent flight levels in crossing routes with angle θ , separated by the horizontal distance (U_x, U_y) . This last function is given, in its matrix form, by:

$$h(U) = \frac{1}{2\pi\sqrt{\det(M)}} \exp\left(-\frac{1}{2}U^T M^{-1}U\right)$$

Equation 34

Where, $\det(M)$ is the determinant of the covariance matrix M of the two aircraft and U is the matrix position of the aircraft B, given by:

$$U = \begin{pmatrix} U_x \\ U_y \end{pmatrix}$$

Equation 35

The function $h(U)$ was acquired considering a conservative approach for the longitudinal distribution of the aircraft along-track route. For each one of the aircraft, it was considered that the along-track and lateral deviations, corresponding to its nominal positions, are ruled by normal distributions. Then, for the normal distribution of the longitudinal position, it was assumed that its variance is equal to the variance of the uniform distribution with limits given by the horizontal separation S_h . For the normal distribution of the lateral deviations, the variance is worth σ_{rc}^2 . Making the rotation of coordinates of the aircraft B in the system (u,w) , to express its position in

the system (x,y) of the aircraft A, the covariance matrix M is acquired, and it is given by:

$$M = \begin{pmatrix} (1 + \cos^2(\theta)) \frac{S_h^2}{6} + \frac{\sigma_{rc}^2}{2} \text{sen}^2(\theta) & \text{sen}(\theta) \cos(\theta) \left(\frac{S_h^2}{6} - \frac{\sigma_{rc}^2}{2} \right) \\ \text{sen}(\theta) \cos(\theta) \left(\frac{S_h^2}{6} - \frac{\sigma_{rc}^2}{2} \right) & \text{sen}^2(\theta) \frac{S_h^2}{6} + \frac{\sigma_{rc}^2}{2} (1 + \cos^2(\theta)) \end{pmatrix}$$

Equation 36

Considering that the normal distribution has its maximum value in the mean point, that in the geometry adopted is the crossing point, and that an aircraft in an adjacent flight level can cross a route intersection with any random distance, $h(U)$ can be assessed only in the point (0,0), that is, for null horizontal separation. In this case, the conservative expression for the horizontal overlap probability is given by:

$$P_h(\theta) = \frac{h(0)\pi\lambda_h^2}{\int_{-Sh}^{Sh} \int_{-\sqrt{Sh^2-x^2}}^{\sqrt{Sh^2-x^2}} h(U) dx dy}$$

Equation 37

This approach is used for any proximity among the aircraft pairs in the crossing routes.

The denominator in Equation 37 can only be obtained by numerical integration.

One interesting property of $P_h(\theta)$ is that $P_h(90^\circ+\theta) = P_h(90^\circ-\theta)$ and $P_h(\theta) = P_h(\theta+180^\circ)$ in $(U_x, U_y) = (0,0)$.

In [Ref. 12], probability of horizontal overlap for crossing angles between 0° and 90° with two different values of λ_h has been calculated. These results have been compared with the ones obtained by the CRM, being both similar. As an example, for



$\lambda_h = 0.02140 \text{ NM}$, the value obtained in [Ref. 12] is $P_h(10^\circ) = 1.325 * 10^{-6}$, whilst the value obtained with the CRM is $P_h(10^\circ) = 1.344 * 10^{-6}$. The small differences may be due to numerical integration.

The results obtained by CRM are always slightly higher than the ones presented in [Ref. 12]. Therefore, they can be considered to be conservative.

4.2.4.1. Application to the EUR/SAM Airspace

As it was previously explained, in the EUR/SAM Corridor there is traffic crossing the Corridor in published routes in SAL, Dakar and Recife, but there is also some traffic crossing the Corridor in non published routes or changing from one route to another. Those trajectories with more than 50 aircraft per year have been analysed. These trajectories are in the Canaries airspace and in SAL airspace.

Probability of horizontal overlap has been calculated for all these routes using Equation 37. The values of S_h and σ_{rc} considered are the same that are used in the CAR/SAM region, i.e., $S_h = 80 \text{ NM}$ and $\sigma_{rc} = 0.3 \text{ NM}$ (this last value is the one established in the Doc 9574 ([Ref. 7])).

The results obtained are shown in Table 27, Table 28, Table 29, Table 30 and Table 31.

Horizontal overlap probability				
Location	Diameter (λ_h)	Route	Angle (°)	$P_h(\theta)$
Canaries	0.03163 NM	EDUMO-APASO	30	1.0151803e-006
			150	1.0151803e-006
		LUMPO-GUNET	25	1.2035805e-006
			155	1.2035805e-006
		TENPA-CVS	20	1.4896045e-006
			160	1.4896045e-006
		CVS-GUNET	17	1.7437125e-006
			163	1.7437125e-006
		LIMAL-ETIBA	17	1.7437125e-006
			163	1.7437125e-006
		COOR3-EDUMO	40	7.8548466e-007
			140	7.8548466e-007
		GAMBA-TENPA	25	1.2035805e-006
			155	1.2035805e-006
		EDUMO-COOR1	7	4.1722595 e-006
			173	4.1722595 e-006

Table 27
Horizontal overlap probabilities for Canaries

Horizontal overlap probability				
Location	Diameter (λ_h)	Route	Angle (°)	$P_h(\theta)$
SAL1	0.03374 NM	UR976/UA-602	85	5.6397142e-007
			95	5.6397142e-007
		ULTEM-LUMPO	90	5.6165779e-007
			90	5.6165779e-007
		TENPA-CVS	20	1.6953279e-006
			160	1.6953279e-006
		CVS-GUNET	15	2.2423955e-006
			165	2.2423955e-006
		GAMBA-COOR1	15	2.2423955e-006
			165	2.2423955e-006
		GAMBA-TENPA	25	1.3698022e-006
			155	1.3698022e-006
		CVS-AMDOL	25	1.3698022e-006
			155	1.3698022e-006
		CVS-BOTNO	25	1.3698022e-006
			155	1.3698022e-006

Table 28
Horizontal overlap probabilities for SAL1



Horizontal overlap probability				
Location	Diameter (λ_h)	Route	Angle (°)	$P_h(\theta)$
SAL2	0.03326 NM	ULTEM-KENOX	40	8.6849102e-007
			140	8.6849102e-007
		KENOX-COOR2	24	1.3832354e-006
			156	1.3832354e-006
		CVS-AMDOL	24	1.3832354e-006
			156	1.3832354e-006
		BOTNO-CVS	24	1.3832354e-006
			156	1.3832354e-006

Table 29
Horizontal overlap probabilities for SAL2

Horizontal overlap probability				
Location	Diameter (λ_h)	Route	Angle (°)	$P_h(\theta)$
Dakar1	0.03326 NM	UL-435	83	5.5013995e-007
			97	5.5013995e-007

Table 30
Horizontal overlap probabilities for Dakar1

Horizontal overlap probability				
Location	Diameter (λ_h)	Route	Angle (°)	$P_h(\theta)$
Recife	0.03326 NM	UL-695	85	5.4797736-007
			95	5.4797736-007

Table 31
Horizontal overlap probabilities for Recife

4.2.5. Relative velocities

Equation 27 contains four relative speed parameters, $2|\bar{v}|$, $|\Delta v|$, $|\bar{y}|$ and $|\bar{z}|$ for the same/opposite vertical risk and relative speeds for each one of the crossing pairs of routes, $v_{rel}(\theta_i)$.



The average along track speed $2|\bar{v}|$ is taken the same as for the lateral collision risk model.

Regarding $|\Delta v|$, it has been calculated, as in the lateral case, from the differences between the speeds of all the pairs of aircraft that constitute a vertical proximate pair in the same direction. The values obtained for the different locations are between 13 and 18kts. Therefore, the conservative value 20 kts will be used for all of them.

For the vertical collision risk model, $|\bar{y}|$ is the mean of the modulus of the relative cross-track speed between aircraft on the same track. Consequently, there is no operational reason why this relative speed should have a particularly large value. In the RVSM Safety Assessment of the Australian Airspace, [Ref. 8], the value considered for this parameter was 13kts. A more conservative value, 20kts, was used by ARINC in [Ref. 2] and in the AFI Region Assessment, [Ref. 16]. This value has been taken here too.

The mean relative vertical speed of the vertical collision risk model applies to aircraft that have lost their assigned vertical separation minimum of S_z . The value $|\bar{z}| = 1.5 kts$ will be taken here as in the lateral collision risk assessment.

As far as relative speed in crossing routes is concerned, it is obtained by:

$$v_{rel}(\theta_i) = \sqrt{v_1^2 + v_2^2 - 2v_1v_2 \cos(\theta_i)}$$

Equation 38

where v_1 and v_2 are the average speeds in each one of the routes and θ , the intersection angle. The relative speeds used in this study are summarized in Table 32 and Table 33. (V_1 refers to the average speed on the corresponding parallel route and V_2 , to the crossing route).

Location	Crossing route	V ₁ (kts)	V ₂ (kts)	θ (°)	V _{rel} (θ) (kts)
Canaries	EDUMO-APASO	468.6	564.1	30	282.7
				150	997.8
	LUMPO-GUNET	468.6	469.6	25	203.1
				155	916.0
	TENPA-CVS	468.6	459.5	20	161.4
				160	914.0
	CVS-GUNET	468.6	447.8	17	137.0
				163	906.3
	LIMAL-ETIBA	468.6	502.7	17	147.5
				163	960.6
	COOR3-EDUMO	468.6	462.5	40	318.5
				140	875.0
	GAMBA-TENPA	468.6	498.1	25	211.2
				155	943.8
EDUMO-COOR1	468.6	456.5	7	57.7	
			173	923.4	
SAL1	UR976/UA-602	466.4	468.7	85	631.8
				95	689.5
	ULTEM-LUMPO	466.4	460.2	90	655.3
				90	655.3
	TENPA-CVS	466.4	0	20	466.4
				160	466.4
	CVS-GUNET	466.4	458.3	15	121.0
				165	916.9
	GAMBA-COOR1	466.4	467.0	15	121.8
				165	925.5
	GAMBA-TENPA	466.4	515.7	25	218.0
				155	959.0
	CVS-AMDOL	466.4	0	25	466.4
				155	466.4
CVS-BOTNO	466.4	0	25	466.4	
			155	466.4	

Table 32
Relative speeds in crossings (Canaries and SAL1)



Location	Crossing route	V ₁ (kts)	V ₂ (kts)	θ (°)	V _{rel} (θ) (kts)
SAL2	ULTEM-KENOX	471.1	473.1	40	322.9
				140	887.3
	KENOX-COOR2	471.1	479.4	24	197.8
				156	929.7
	CVS-AMDOL	471.1	454.6	24	193.1
				156	905.4
BOTNO-CVS	471.1	461.8	24	194.2	
			156	912.4	
Recife	UL-695/UL-375	476.3	471.8	85	640.5
				95	699.0

Table 33
Relative speeds in crossings (SAL2 and Recife)

4.2.6. Vertical overlap probability: $P_z(S_z)$

The probability of vertical overlap of a pair of aircraft nominally flying at adjacent flight levels separated by S_z is denoted $P_z(S_z)$. It is defined by:

$$P_z(S_z) = \int_{-\lambda_z}^{\lambda_z} f^{z_{12}}(z) dz$$

Equation 39

Where $f^{z_{12}}(z)$ denotes the probability density of the vertical distance z_{12} between the two aircraft. This distance may be defined as:

$$z_{12} = S_z + z_1 - z_2$$

Equation 40



with z_1 and z_2 representing the height-keeping deviations of two aircraft. Height-keeping deviations of aircraft are usually defined in terms of Total Vertical Error (TVE), measured in geometric feet:

$$TVE = \text{actual pressure altitude flown by an aircraft} - \text{assigned altitude}$$

Assuming that the height-keeping deviations of the two aircraft are independent and denoting their probability densities by $f_1^{TVE}(z_1)$ and $f_2^{TVE}(z_2)$, the probability density $f^{z_{12}}(z)$ and the probability of vertical overlap can be written as:

$$f^{z_{12}}(z) = \int_{-\infty}^{\infty} f_1^{TVE}(z_1) f_2^{TVE}(S_z + z_1 - z) dz_1$$

Equation 41

$$P_z(S_z) = \int_{-\lambda_z}^{\lambda_z} \int_{-\infty}^{\infty} f_1^{TVE}(z_1) f_2^{TVE}(S_z + z_1 - z) dz_1 dz$$

Equation 42

This equation can be approximated by:

$$P_z(S_z) \approx 2\lambda_z \int_{-\infty}^{\infty} f_1^{TVE}(z_1) f_2^{TVE}(S_z + z_1) dz_1$$

Equation 43

The probability distribution of the height-keeping deviations, $f^{TVE}(z)$, depends on the height-keeping characteristics of the aircraft as specified by the MASPS. Data on the height-keeping performance of MASPS-approved aircraft can be obtained by means of aircraft height monitoring. Currently, height monitoring data are not available from the SAT. However, as the majority of the aircraft types in the EUR/SAM Corridor are also flying in the European RVSM height monitoring programme, these data will be used.



$f^{TVE}(z)$ can be obtained modelling separately the two components of TVE: Altimetry System Error (ASE) and Flight Technical Error (FTE):

$$TVE = ASE + FTE$$

Equation 44

where

ASE = actual pressure altitude flown by an aircraft – displayed altitude

FTE = displayed altitude – assigned altitude

Assuming that the two components are statistically independent:

$$f^{TVE}(z) = \int_{-\infty}^{\infty} f^{ASE}(a) f^{FTE}(z - a) da$$

Equation 45

In practice, FTE is difficult to determine and it is approximated by Assigned Altitude Deviation (AAD):

AAD = transponded altitude – assigned altitude

Equation 45 can then be approximated by:

$$f^{TVE}(z) = \int_{-\infty}^{\infty} f^{ASE}(a) f^{AAD}(z - a) da$$

Equation 46

The difference between FTE and AAD is referred to as correspondence error. It arises due to the rounding of the altimeter reading before transmission by the aircraft transponder. Data on AAD can be obtained by evaluating archived mode C data.

Figure 26 shows a diagram of the components of the Total Vertical Error:

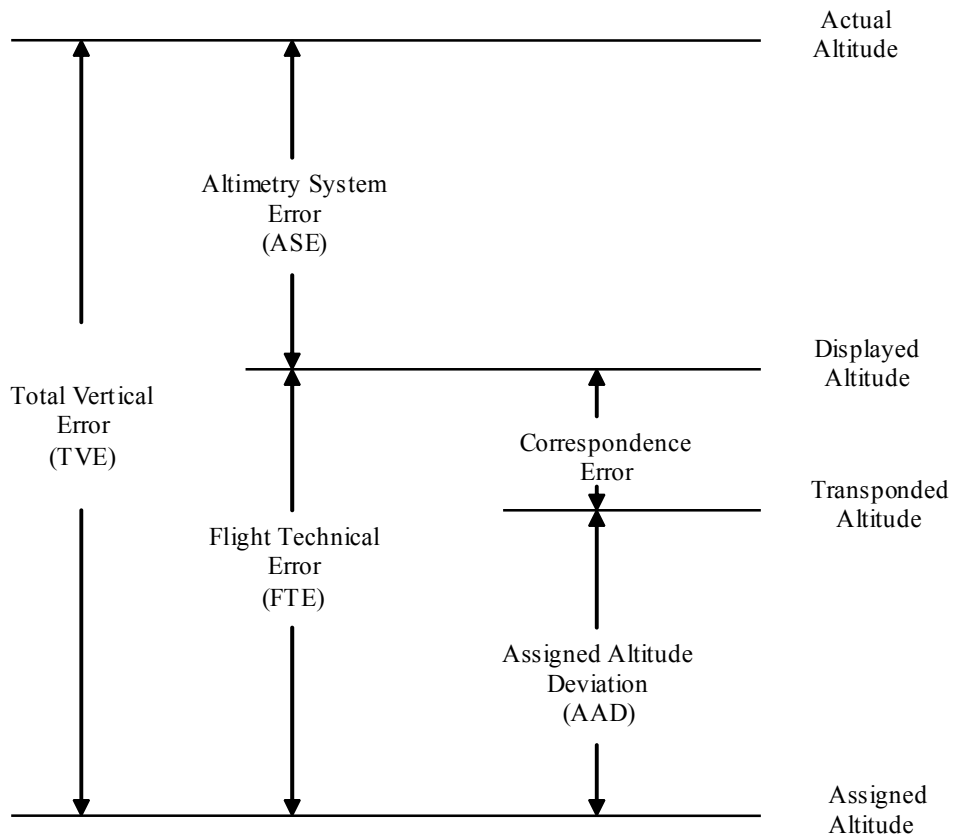


Figure 26
Breakdown of height-keeping errors

The modelling of the two component densities, ASE and AAD, is described below.

4.2.6.1. ASE Distribution Modelling

The overall ASE distribution is a combination of ASE distributions for each aircraft monitoring group, weighted by the proportion of flights made by the group, i.e.

$$f^{ASE}(a) = \sum_{i=1}^{n_{ig}} \beta_i f_i^{ASE}(a)$$

Equation 47

where n_{tg} denotes the number of different aircraft type groups, β_i is the proportion of flight time contributed by aircraft type group i and $f_i^{ASE}(a)$ is the probability density of the ASE of aircraft type group i , $i=1, \dots, n_{tg}$. Each monitoring group's ASE probability density, $f_i^{ASE}(a)$, is the result of both within and between airframe ASE variability of all the airframes making up the group.

The probability densities $f_i^{ASE}(a)$ are to be determined on the basis of height monitoring data of RVSM approved aircraft. As it was mentioned before, such monitoring data are not available from the SAT. However, as the normal height-keeping performance of RVSM approved aircraft is not dependent on the region of operation, HMU data collected in other ICAO Regions may be used for the modelling of a monitoring group's ASE probability density, $f_i^{ASE}(a)$. Therefore, for the current collision risk assessment, height monitoring data from the European programme, collected for the EUR RVSM Safety Monitoring Report 2008 have been used.

The RVSM Tool, developed by Eurocontrol, has also been used to model the monitoring group's ASE probability densities, $f_i^{ASE}(a)$, for the aircraft that fly in the EUR/SAM Corridor, to obtain the overall ASE distribution and to calculate the vertical overlap probability, $P_z(1000)$.

This software has been recently updated. Firstly, the families of within and between airframe ASE probability densities have been extended to mixtures of up to three Generalised Laplace probability densities (instead of only Gaussians or Double Exponential). The second refinement concerns the removal of a conservative analytical approximation (use of a Double Exponential distribution) in the process of combining within and between airframe ASE probability densities in favour of a numerical evaluation, as it was found that, for certain combinations, the DE approximation resulted in unrealistically conservative results.

In the European airspace, the aircraft-operator combinations are used in order to obtain the different monitoring groups’ ASE probability densities. However, only 11% of the aircraft-operator combinations obtained for the EUR/SAM Corridor could be matched to those in the EUR Region. For this reason, a different approach was used for this study and only the type of aircraft was considered, with the proportion of flights of each type as weighting factors for the overall ASE distribution. Doing it this way, only 0.21% of the flights of the EUR/SAM Corridor could not be assigned to any monitoring group. These flights were discarded and the proportions of the rest of flights renormalized to ensure that the weighting factors β_i add up to one.

Table A1. 1, in Annex 2, shows the proportion of flight time and the ASE probability density used for each of the monitoring groups in the EUR/SAM Corridor.

4.2.6.2. AAD Distribution Modelling

AAD performance is subdivided into typical and atypical performance. For the assessment of technical vertical risk, only typical AAD will be taken into account for the AAD component of TVE. All data on atypical AAD will be included in the assessment of the vertical risk due to all causes.

In [Ref. 12] typical AAD performance is taken to be that which is not greater than 300ft in magnitude and any AAD greater than that value is considered to be atypical.

AAD data on typical performance should be obtained from the height monitoring process, while AAD data on atypical performance should be obtained from incident reports.

The typical AAD distribution to be used in this study has been obtained using the Eurocontrol RVSM Tool with the aircraft monitoring groups of the EUR/SAM Corridor. It is a Double Exponential (DE) with mean -0.0356 ft and standard deviation 39.727 ft, whose equation is:

$$f^{AAD}(a) = \frac{1}{2b_{AAD}} \exp\left[-\left|\frac{a - m_{AAD}}{b_{AAD}}\right|\right], \quad \text{with } b_{AAD} = s/\sqrt{2}$$

Equation 48

Where m_{AAD} is the mean value and s is the standard deviation of the AAD function.

4.2.6.3. TVE Distribution Modelling

Substitution of the ASE and AAD densities of the foregoing two subsections into Equation 46 yields the TVE density $f^{TVE}(z)$. Then, the probability of vertical overlap is calculated by means of Equation 43, using the Eurocontrol RVSM Tool, being the resulting value $P_z(1000) = 4 \times 10^{-9}$.

In addition to the TLS of 2.5×10^{-9} for technical vertical risk, there are some constraints to be met by the TVE performance of aircraft. Firstly, the Global System Performance Specification requires the probability of vertical overlap, $P_z(1000)$, not to be greater than 1.7×10^{-8} . The value obtained does satisfy this requirement.

Apart from this requirement, section 2.3.1 of ICAO Document 9574 (2nd Edition), [Ref. 7], states that the aggregate of Total Vertical Error (TVE) performance in the airspace simultaneously satisfies the following four requirements, constituting the Global Height-Keeping Performance Specification:



- The proportion of TVE beyond 90m (300ft) in magnitude must be less than 2.0×10^{-3}
- The proportion of TVE beyond 150m (500ft) in magnitude must be less than 3.5×10^{-6}
- The proportion of TVE beyond 200m (650ft) in magnitude must be less than 1.6×10^{-7}
- The proportion of TVE between 290 and 320m (950ft and 1050ft) in magnitude must be less than 1.7×10^{-8}

Meeting the criteria of the global height-keeping performance specification provides additional confidence in the estimate of the probability of vertical overlap.

These proportions can also be calculated with the Eurocontrol RVSM Tool. The values obtained with the probability density $f^{TVE}(z)$ used in this study are shown in the following table:

Quantity	Estimate	Upper Bound
$Pr ob\{ TVE \geq 300\}$	3.1061×10^{-4}	2.0×10^{-3}
$Pr ob\{ TVE \geq 500\}$	8.9791×10^{-7}	3.5×10^{-6}
$Pr ob\{ TVE \geq 650\}$	9.9615×10^{-8}	1.6×10^{-7}
$Pr ob\{950 \leq TVE \leq 1050\}$	3.2234×10^{-9}	1.7×10^{-8}

Table 34
Estimates of Proportions of Height-Keeping Errors

The results show that all the criteria are met. Nevertheless, it must be taken into account that this part of the RVSM Software is not validated yet.



4.2.7. Vertical occupancy

Vertical occupancy can be defined for same and opposite direction traffic in the same way as lateral occupancy. Thus, “same direction, single separation minimum vertical occupancy” is the average number of aircraft, which are, in relation to the typical aircraft:

- flying in the same direction as it;
- nominally on the same track as it;
- nominally flying at flight levels one vertical separation minimum away from it; and
- within a longitudinal segment centred on it, whose length is $2S_x$.

A similar set of criteria can be used to define opposite direction vertical occupancy.

Therefore,

$$E_z = \frac{2T_z}{H}$$

Equation 49

Where

- T_z : The total same (opposite) direction proximity time generated in the system, i.e. the total time spent by same (opposite) direction aircraft pairs on the same flight paths at adjacent flight levels and within a longitudinal distance S_x of each other; and

- H: The total number of flying hours generated in the system during the period considered.

The same method used to estimate lateral occupancy, “direct estimation from time at waypoint passing”, can also be used to estimate same and opposite direction vertical occupancy. In this case, the condition that the points utilized should be approximately on a plane at right angles to the track system is automatically satisfied for aircraft on the same track. Thus, occupancy can be obtained using the following equation:

$$E_z = \frac{2n_z}{n}$$

Equation 50

where n_z is the total number of vertically proximate pairs and n is the total number of aircraft.

It was verified that the relationship between S_x and vertical occupancy was linear. The vertical collision risk has been calculated on the basis of $S_x = 80NM$.

For crossing routes, with intersection angle θ , a similar procedure can be used to obtain the vertical occupancy, $E(\theta)$. It is given by:

$$E_z(\theta) = \begin{cases} \frac{t_{sh}(\theta)}{t_F} \frac{2K(\theta)}{N}; & \text{for } t_{sh} < t_F \\ \frac{2K(\theta)}{N}; & \text{for } t_{sh} > t_F \end{cases}$$

Equation 51

where,



- N is the number of aircraft in the system during the observation period,
- $K(\theta_i)$ is the number of aircraft pairs in the crossing routes with angle θ_i ,
- t_{sh} is the average proximity time of pairs of aircraft in the crossing routes with angle θ
- t_F is the average flight time in the crossing routes,

In this assessment, as it was done in the CAR/SAM study, the conservative expression $2K(\theta)/N$ will be used.

The “direct estimation from time at waypoint passing”, can also be used in this case to estimate crossing occupancy. The way proximate events are obtained is explained in Annex 1.

4.2.7.1. Vertical occupancy values obtained

This section presents the vertical occupancy values provided by the CRM programme for the current time and an estimate of the occupancy until 2018, with the annual traffic growth rate indicated before, 8%.



4.2.7.1.1 Canaries

Table 35 shows some results on same and opposite vertical occupancy in Canaries location, based on traffic levels representative of 2008, (from July 2007 to July 2008).

Vertical occupancy	
Number of flights on UN-741	8439
Number of flights on UN-866	8461
Number of flights on UN-873	13174
Number of flights on UN-857	3822
Total number of flights (excluding flights on route RANDOM)	33896
Number of same direction vertical proximate events for UN-741	1456
Number of same direction vertical proximate events for UN-866	717
Number of opposite direction vertical proximate events for UN-873	492
Number of opposite direction vertical proximate events for UN-857	64
Total number of same direction proximate events	2173
Total number of opposite direction proximate events	556
Same direction vertical occupancy ($S_x=80\text{NM}$)	0.1282
Opposite direction vertical occupancy ($S_x=80\text{NM}$)	0.0328

Table 35
Vertical occupancy due to same and opposite direction traffic in Canaries location with current traffic levels

Apart from the traffic on the main routes, in the Canaries airspace there are some non published crossing trajectories with more than 50 aircraft per year, as it was explained before.

The number of flights on these routes can be found in the following table:



Number of flights on EDUMO-APASO	163
Number of flights on LUMPO-GUNET	65
Number of flights on TENPA-CVS	18
Number of flights on CVS-GUNET	282
Number of flights on LIMAL-ETIBA	213
Number of flights on COOR3-EDUMO	93
Number of flights on GAMBA-TENPA	52
Number of flights on EDUMO-COOR1	46
Number of flights on main routes (UN-741, UN-866, UN-873 and UN-857)	33896
Total number of aircraft	34098

Table 36
Number of aircraft in the Canaries airspace

All the aircraft on the crossing routes are already included in the number of flights on the main routes except for 202 of them, for most of them correspond to a change between routes. Therefore, the total number of aircraft in this case is 34098.

To calculate crossing occupancies, it is necessary to obtain the number of proximate pairs, i.e., the number of pairs for which horizontal separation is less than S_h . The value selected for S_h is the value used in the CAR/SAM study, [Ref. 12], i.e. $S_h = 80NM$.

Proximate events can be obtained comparing differences of passing times at the crossing point. The time window to be used in each case depends on the speeds and intersection angle of the routes, as it is explained in Annex 1. The values obtained for the Canaries are shown in Table 37, where V_1 refers to the average speed on the corresponding parallel route, V_2 refers to the average speed on the crossing route, and θ_1 and θ_2 are the two possible crossing angles, depending on the headings.

Time windows for crossing routes					
EDUMO-APASO	EDUMO	V ₁ = 465.7kts	V ₂ =564.1 kts	θ ₁ =150°	t ₁ =37 min
				θ ₂ =30°	t ₂ =11 min
	APASO	V ₁ =484.4 kts	V ₂ =564.1 kts	θ ₁ =150°	t ₁ =36 min
				θ ₂ =30°	t ₂ =10 min
LUMPO-GUNET	GUNET	V ₁ =467.3 kts	V ₂ =469.6 kts	θ ₁ =155°	t ₁ =48 min
				θ ₂ =25°	t ₂ =11 min
TENPA-CVS	TENPA	V ₁ =484.4 kts	V ₂ =459.5 kts	θ ₁ =160°	t ₁ =59 min
				θ ₂ =20°	t ₂ =11 min
CVS-GUNET	GUNET	V ₁ =467.3 kts	V ₂ =447.8 kts	θ ₁ =163°	t ₁ =71 min
				θ ₂ =17°	t ₂ =11 min
LIMAL-ETIBA	LIMAL	V ₁ =463.4kts	V ₂ =502.7 kts	θ ₁ =163°	t ₁ =68 min
				θ ₂ =17°	t ₂ =11 min
	ETIBA	V ₁ =467.3 kts	V ₂ =502.7 kts	θ ₁ =163°	t ₁ =67 min
				θ ₂ =17°	t ₂ =11 min
COOR3-EDUMO	EDUMO	V ₁ =465.7 kts	V ₂ =462.5 kts	θ ₁ =140°	t ₁ =31 min
				θ ₂ =40°	t ₂ =11 min
GAMBA-TENPA	TENPA	V ₁ =484.4 kts	V ₂ =498.1 kts	θ ₁ =155°	t ₁ =46 min
				θ ₂ =25°	t ₂ =10 min
EDUMO-COOR1	EDUMO	V ₁ =465.7 kts	V ₂ =456.5 kts	θ ₁ =173°	t ₁ =171 min
				θ ₂ =7°	t ₂ =11 min

Table 37
Time windows for crossing occupancies in the Canaries

With these time windows, the number of proximate pairs obtained can be seen in Table 38.



Number of proximate events due to crossing traffic				
EDUMO-APASO	EDUMO	$\theta_1=150$	At adjacent flight levels	9
			At the same flight level	5
		$\theta_2=30$	At adjacent flight levels	13
			At the same flight level	0
	APASO	$\theta_1=150$	At adjacent flight levels	12
			At the same flight level	1
		$\theta_2=30$	At adjacent flight levels	11
			At the same flight level	7
LUMPO-GUNET	GUNET	$\theta_1=155$	At adjacent flight levels	10
			At the same flight level	1
		$\theta_2=25$	At adjacent flight levels	16
			At the same flight level	0
TENPA-CVS	TENPA	$\theta_1=160$	At adjacent flight levels	0
			At the same flight level	0
		$\theta_2=20$	At adjacent flight levels	0
			At the same flight level	0
CVS-GUNET	GUNET	$\theta_1=163$	At adjacent flight levels	46
			At the same flight level	0
		$\theta_2=17$	At adjacent flight levels	0
			At the same flight level	1
LIMAL-ETIBA	LIMAL	$\theta_1=163$	At adjacent flight levels	57
			At the same flight level	13
		$\theta_2=17$	At adjacent flight levels	8
			At the same flight level	24
	ETIBA	$\theta_1=163$	At adjacent flight levels	29
			At the same flight level	2
COOR3-EDUMO	EDUMO	$\theta_1=140$	At adjacent flight levels	7
			At the same flight level	5
		$\theta_2=40$	At adjacent flight levels	1
			At the same flight level	1
GAMBA-TENPA	TENPA	$\theta_1=155$	At adjacent flight levels	0
			At the same flight level	0
		$\theta_2=25$	At adjacent flight levels	8
			At the same flight level	1
EDUMO-COOR1	EDUMO	$\theta_1=173$	At adjacent flight levels	0
			At the same flight level	0
		$\theta_2=7$	At adjacent flight levels	18
			At the same flight level	2

Table 38
Number of proximate events due to crossing traffic in the Canaries



It can be seen that some proximate events involve aircraft at the same flight level. 53 of these events at the same level involve aircraft within eleven minutes of each other and for 32 of them the time difference at the crossing point is below or equal to nine minutes. Possible explanations for this apparent violation of the required separation would be an error in the flight level or passing time included in Palestra database or an operational error that was not registered by the air traffic controller and/or by the aircraft.

Further analysis would be required for these cases to identify whether they are in fact proximate events at the same level or not. No more information is available for further clarification and no deviation reports have been received. Therefore, in this assessment, for the purpose of accounting for these events in the collision risk model, the “same flight level” crossing proximity events are counted as “adjacent flight level” proximity events. This approach was also followed by ARINC in [Ref. 2]. Nevertheless, if it could be shown that these events were in fact violations of the vertical separation standard, then these events should be treated as large height keeping deviations and be accounted for in the total vertical collision risk.

With these considerations, once vertical occupancy is calculated based on current traffic levels, it is possible to estimate the occupancy in the following years taking into account the annual traffic growth rate forecasted. Vertical occupancy values from 2008 to 2018 with an annual traffic growth rate of 8% are shown in Table 39.



8% annual traffic growth			2008	20010	2012	2014	2016	2018
Same direction vertical occupancy			0.1282	0.1496	0.1744	0.2035	0.2373	0.2768
Opposite direction vertical occupancy			0.0328	0.0383	0.0446	0.0521	0.0607	0.0708
Crossing occupancy	EDUMO- APASO	150°	0.0016	0.0018	0.0022	0.0025	0.0029	0.0034
		30°	0.0018	0.0021	0.0025	0.0029	0.0034	0.0039
	LUMPO-GUNET	155	0.0006	0.0008	0.0009	0.0010	0.0012	0.0014
		25	0.0009	0.0011	0.0013	0.0015	0.0017	0.0020
	TENPA-CVS	160°	0	0	0	0	0	0
		20°	0	0	0	0	0	0
	CVS-GUNET	163°	0.0027	0.0031	0.0037	0.0043	0.0050	0.0058
		17°	5.87*10 ⁻⁵	6.84*10 ⁻⁵	7.98*10 ⁻⁵	9.31*10 ⁻⁵	1.09*10 ⁻⁴	1.27*10 ⁻⁴
	LIMAL-ETIBA	163°	0.0059	0.0069	0.0081	0.0094	0.0110	0.0128
		17°	0.0049	0.0057	0.0067	0.0078	0.0091	0.0106
	COOR3- EDUMO	140°	0.0007	0.0008	0.0010	0.0011	0.0013	0.0015
		40°	1.17*10 ⁻⁴	1.37*10 ⁻⁴	1.60*10 ⁻⁴	1.86*10 ⁻⁴	2.17*10 ⁻⁴	2.53*10 ⁻⁴
	GAMBA- TENPA	155°	0	0	0	0	0	0
		25°	0.0005	0.0006	0.0007	0.0008	0.0010	0.0011
	EDUMO- COOR1	173°	0	0	0	0	0	0
		7°	0.0012	0.0014	0.0016	0.0019	0.0022	0.0025

Table 39
Vertical occupancy estimate for the Canaries until 2018 with an annual traffic growth rate of 8%

4.2.7.1.2 SAL1

Table 40 collects some results on same and opposite vertical occupancy in SAL1, obtained with data from 1st November 2007 till 31st January 2008 and from 1st April till 30th June 2008. These values will be representative for year 2008.



Vertical occupancy	
Number of flights on UN-741	4144
Number of flights on UN-866	4155
Number of flights on UN-873	4179
Number of flights on UN-857	1727
Total number of flights (excluding flights on route RANDOM)	14205
Number of same direction vertical proximate events for UN-741	705
Number of same direction vertical proximate events for UN-866	455
Number of opposite direction vertical proximate events for UN-873	66
Number of opposite direction vertical proximate events for UN-857	8
Total number of same direction proximate events	1160
Total number of opposite direction proximate events	74
Same direction vertical occupancy ($S_x=80\text{NM}$)	0.1633
Opposite direction vertical occupancy ($S_x=80\text{NM}$)	0.0104

Table 40
Vertical occupancy due to same and opposite direction traffic in SAL1 with current traffic levels

Apart from the traffic on the main routes, in SAL1 there is also some traffic crossing the Corridor on routes UR-976/UA-602 and on non published routes.

The number of flights on these routes can be found in the following table:

Number of flights on UR-976/UA-602	755
Number of flights on ULTEM-LUMPO (“direct to”)	1136
Number of flights on TENPA-CVS	12
Number of flights on CVS-GUNET	155
Number of flights on GAMBA-COOR1	12
Number of flights on GAMBA-TENPA	18
Number of flights on CVS-AMDOL	21
Number of flights on CVS-BOTNO	23
Number of flights on main routes (UN-741, UN-866, UN-873 and UN-857)	14205
Total number of flights	16125

Table 41
Number of flights in SAL1



All the aircraft on the non published crossing routes are already included in the number of flights on the main routes, except for those on the direct route ULTEM-LUMPO and 29 of the rest of routes.

The time windows to obtain proximate pairs are, in this case, the ones shown in Table 42.

Time windows for crossing routes					
UR-976/UA-602		V ₁ = 466.4 kts	V ₂ =468.7 kts	θ ₁ =95°	t ₁ =16 min
				θ ₂ =85°	t ₂ =14 min
ULTEM-LUMPO (“Direct to”)		V ₁ =466.4 kts	V ₂ =460.2 kts	θ ₁ =90°	t ₁ =15 min
				θ ₂ =90°	t ₂ =15 min
TENPA-CVS	CVS	V ₁ =464.4 kts	V ₂ =0 kts	θ ₁ =160°	t ₁ =0 min
				θ ₂ =20°	t ₂ =0 min
CVS-GUNET	CVS	V ₁ =464.4 kts	V ₂ =458.3 kts	θ ₁ =165°	t ₁ =80 min
				θ ₂ =15°	t ₂ =11 min
GAMBA-COOR1	GAMBA	V ₁ =452.5 kts	V ₂ =467.0 kts	θ ₁ =165°	t ₁ =80 min
				θ ₂ =15°	t ₂ =11 min
GAMBA-TENPA	GAMBA	V ₁ = 452.5 kts	V ₂ =515.7 kts	θ ₁ =155°	t ₁ =46 min
				θ ₂ =25°	t ₂ =11 min
CVS-AMDOL	CVS	V ₁ =464.4 kts	V ₂ =0 kts	θ ₁ =155°	t ₁ =0 min
				θ ₂ =25°	t ₂ =0 min
CVS-BOTNO	CVS	V ₁ =464.4 kts	V ₂ =0 kts	θ ₁ =155°	t ₁ =0 min
				θ ₂ =25°	t ₂ =0 min

Table 42
Time windows for crossing occupancies in SAL1

With these values, the number of proximate events obtained is:



Number of proximate events due to crossing traffic				
UR-976/UA-602	GAMBA	$\theta_1=95^\circ$	At adjacent flight levels	32
			At the same flight level	15
		$\theta_2=85^\circ$	At adjacent flight levels	145
			At the same flight level	58
	IREDO	$\theta_1=95^\circ$	At adjacent flight levels	197
			At the same flight level	110
		$\theta_2=85^\circ$	At adjacent flight levels	16
			At the same flight level	11
	CVS	$\theta_1=95^\circ$	At adjacent flight levels	71
			At the same flight level	137
		$\theta_2=85^\circ$	At adjacent flight levels	21
			At the same flight level	12
	UGAMA	$\theta_1=95^\circ$	At adjacent flight levels	10
			At the same flight level	7
		$\theta_2=85^\circ$	At adjacent flight levels	19
			At the same flight level	8
	ORABI	$\theta_1=95^\circ$	At adjacent flight levels	3
			At the same flight level	2
		$\theta_2=85^\circ$	At adjacent flight levels	18
			At the same flight level	0
ULTEM-LUMPO (“Diret-to”)	Intersection with UN-741	$\theta_1=\theta_2=90^\circ$	At adjacent flight levels	208
			At the same flight level	132
	Intersection with UN-866	$\theta_1=\theta_2=90^\circ$	At adjacent flight levels	153
			At the same flight level	85
	Intersection with UN-873	$\theta_1=\theta_2=90^\circ$	At adjacent flight levels	105
			At the same flight level	125
	Intersection with UN-857	$\theta_1=\theta_2=90^\circ$	At adjacent flight levels	117
			At the same flight level	35
TENPA-CVS	CVS	$\theta_1=160^\circ$	At adjacent flight levels	0
			At the same flight level	0
		$\theta_2=20^\circ$	At adjacent flight levels	0
			At the same flight level	0
CVS-GUNET	CVS	$\theta_1=165^\circ$	At adjacent flight levels	2
			At the same flight level	0
		$\theta_2=15^\circ$	At adjacent flight levels	0
			At the same flight level	0

Table 43
Number of proximate events due to crossing traffic in SAL1



Number of proximate events due to crossing traffic				
GAMBA-COOR1	GAMBA	$\theta_1=165^\circ$	At adjacent flight levels	1
			At the same flight level	2
		$\theta_2=15^\circ$	At adjacent flight levels	0
			At the same flight level	0
GAMBA-TENPA	GAMBA	$\theta_1=155^\circ$	At adjacent flight levels	6
			At the same flight level	2
		$\theta_2=25^\circ$	At adjacent flight levels	0
			At the same flight level	0
CVS-AMDOL	CVS	$\theta_1=155^\circ$	At adjacent flight levels	0
			At the same flight level	0
		$\theta_2=25^\circ$	At adjacent flight levels	0
			At the same flight level	0
CVS-BOTNO	CVS	$\theta_1=155^\circ$	At adjacent flight levels	0
			At the same flight level	0
		$\theta_2=25^\circ$	At adjacent flight levels	0
			At the same flight level	0

Table 43 (Cont.)
Number of proximate events due to crossing traffic in SAL1

It can be seen in Table 43 that a lot of proximate events at the same flight level, within less than 15 minutes of each other, have been detected, as it happened in the Canaries location. For 426 of them, the time difference at the crossing point is below or equal to 9 minutes. Several reasons are possible for this, such as:

- A tactical flight level change to separate crossing traffic was not included in the data provided;
- There was an error in the time provided in the data;
- The air traffic controller did not register a flight level change;
- The aircraft made contact too late to allow an action by the air traffic controller;
- There was an operational error that was not registered by the air traffic controller and/or by the aircraft;



- Passing times at the crossing point are not precise, due to the need of extrapolation of the traffic data

Given that such a great amount of proximate events is not possible and that no deviation reports have been received for those aircraft, it will be assumed that they are due to the extrapolation of data and the lack of data regarding flight level changes in the traffic data provided, and they will be considered as adjacent level proximate events. Nevertheless, this hypothesis should be verified when more information is available, because it may have an impact in the results in case that any of the proximate events were, in fact, at the same flight level.

With these considerations, vertical occupancy from 2008 to 2018 with an annual traffic growth rate of 8% is calculated and presented in Table 44.

8% annual traffic growth		2008	2010	2012	2014	2016	2018	
Same direction vertical occupancy		0.1633	0.1905	0.2222	0.2592	0.3023	0.3526	
Opposite direction vertical occupancy		0.0104	0.0122	0.0142	0.0165	0.0193	0.0225	
Crossing occupancy	UR-976/UA-602	95°	0.0724	0.0845	0.0985	0.1149	0.1341	0.1564
		85°	0.0382	0.0446	0.0520	0.0606	0.0707	0.0825
	ULTEM-LUMPO	90°	0.1191	0.1389	0.1620	0.1889	0.2204	0.2571
		TENPA-CVS	160°	0	0	0	0	0
		20°	0	0	0	0	0	0
	CVS-GUNET	165°	2.48*10 ⁻⁴	2.89*10 ⁻⁴	3.38*10 ⁻⁴	3.94*10 ⁻⁴	4.59*10 ⁻⁴	5.36*10 ⁻⁴
		15°	0	0	0	0	0	0
	GAMBA-COOR1	165°	3.72*10 ⁻⁴	4.34*10 ⁻⁴	5.06*10 ⁻⁴	5.91*10 ⁻⁴	6.89*10 ⁻⁴	8.03*10 ⁻⁴
		15°	0	0	0	0	0	0
	GAMBA-TENPA	155°	0.0010	0.0012	0.0013	0.0016	0.0018	0.0021
		25°	0	0	0	0	0	0
	CVS-AMDOL	155°	0	0	0	0	0	0
		25°	0	0	0	0	0	0
	CVS-BOTNO	155°	0	0	0	0	0	0
		25°	0	0	0	0	0	0

Table 44
Vertical occupancy estimate for SAL1 until 2018 with an 8% annual traffic growth rate



4.2.7.1.3 SAL2

Table 45 shows some results on same and opposite vertical occupancy in SAL2. These results are obtained with data from 1st November 2007 till 31st January 2008 and from 1st April till 30th June 2008, that are representative for year 2008.

Vertical occupancy	
Number of flights on UN-741	4319
Number of flights on UN-866	4169
Number of flights on UN-873	4654
Number of flights on UN-857	1757
Total number of flights (excluding flights on route RANDOM)	14899
Number of same direction vertical proximate events for UN-741	720
Number of same direction vertical proximate events for UN-866	410
Number of opposite direction vertical proximate events for UN-873	73
Number of opposite direction vertical proximate events for UN-857	31
Total number of same direction proximate events	1130
Total number of opposite direction proximate events	104
Same direction vertical occupancy ($S_x=80\text{NM}$)	0.1517
Opposite direction vertical occupancy ($S_x=80\text{NM}$)	0.0140

Table 45
Vertical occupancy due to same and opposite direction traffic in SAL2 with current traffic levels

Apart from the traffic on the main routes, in SAL2 there is also some traffic crossing the Corridor on non published route. The number of flights on these routes during these six months is indicated in Table 46:



Number of flights on ULTEM-KENOX	61
Number of flights on KENOX-COOR2	21
Number of flights on CVS-AMDOL	21
Number of flights on BOTNO-CVS	23
Number of flights on main routes (UN-741, UN-866, UN-873 and UN-857)	14899
Total number of flights	14922

Table 46
Number of flights in SAL2

All the aircraft on the crossing routes are already included in the number of flights on the main routes except for 23 of them. Therefore, the total number of aircraft in this case is 14922.

The time windows to obtain proximate pairs are, in this case, the ones shown in Table 47.

Time windows for crossing routes					
ULTEM-KENOX	KENOX	$V_1=451.7$ kts	$V_2=473.1$ kts	$\theta_1=140^\circ$	$t_1=31$ min
				$\theta_2=40^\circ$	$t_2=11$ min
KENOX-COOR2	KENOX	$V_1=451.7$ kts	$V_2=479.4$ kts	$\theta_1=156^\circ$	$t_1=50$ min
				$\theta_2=24^\circ$	$t_2=11$ min
CVS-AMDOL	AMDOL	$V_1=495.3$ kts	$V_2=454.6$ kts	$\theta_1=156^\circ$	$t_1=49$ min
				$\theta_2=24^\circ$	$t_2=11$ min
BOTNO-CVS	BOTNO	$V_1=470.8$ kts	$V_2=461.8$ kts	$\theta_1=156^\circ$	$t_1=50$ min
				$\theta_2=24^\circ$	$t_2=11$ min

Table 47
Time windows for crossing occupancies in SAL2

With these values, the number of proximate events obtained is:



Number of proximate events due to crossing traffic				
ULTEM-KENOX	KENOX	$\theta_1=140$	At adjacent flight levels	0
			At the same flight level	0
		$\theta_2=40$	At adjacent flight levels	4
			At the same flight level	3
KENOX-COOR2	KENOX	$\theta_1=156$	At adjacent flight levels	3
			At the same flight level	3
		$\theta_2=24$	At adjacent flight levels	7
			At the same flight level	2
CVS-AMDOL	AMDOL	$\theta_1=156$	At adjacent flight levels	2
			At the same flight level	0
		$\theta_2=24$	At adjacent flight levels	1
			At the same flight level	0
BOTNO-CVS	BOTNO	$\theta_1=156$	At adjacent flight levels	4
			At the same flight level	0
		$\theta_2=24$	At adjacent flight levels	1
			At the same flight level	0

Table 48
Number of proximate events due to crossing traffic in SAL2

Here again, as it happened in SAL1 or Canaries, there are proximate events at the same flight level. In this case, for 3 of the proximate pairs detected at the same flight level, the time difference at the crossing point is less than 9 minutes. The same reasons explained before are of application here.

No deviation reports have been received for these cases either, and therefore, the hypothesis of considering proximate events at the same flight level as proximate at adjacent flight levels will also be made for this location. Nevertheless, this hypothesis should be verified.

With these considerations, the results obtained with an annual traffic growth rate of 8% are presented in Table 49.



8% annual traffic growth			2008	2010	2012	2014	2016	2018
Same direction vertical occupancy			0.1517	0.1769	0.2064	0.2407	0.2808	0.3275
Opposite direction vertical occupancy			0.0140	0.0163	0.0190	0.0221	0.0258	0.0301
Crossing occupancy	ULTEM- KENOX	140°	0	0	0	0	0	0
		40°	0.0009	0.0011	0.0013	0.0015	0.0017	0.0020
	KENOX-COOR2	156°	0.0008	0.0009	0.0011	0.0013	0.0015	0.0017
		24°	0.0012	0.0014	0.0016	0.0019	0.0022	0.0026
	CVS-AMDOL	156°	2.68*10 ⁻⁴	3.13*10 ⁻⁴	3.65*10 ⁻⁴	4.25*10 ⁻⁴	4.96*10 ⁻⁴	5.79*10 ⁻⁴
		24°	1.34*10 ⁻⁴	1.56*10 ⁻⁴	1.82*10 ⁻⁴	2.13*10 ⁻⁴	2.48*10 ⁻⁴	2.89*10 ⁻⁴
	CVS-BOTNO	156°	0.0005	0.0006	0.0007	0.0009	0.0010	0.0012
		24°	1.34*10 ⁻⁴	1.56*10 ⁻⁴	1.82*10 ⁻⁴	2.13*10 ⁻⁴	2.48*10 ⁻⁴	2.89*10 ⁻⁴

Table 49
Vertical occupancy estimate for SAL2 until 2018 with an 8% annual traffic growth rate

4.2.7.1.4 Dakar1

Table 50 collects some results on same and opposite vertical occupancy in Dakar1 for the period 1st November 2007-31st January 2008 and 1st April 2008-30th June 2008.

Vertical occupancy	
Number of flights on UN-741	4302
Number of flights on UN-866	4171
Number of flights on UN-873	4650
Number of flights on UN-857	1759
Total number of flights (excluding flights on route RANDOM)	14882
Number of same direction vertical proximate events for UN-741	722
Number of same direction vertical proximate events for UN-866	451
Number of opposite direction vertical proximate events for UN-873	111
Number of opposite direction vertical proximate events for UN-857	27
Total number of same direction proximate events	1173
Total number of opposite direction proximate events	138
Same direction vertical occupancy (S _x =80NM)	0.1576
Opposite direction vertical occupancy (S _x =80NM)	0.0185

Table 50
Vertical occupancy due to same and opposite direction traffic in Dakar1 with current traffic levels



No traffic data from Dakar has been received for this study. Therefore, it has not been possible to analyse occupancy due to the crossing route UL-435. For this reason, the results obtained for this location may be underestimated.

Taking this into account, the vertical occupancy values obtained with an annual traffic growth rate of 8% are the ones shown in Table 51:

8% annual traffic growth			2008	2010	2012	2014	2016	2018
Same direction vertical occupancy			0.1576	0.1839	0.2145	0.2502	0.2918	0.3403
Opposite direction vertical occupancy			0.0185	0.0216	0.0252	0.0294	0.0343	0.0400
Crossing occupancy	UL-435	97°	---	---	---	---	---	---
		83°	---	---	---	---	---	---

Table 51
Vertical occupancy estimate for Dakar1 until 2018 with an 8% annual traffic growth rate

4.2.7.1.5 Dakar2

Table 52 shows the number of flights, the number of proximate events and the values for same and opposite vertical occupancy obtained with data from 1st November 2007 to 31st January 2008 and from 1st April 2008 to 30th June 2008 in Dakar2 location. There is no crossing traffic in this location and, therefore, no crossing occupancy.

Vertical occupancy values obtained until 2018, assuming an annual traffic growth rate of 8% can be seen in Table 53:



Vertical occupancy	
Number of flights on UN-741	4302
Number of flights on UN-866	4178
Number of flights on UN-873	4645
Number of flights on UN-857	1760
Total number of flights (excluding flights on route RANDOM)	14885
Number of same direction vertical proximate events for UN-741	721
Number of same direction vertical proximate events for UN-866	448
Number of opposite direction vertical proximate events for UN-873	103
Number of opposite direction vertical proximate events for UN-857	28
Total number of same direction proximate events	1169
Total number of opposite direction proximate events	131
Same direction vertical occupancy ($S_x=80\text{NM}$)	0.1571
Opposite direction vertical occupancy ($S_x=80\text{NM}$)	0.0176

Table 52
Vertical occupancy due to same and opposite direction traffic in Dakar2 with current traffic levels

8% annual traffic growth	2008	2010	2012	2014	2016	2018
Same direction vertical occupancy	0.1571	0.1832	0.2137	0.2493	0.2907	0.3391
Opposite direction vertical occupancy	0.0176	0.0205	0.0239	0.0279	0.0326	0.0380

Table 53
Vertical occupancy estimate for Dakar2 until 2018 with an 8% annual traffic growth rate

4.2.7.1.6 Recife

Table 54 presents results on same and opposite vertical occupancy in Recife location, based on data from 1st November 2007 to 31st January 2008 and from 1st April 2008 to 30th June 2008.



Vertical occupancy	
Number of flights on UN-741	4302
Number of flights on UN-866	4178
Number of flights on UN-873	4640
Number of flights on UN-857	1759
Total number of flights (excluding flights on route RANDOM)	14879
Number of same direction vertical proximate events for UN-741	721
Number of same direction vertical proximate events for UN-866	450
Number of opposite direction vertical proximate events for UN-873	96
Number of opposite direction vertical proximate events for UN-857	20
Total number of same direction proximate events	1171
Total number of opposite direction proximate events	116
Same direction vertical occupancy ($S_x=80\text{NM}$)	0.1574
Opposite direction vertical occupancy $S_x=80\text{NM}$	0.0156

Table 54
Vertical occupancy due to same and opposite direction traffic in Recife with current traffic levels

In Recife, there is some traffic crossing the Corridor on routes UL-695/UL-375. The number of aircraft on these routes is:

Number of flights on UL-695/UL-375	93
Number of flights on main routes (UN-741, UN-866, UN-873 and UN-857)	14879
Total number of flights	14972

Table 55
Number of flights in Recife

The time windows obtained in this case are the ones shown in the following table (V_1 refers to the average speed on the parallel routes and V_2 , to the average speed on the crossing route)

Time windows for crossing occupancy				
UL-695/UL-375	V ₁ =476.3 kts	V ₂ =471.8 kts	$\theta_1=96^\circ$	t ₁ =16 min
			$\theta_2=84^\circ$	t ₂ =14 min

Table 56
Time windows for crossing occupancy in Recife

With these time windows, the number of proximate pairs obtained is:

Number of proximate events due to crossing traffic				
UL-695/UL-375	DIKEB	$\theta_1=96^\circ$	At adjacent flight levels	23
			At the same flight level	9
		$\theta_2=84^\circ$	At adjacent flight levels	1
			At the same flight level	0
	OBKUT	$\theta_1=96^\circ$	At adjacent flight levels	5
			At the same flight level	2
		$\theta_2=84^\circ$	At adjacent flight levels	7
			At the same flight level	2
	ORARO	$\theta_1=96^\circ$	At adjacent flight levels	3
			At the same flight level	7
		$\theta_2=84^\circ$	At adjacent flight levels	4
			At the same flight level	0
NOISE	$\theta_1=96^\circ$	At adjacent flight levels	0	
		At the same flight level	3	
	$\theta_2=84^\circ$	At adjacent flight levels	6	
		At the same flight level	0	

Table 57
Number of proximate events due to crossing traffic in Recife

As it occurred in other locations, some proximate pairs at the same flight level have been detected. In this case, 23 of the 72 proximate pairs found are at the same flight level, and from these 23, the time difference at the crossing point is less than ten minutes for 8 of them.

As no large height deviation reports have been received for these events, it will be considered that they are proximate events at adjacent flight levels, as it has been

done in other locations, assuming that they are due to the need of extrapolation and the lack of data about flight level changes. Nevertheless, this hypothesis should be verified, because it may have an impact on the results, as it has been explained before.

With these considerations, the results obtained with an annual traffic growth rate of 8% are shown in Table 58.

8% annual traffic growth			2008	2010	2012	2014	2016	2018
Same direction vertical occupancy			0.1574	0.1836	0.2142	0.2498	0.2913	0.3398
Opposite direction vertical occupancy			0.0156	0.0182	0.0212	0.0247	0.0289	0.0337
Crossing occupancy	UL-695/UL-375	96°	0.0069	0.0081	0.0095	0.0110	0.0129	0.0150
		84°	0.0027	0.0031	0.0036	0.0042	0.0049	0.0058

Table 58
Vertical occupancy estimate for Recife until 2018 with an 8% annual traffic growth rate

4.2.8. Technical vertical collision risk

The technical vertical collision risk values obtained until 2018 in the different locations are the ones summarized in the following sections.

4.2.8.1 Canaries

Table 59 shows the estimate of the vertical collision risk, in Canaries location, considering that the traffic growth factor is 8% per annum. These results can also be seen in Figure 27 and Figure 28.



Technical Vertical Collision Risk	8% annual traffic growth
2008	0.2725×10^{-9}
2009	0.2943×10^{-9}
2010	0.3178×10^{-9}
2011	0.3433×10^{-9}
2012	0.3707×10^{-9}
2013	0.4004×10^{-9}
2014	0.4324×10^{-9}
2015	0.4670×10^{-9}
2016	0.5044×10^{-9}
2017	0.5447×10^{-9}
2018	0.5883×10^{-9}

Table 59
Technical vertical collision risk for the period 2008-2018 in the Canaries

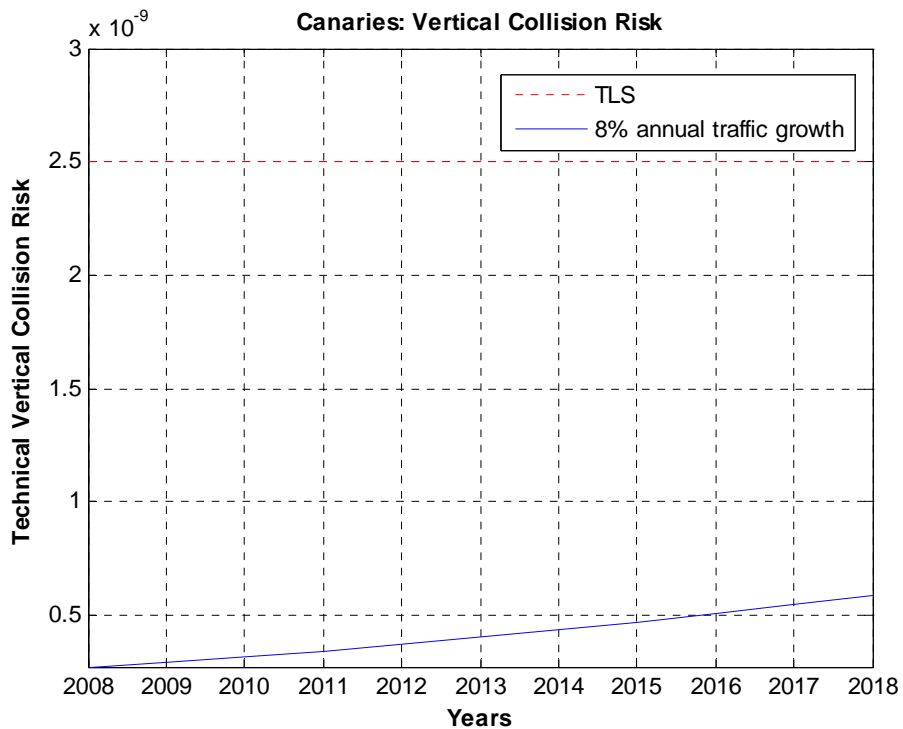


Figure 27
Technical vertical collision risk for the period 2008-2018 in the Canaries



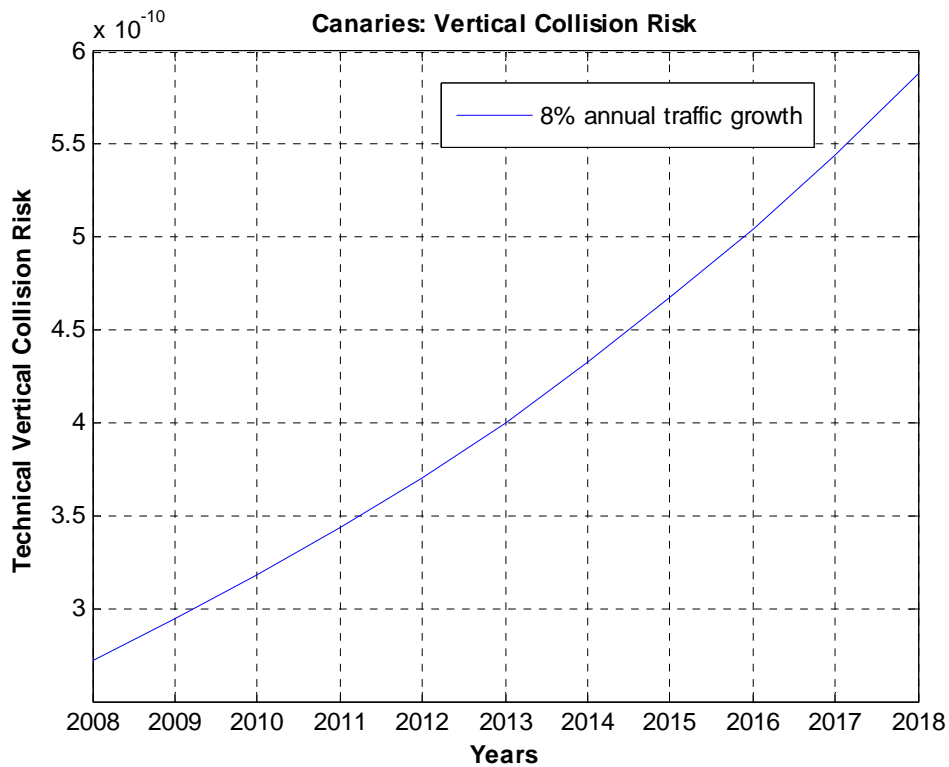


Figure 28
Technical vertical collision risk for the period 2008-2018 in the Canaries - Enlarged

4.2.8.2 SAL1

Table 60 shows the estimate of the technical vertical collision risk, in SAL1 location, considering that the traffic growth factor is 8% per annum. These results are also depicted in Figure 29 and Figure 30.



Technical Vertical Collision Risk	8% annual traffic growth
2008	0.1337*10 ⁻⁹
2009	0.1444*10 ⁻⁹
2010	0.1560*10 ⁻⁹
2011	0.1684*10 ⁻⁹
2012	0.1819*10 ⁻⁹
2013	0.1965*10 ⁻⁹
2014	0.2122*10 ⁻⁹
2015	0.2292*10 ⁻⁹
2016	0.2475*10 ⁻⁹
2017	0.2673*10 ⁻⁹
2018	0.2887*10 ⁻⁹

Table 60
Technical vertical collision risk for the period 2008-2018 in SAL1

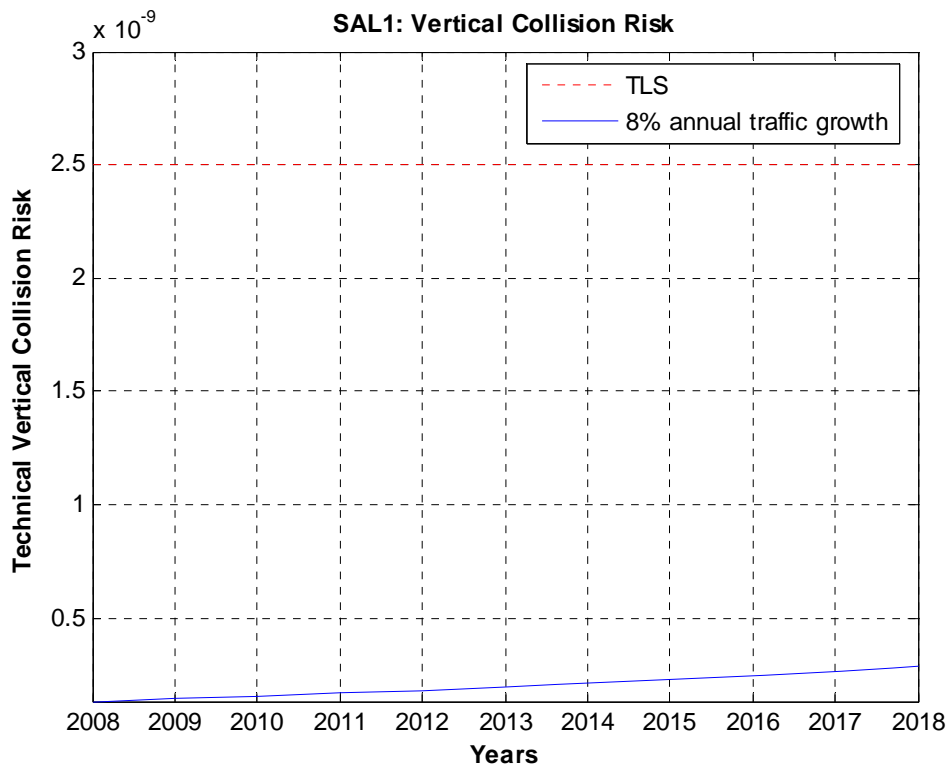


Figure 29
Technical vertical collision risk for the period 2008-2018 in SAL1



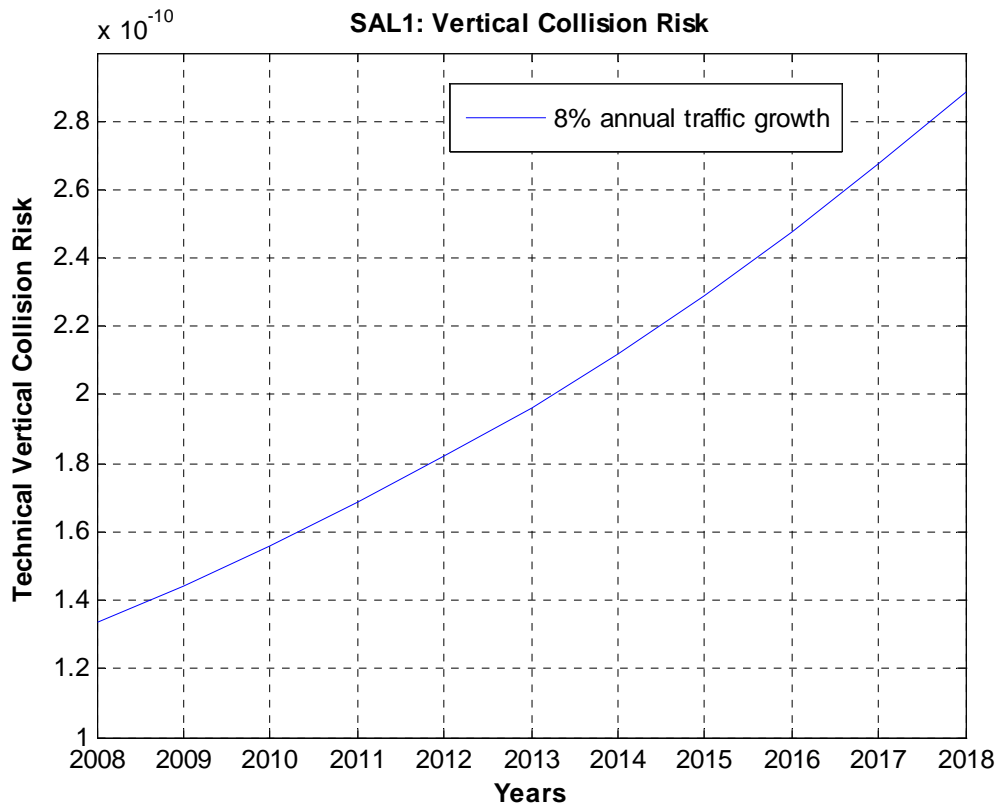


Figure 30
Technical vertical collision risk for the period 2008-2018 in SAL1 - Enlarged

4.2.8.3 SAL2

An estimate of the technical vertical risk, in SAL2 location, considering that the traffic growth factor is 8% per annum, is presented in Table 61. These results can also be seen in Figure 31 and Figure 32.

Technical Vertical Collision Risk	8% annual traffic growth
2008	0.1488*10 ⁻⁹
2009	0.1607*10 ⁻⁹
2010	0.1735*10 ⁻⁹
2011	0.1874*10 ⁻⁹
2012	0.2024*10 ⁻⁹
2013	0.2186*10 ⁻⁹
2014	0.2361*10 ⁻⁹
2015	0.2550*10 ⁻⁹
2016	0.2754*10 ⁻⁹
2017	0.2974*10 ⁻⁹
2018	0.3212*10 ⁻⁹

Table 61
Technical vertical collision risk for the period 2008-2018 in SAL2

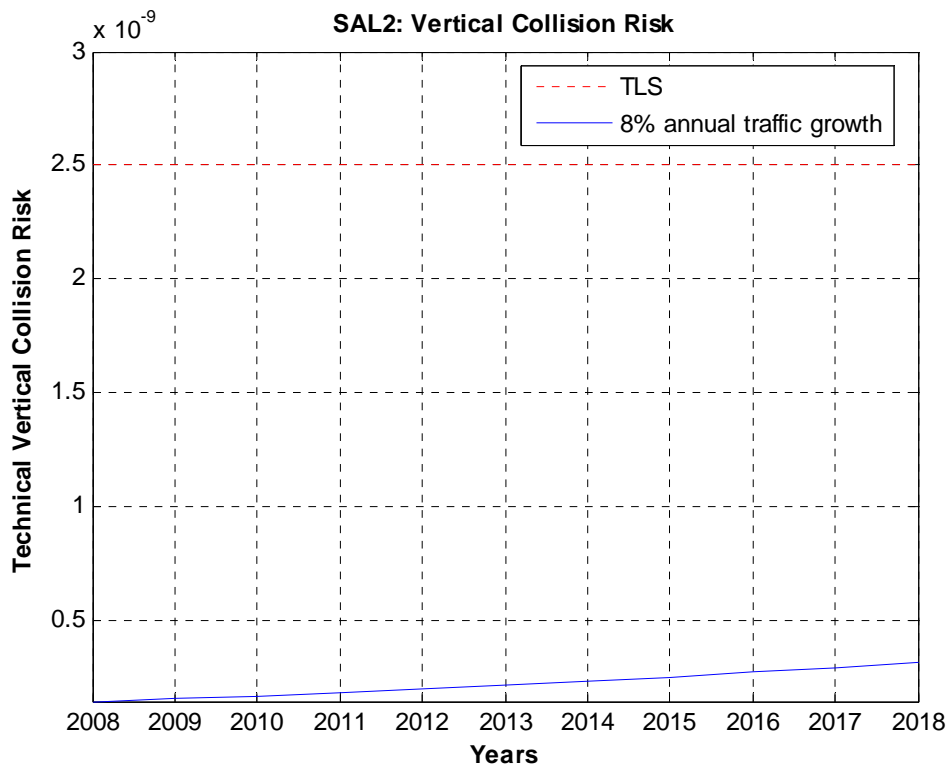


Figure 31
Technical vertical collision risk for the period 2008-2018 in SAL2



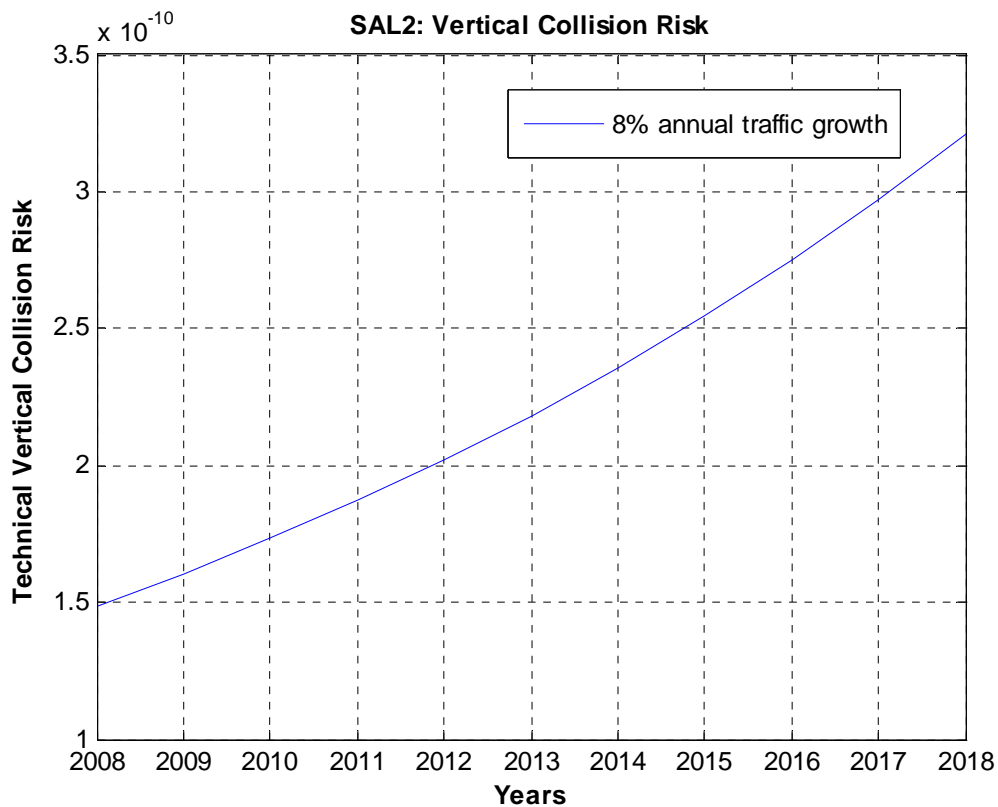


Figure 32
Technical vertical collision risk for the period 2008-2018 in SAL2 - Enlarged

4.2.8.4. Dakar1

Table 62 collects the estimate of the technical vertical collision risk, in Dakar1 location, considering that the traffic growth factor is 8% per annum. These results can also be found in Figure 33 and Figure 34.



Technical Vertical Collision Risk	8% annual traffic growth
2008	0.1822*10 ⁻⁹
2009	0.1968*10 ⁻⁹
2010	0.2126*10 ⁻⁹
2011	0.2296*10 ⁻⁹
2012	0.2479*10 ⁻⁹
2013	0.2678*10 ⁻⁹
2014	0.2892*10 ⁻⁹
2015	0.3123*10 ⁻⁹
2016	0.3373*10 ⁻⁹
2017	0.3643*10 ⁻⁹
2018	0.3935*10 ⁻⁹

Table 62
Technical vertical collision risk for the period 2008-2018 in Dakar1

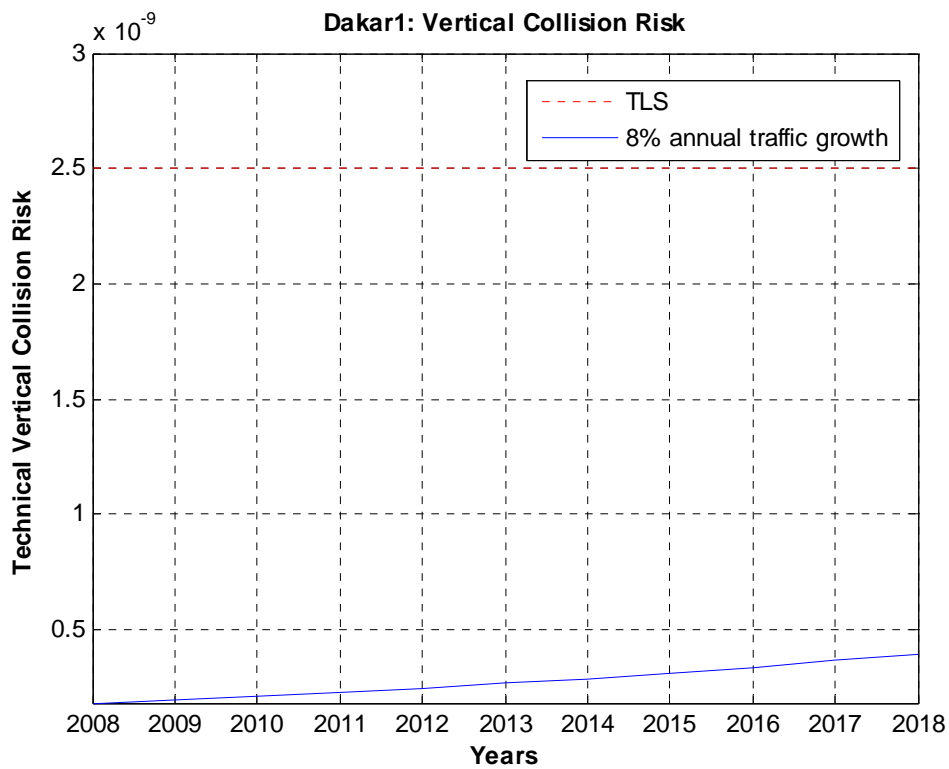


Figure 33
Technical vertical collision risk for the period 2008-2018 in Dakar1



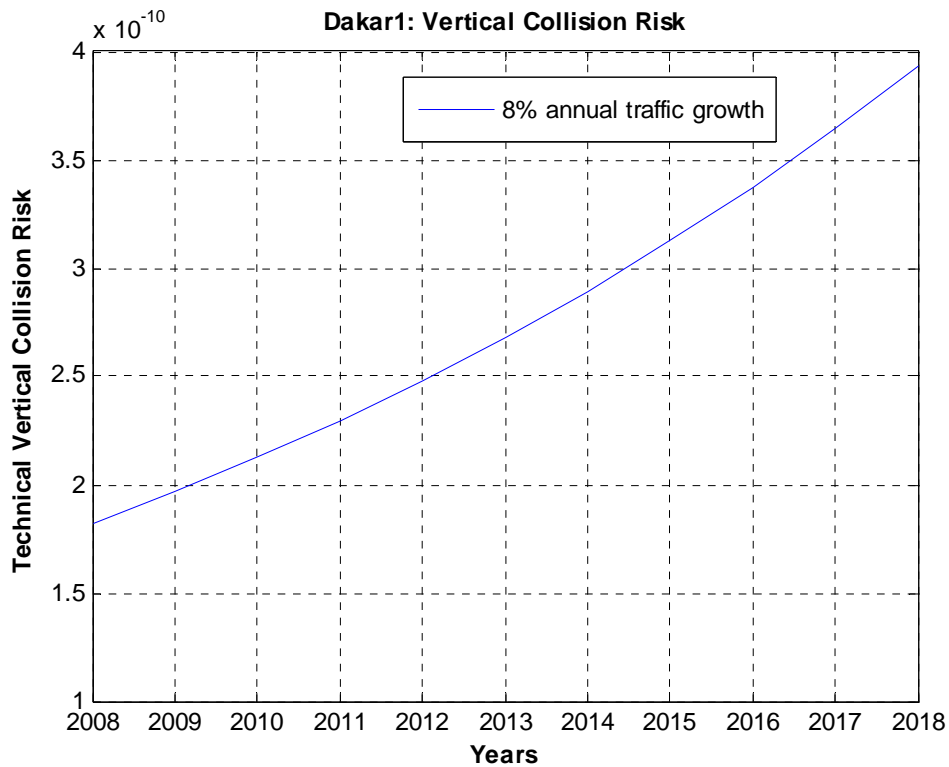


Figure 34
Technical vertical collision risk for the period 2008-2018 in Dakar1 - Enlarged

4.2.8.5. Dakar2

Table 63 shows the estimate of the technical vertical collision risk, in Dakar2 location, considering that the traffic growth factor is 8% per annum. These results are also depicted in Figure 35 and Figure 36.



Technical Vertical Collision Risk	8% annual traffic growth
2008	0.1776*10 ⁻⁹
2009	0.1918*10 ⁻⁹
2010	0.2072*10 ⁻⁹
2011	0.2238*10 ⁻⁹
2012	0.2417*10 ⁻⁹
2013	0.2610*10 ⁻⁹
2014	0.2819*10 ⁻⁹
2015	0.3044*10 ⁻⁹
2016	0.3288*10 ⁻⁹
2017	0.3551*10 ⁻⁹
2018	0.3835*10 ⁻⁹

Table 63
Technical vertical collision risk for the period 2008-2018 in Dakar2

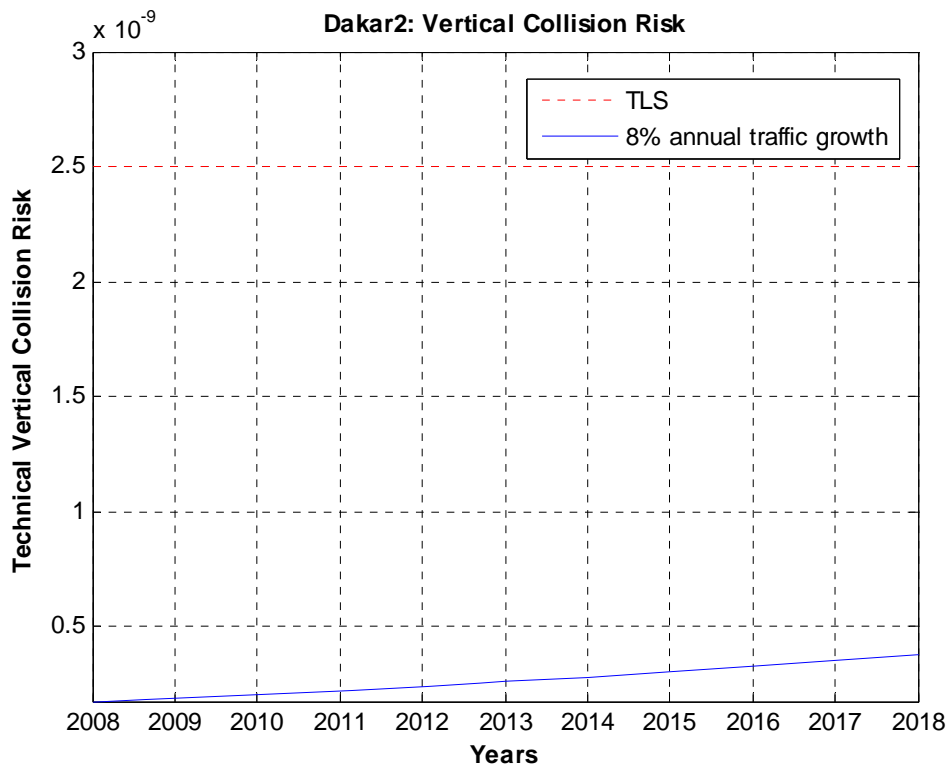


Figure 35
Technical vertical collision risk for the period 2008-2018 in Dakar2



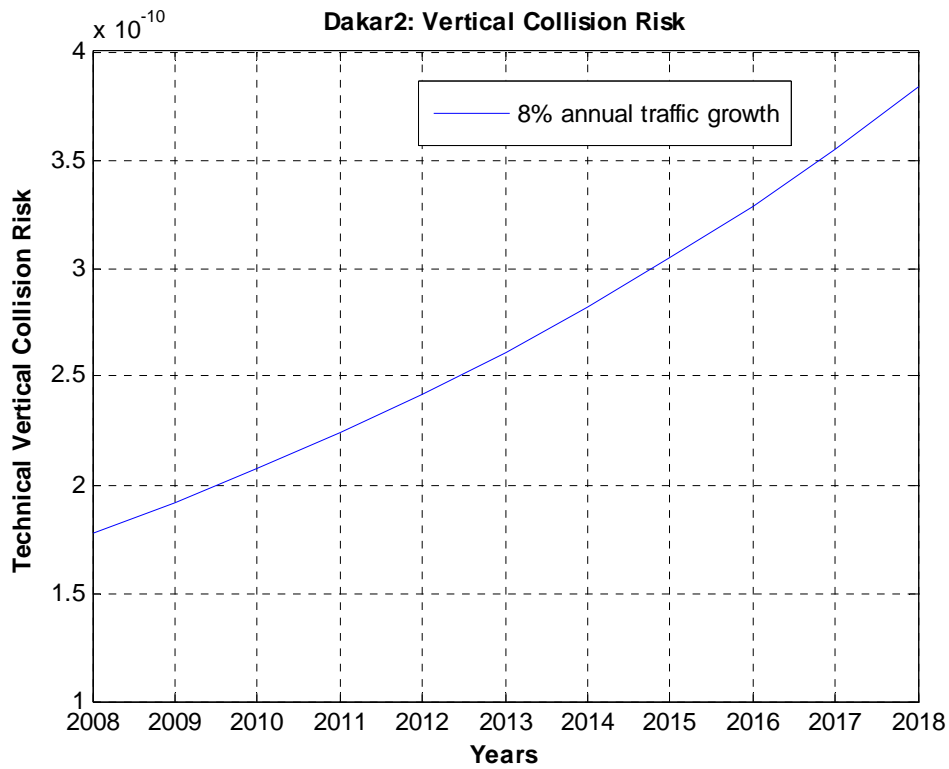


Figure 36
Technical vertical collision risk for the period 2008-2018 in Dakar2 - Enlarged

4.2.8.6. Recife

The estimate of the technical vertical collision risk, in Recife location, assuming that the traffic growth factor is 8% per annum, is summarized in Table 64. These results can also be seen in Figure 37 and Figure 38.



Technical Vertical Collision Risk	8% annual traffic growth
2008	0.1633*10 ⁻⁹
2009	0.1764*10 ⁻⁹
2010	0.1905*10 ⁻⁹
2011	0.2058*10 ⁻⁹
2012	0.2222*10 ⁻⁹
2013	0.2400*10 ⁻⁹
2014	0.2592*10 ⁻⁹
2015	0.2799*10 ⁻⁹
2016	0.3023*10 ⁻⁹
2017	0.3265*10 ⁻⁹
2018	0.3527*10 ⁻⁹

Table 64
Technical vertical collision risk for the period 2008-2018 in Recife

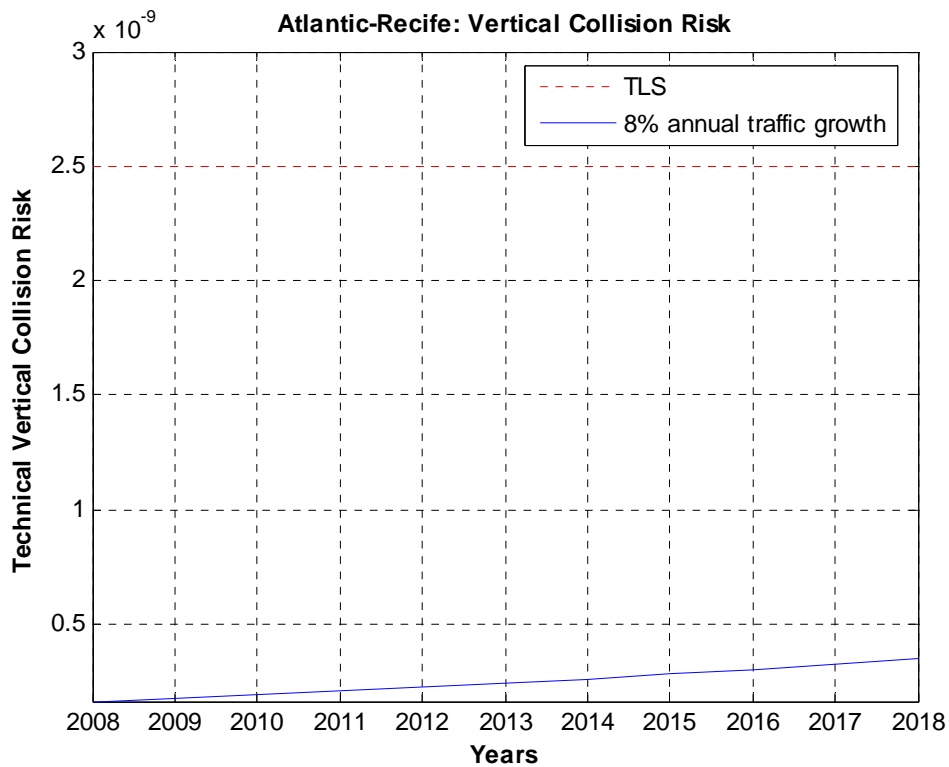


Figure 37
Technical vertical collision risk for the period 2008-2018 in Recife



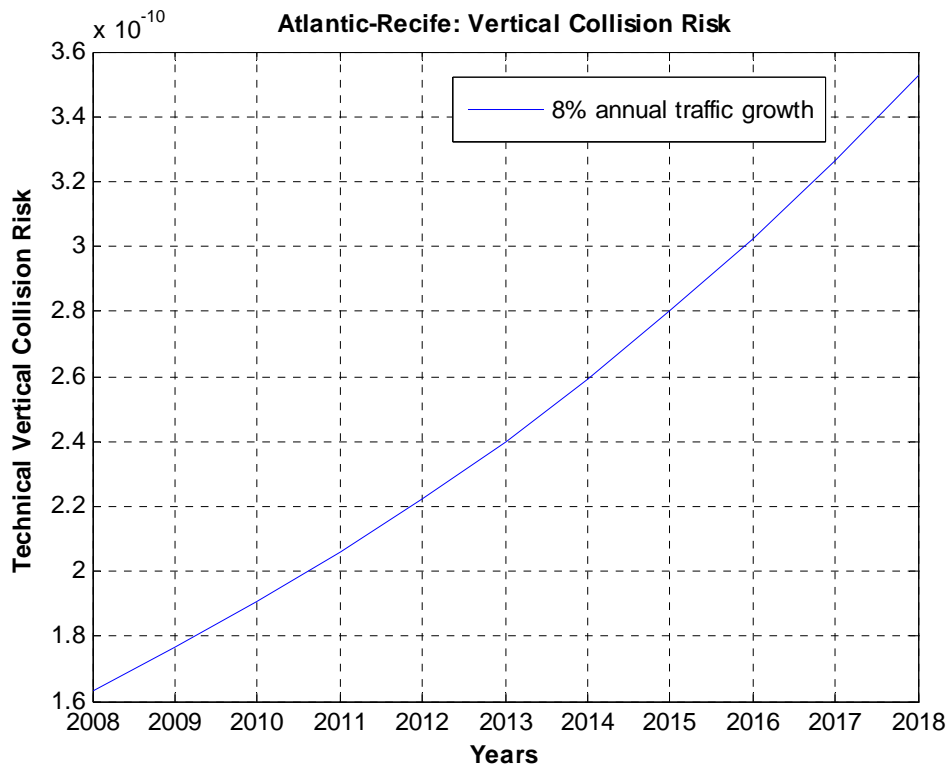


Figure 38
Technical vertical collision risk for the period 2008-2018 in Recife - Enlarged

4.2.9. Considerations on the results

4.2.10.1. Parallel and crossing routes

It can be seen that the estimates of the technical vertical risk are below the technical TLS even in 2018, being similar the values obtained in all the locations.

Comparing these results with those obtained for the pre-implementation safety assessment, [Ref. 15], it can be seen that the new values are higher. This is due to the traffic growth in the Corridor (higher than expected), the different distribution of traffic on the flight levels of unidirectional routes and the use of a much more conservative value for the probability of lateral overlap, $P_y(0)$.



4.2.10.2. RANDOM route

Although traffic on the direct routes (RANDOM) has not been considered, it is assumed that the risk due to these routes will not dramatically change the results obtained for technical vertical risk. This is due to the fact that, as it has been explained in 3.10.2, on these routes there is mainly traffic on even or odd levels and, therefore, there will not be proximate pairs at adjacent flight levels of the same route.

4.3. TOTAL VERTICAL COLLISION RISK ASSESSMENT

In order to assess the total vertical risk, the risk due to large, atypical height deviations⁸ must be assessed and added to the technical vertical risk.

Whilst the technical vertical risk for aircraft on non-adjacent flight levels is negligible in comparison with those on adjacent flight levels, the same is not true for the risk due to atypical height deviations.

Atypical height deviations can be due to exceptional technical errors or due to operational errors.

Altitude deviations resulting from exceptional technical errors are subdivided into five categories, according to the cause of deviation. These are:

- Turbulence: Incidents in which an aircraft deviates from its assigned altitude as a result of pressure turbulence, or turbulence from another aircraft.
- TCAS: false RA-TCAS alerts when there is no other aircraft nearby.

⁸ A RVSM large height deviation (LHD) is defined as any vertical deviation of 90metres/300 feet or more from the flight level expected to be occupied by the flight.



- TCAS: nuisance RA-TCAS alerts against an aircraft that is not posing a threat; for example, an aircraft that is climbing to the level below.
- Autopilot failure: the aircraft deviates from its assigned flight level due to a malfunction in the autopilot system.
- Other technical malfunctions: for example, an electrical fault or engine problem.

On the other side, altitude deviations due to operational errors are due to ATC-pilot loop errors and incorrect clearances. These include:

- Climb/descend without ATC clearance.
- Failure to climb/descend as cleared.
- Entry to RVSM airspace at an incorrect level.
- ATC system loop error (e.g. pilot misunderstands clearance or ATC issues incorrect clearance).
- Errors in coordination of the transfer of control responsibility between adjacent ATC units, resulting in flight at incorrect flight level.

A large atypical deviation can follow three main paths, which are illustrated in Figure 39. The figure depicts a scenario where aircraft 1 should climb to a certain flight level. The correct path of the aircraft is shown by the solid line. The three possible types of deviation which aircraft 1 might make are depicted by dotted line paths A, B and C.

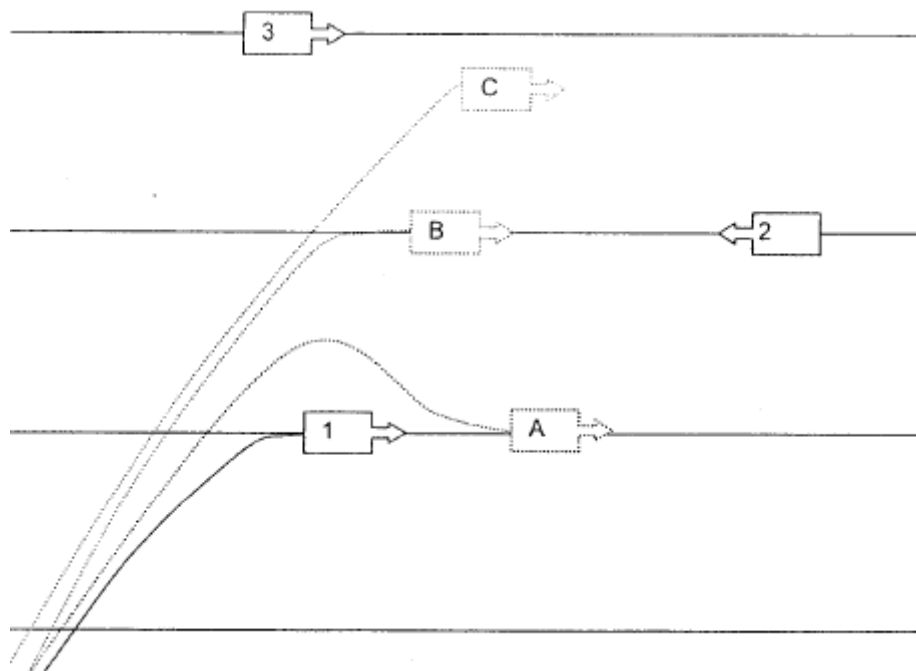


Figure 39
Illustration of the three basic deviation paths

In scenario A, aircraft 1 fails to capture its correct flight level, and performs a height bust. In scenario B, aircraft 1 climbs to and joins an incorrect flight level and in scenario C, aircraft 1 climbs through an incorrect level.

Height deviations due to TCAS do not usually involve whole number of flight levels, i.e. climbing or descending through one or more flight levels without clearance or levelling off at a wrong flight level, but may be much larger than the normal deviations of MASPS approved aircraft. However, deviations caused by the remaining types of error may involve whole number of flight levels.

In relation to this, a distinction between large height deviations involving whole numbers of flight levels and large height deviations not involving whole numbers of flight levels was made for the NAT and different models for the associated probabilities of vertical overlap were developed. These models are described in the following section.

4.3.1. Vertical Collision Risk Models for large height deviations

The models used to estimate the risk due to large height deviations differ from the technical vertical risk model only in the computation of the probability of vertical overlap, P_z , and the relative vertical speed, $|\dot{z}|$.

Three sub-models will be used for large height deviations not involving whole numbers of flight levels, aircraft climbing or descending through a flight level and aircraft levelling off at a wrong level.

4.3.1.1. Aircraft levelling off at a wrong level

To estimate the vertical overlap probability for events where an aircraft joins an incorrect level it is necessary to estimate the probability that an aircraft is at an incorrect level, P_i , and then multiply this by the probability that two aircraft nominally at the same level will be in vertical overlap ($P_z(0)$).

The probability that an aircraft is flying at an incorrect level, P_i , is estimated from the proportion of the total flying time spent at an incorrect level. It is determined by summing the individual times spent at an incorrect level for each large height deviation and dividing this by the total system flight time.

An aircraft levelling off at a wrong flight level is still in level flight and, therefore, the same type of collision risk model is applicable as for aircraft at adjacent flight levels but with a modified calculation of the probability of vertical overlap. The collision risk in this case is given by:



$$N_{az}^{wl} = P_y(0) \frac{\lambda_x}{S_x} \left\{ \begin{aligned} & P_z^{wl}(S_z)_{same} E_{zsame} \left[\frac{|\Delta v|}{2\lambda_x} + \frac{|\bar{y}|}{2\lambda_y} + \frac{|\bar{z}|}{2\lambda_z} \right] + \\ & + P_z^{wl}(S_z)_{opp} E_{zopp} \left[\frac{2|\bar{v}|}{2\lambda_x} + \frac{|\bar{y}|}{2\lambda_y} + \frac{|\bar{z}|}{2\lambda_z} \right] \end{aligned} \right\} + \\
 + \frac{P_z(0) \times t^{wl}}{T} \sum_{i=1}^n P_h(\theta_i) E(\theta_i) \left[\frac{v_{rel}(\theta_i)}{\pi\lambda_h} + \frac{|\dot{z}|}{2\lambda_z} \right]$$

Equation 52

where the superscript “wl” refers to levelling off at a wrong level and $P_z(S_z)^{wl}$ is given by:

$$P_z^{wl}(S_z)_{same} = \frac{P_z(0) \times t_{same}^{wl}}{T}$$

$$P_z^{wl}(S_z)_{opp} = \frac{P_z(0) \times t_{opp}^{wl}}{T}$$

Equation 53

In these equations the different parameters are:

- N_{az}^{wl} : the expected number of fatal aircraft accidents per flight hour due to aircraft levelling off at a wrong flight level
- $P_z(S_z)^{wl}$ is the probability of vertical overlap due to aircraft levelling off at a wrong flight level. The subscript “same” indicates same direction and “opp” opposite direction.



- $P_z(0)$ is the probability of vertical overlap for aircraft nominally flying at the same flight level. It accounts for the normal technical height deviations of aircraft that are flying at the same level and it can be calculated as in 3.3.
- T is the amount of flying time during the period of time the incident data were collected.
- t^{wl} is the total time aircraft have stayed at a wrong flight level after incorrectly levelling off during a period of time with T flying hours. The subscript “same” or “opp” indicates whether there is traffic on the same or opposite direction in this level.

Information on the number of times an aircraft levels off at a wrong level and the duration of its stay at the wrong level are to be obtained from the incident reports.

4.3.1.2. Aircraft climbing or descending through a flight level

The two main elements of a collision risk model for aircraft climbing or descending through a flight level without clearance depend on the probability of two aircraft being in joint longitudinal and vertical overlap and on the average duration of a joint overlap in the vertical plane. The relative vertical speed depends on the rate of climb/descent during the event and determines the angle at which the flight level is crossed.

The model described here is employed for climb/descent rates less than or equal to 4000 ft/min (approximately 40 knots). Slowly descending aircraft are assumed to maintain the same attitude as in level flight and it is assumed that the lateral path-keeping performance is no worse than that for aircraft in level flight. For large height deviations of aircraft with climb/descent rates higher than 40 kts, (emergencies or pressurization failures) a different model should be applied.

The collision risk model for aircraft climbing or descending through a flight level is given by:

$$N_{az}^{cl/d} = P_y(0) \frac{\lambda_x}{S_x} \left\{ \begin{aligned} &P_z^{cl/d}(S_z)_{same} E_{zsame} \left[\frac{|\overline{\Delta v}|}{2\lambda_x} + \frac{|\overline{y}|}{2\lambda_y} + \frac{|\overline{z}|}{2\lambda_z} \right] + \\ &+ P_z^{cl/d}(S_z)_{opp} E_{zopp} \left[\frac{2|\overline{v}|}{2\lambda_x} + \frac{|\overline{y}|}{2\lambda_y} + \frac{|\overline{z}|}{2\lambda_z} \right] \end{aligned} \right\} + \\ + P_z^{cl/d} \sum_{i=1}^n P_h(\theta_i) E(\theta_i) \left[\frac{v_{rel}(\theta_i)}{\frac{\pi\lambda_h}{2}} + \frac{|\dot{z}|}{2\lambda_z} \right]$$

Equation 54

where the superscript “cl/d” refers to an aircraft climbing or descending through a flight level without a proper clearance.

Per event, that is, an aircraft crossing a flight level, it is in vertical overlap, in average, for t_z flight hours,

$$t_z = \frac{2\lambda_z}{|\dot{z}_c|}$$

Equation 55

where λ_z is the average aircraft height and \dot{z}_c , the relative vertical speed.

Therefore, if N is the total number of flight levels crossed, the total time in vertical overlap for aircraft climbing or descending through a flight level is $N \times t_z$ and the probability of vertical overlap, $P_z(S_z)^{cl/d}$, is given by:



$$P_z(S_z)^{cl/d} = \frac{N \times t_z}{T} = \frac{N \times 2\lambda_z / |\dot{z}_c|}{T}$$

Equation 56

In these equations:

- $N_{az}^{cl/d}$ is the expected number of fatal aircraft accidents per flight hour due to aircraft climbing or descending through a flight level without a proper clearance.
- $P_z(S_z)^{cl/d}$ is the probability of vertical overlap due to aircraft climbing or descending through a flight level without a proper clearance. The subscripts “same” and “opp” indicate whether the crossed levels are levels in the same direction or in the opposite direction.
- N is the number of flight levels crossed.
- \dot{z}_c is the average climb or descent rate for aircraft climbing or descending through a flight level without a proper clearance.

Information on the number of incorrect flight level crossings and the pertinent vertical speeds is to be obtained from the incident reports. When the vertical speed is not indicated, a default value is used for the relative vertical speed. This value is usually considered to be 15 knots.

4.3.1.3. Large height deviations not involving whole numbers of flight levels

The vertical collision risk due to large height deviations not involving whole numbers of flight levels can be modelled in the same way as the technical vertical collision risk, i.e.:



$$N_{az}^* = P_y(0) \frac{\lambda_x}{S_x} \left\{ \begin{aligned} &P_z^*(S_z) E_{zsame} \left[\frac{|\Delta v|}{2\lambda_x} + \frac{|\bar{y}|}{2\lambda_y} + \frac{|\bar{z}|}{2\lambda_z} \right] + \\ &+ P_z^*(S_z) E_{zopp} \left[\frac{2|\bar{v}|}{2\lambda_x} + \frac{|\bar{y}|}{2\lambda_y} + \frac{|\bar{z}|}{2\lambda_z} \right] \end{aligned} \right\} + \\ + P_z^*(S_z) \sum_{i=1}^n P_h(\theta_i) E(\theta_i) \left[\frac{v_{rel}(\theta_i)}{\frac{\pi\lambda_h}{2}} + \frac{|\bar{z}|}{2\lambda_z} \right]$$

Equation 57

Superscript “*” is used to distinguish this type of vertical risk from the technical vertical collision risk. The probability of vertical overlap $P_z(S_z)^*$ can be calculated in the same way as for the technical vertical collision risk, by means of Equation 43.

4.3.2. Data on EUR/SAM large height deviations

As it has been explained in the previous sections, data needed for the different models should be obtained from the large height deviation reports received from the different UIRs.

The information that has been made available for this assessment can be seen in the following tables. Table 65, Table 66 and Table 67 show the details of the deviations provided by SAL, Dakar and Recife, respectively.



Date	Callsign	Aircraft	Route	Duration	Coordinated FL	Observed FL	Deviation	Cause
141007	KLM792	B772	UN866		FL340	FL350	1000 ft	Coordination error
141007	TAM8061	MD11	UN873		FL320	FL310	1000 ft	Coordination error
151007	LVWSS	GLF4	UN873			FL400		Coordination error
211007	VRN8740	B763	UN866		FL330	FL350	2000 ft	Coordination error
291007	TCV659	B752	UN873			FL360		Coordination error
140208	IBE6820	A343	UN866			FL 370		Coordination error
140208	AFR447	A332	UN866			FL 360		Coordination error
140208	AFR459	A343	UN866			FL 350		Coordination error
140208	TAM8064	A332	UN873			FL 390		Coordination error
140308	TAM8075	A332	UN741		FL 370	FL 380	1000 ft	Coordination error
280308	TAM8070	A332	UN866		FL 350	FL 370	2000 ft	Coordination error
290308	AFR6911	B744	UN873		FL 410	FL 450	4000ft	Coordination error
070708	TAP168	A332	UN866		FL 390	FL 400	1000ft	Coordination error
180708	ARG1986	A342	UN866		FL 390	FL 400	1000 ft	Coordination error
180708	IBE6824	A346	UN873		FL 390	FL 370	2000 ft	Coordination error
180708	AFR455	B772	UN873		FL 350	FL 370	2000 ft	Coordination error

Table 65
Large height deviations reported by SAL

Date	Callsign	Aircraft	Route	Duration	Coordinated FL	Observed FL	Deviation	Cause
270807	AFR418	B772	UN741		FL 330	FL 350	2000 ft	Coordination error
100907	IBE6841	A346	UN741		FL 310	FL 340	3000 ft	Coordination error
110907	BAW247	B744	UN741		FL 340	FL 350	1000 ft	Coordination error
110907	PUA803	B763	UN857		FL 320	FL 340	2000ft	Coordination error
110907	VRN8741	A343	UN741		FL 330	FL 350	2000 ft	Coordination error
110907	TAM8097	B744	UN741		FL 330	FL 350	2000 ft	Coordination error
281207	VLO7447	MD11	UN873		FL 320	FL 340	2000 ft	Coordination error
270208	TAP139	A332	UN741		FL 340	FL 400	6000 ft	Coordination error
270208	TAP173	A332	UN741		FL 390	FL 400	1000 ft	Coordination error
110408	MPD301	A310			FL 380	FL 360	2000 ft	Coordination error
080508	TAP139	A346			FL 350	FL 380	3000 ft	Coordination error

Table 66
Large height deviations reported by Dakar



Date	Callsign	Aircraft	Route	Duration	Coordinated FL	Observed FL	Desviation	Cause
240707	BRB7553	B763	UN873	45 min	FL 360	FL 340	2000 ft	Coordination error
070807	IBE6842	A346	UN 866	120 s	FL 370	FL 350	2000 ft	Coordination error
200807	VP-BOZ	F900	UN741	300 s	FL 400	FL 430	3000 ft	Coordination error
210807	IBE6845	A346	UN741	60 s	FL 360	FL 380	2000 ft	Coordination error
010907	ARG1134	B744	UN857	80 s	FL 330	FL 350	2000 ft	Coordination error
030907	TAP156	A332	UN873	240 s	FL 370	FL 390	2000 ft	Coordination error
271007	AFR443	B744	UN873	240 s	FL 310	FL 330	2000 ft	Coordination error
031207	ARG1141	A342	UN873	180 s	FL 340	FL 360	2000 ft	Coordination error
031207	TAP176	A332	UN866	120 s	FL 370	FL 390	2000 ft	Coordination error
181207	AFR459	A342	UN873	1320 s	FL 350	FL 370	2000 ft	Coordination error
181207	DMJ1005	B737	UN741	3600 s	FL 330	FL 320	1000 ft	Coordination error
211207	IBE6821	A343	UN741	1980 s	FL 340	FL 350	1000 ft	Coordination error
290108	TAM8097	MD11	UN741	60 s	FL340	FL 360	2000 ft	Coordination error
050308	IBE6013	A343	UN741	360 s	FL370	FL360	1000 ft	Coordination error
130308	TAM8061	MD11	UN741	300 s	FL350	FL 360	1000 ft	Coordination error
170308	CSTFN	F900	UN873	2400 s	FL 400	FL 430	3000 ft	Coordination error
260408	VRN8731	B763	UN741			FL 330		Coordination error
240608	AFR459	A332	UN866	1860 s	FL350	FL360	1000 ft	Coordination error

Table 67
Large height deviations reported by Atlantic-Recife

After an exhaustive analysis of the deviation reports, it has been possible conclude that all the registered deviations are due to errors in coordination between adjacent ATC units, resulting in either no notification of the transfer or in transfer at an unexpected flight level.

4.3.3. Total vertical collision risk

The total vertical risk is the sum of the technical risk and the risks due to large height deviations involving whole numbers of flight levels (both climbing/descending aircraft and level flight aircraft) and the risk due to large height deviations not involving whole numbers of flight levels. As it has been said, it is assumed that the same type of collision risk model applies to the different risk components, being only



different the probability of vertical overlap, $P_z(S_z)$, and the average relative vertical speed used in each case. So,

$$N_{az}^{total} = N_{az}^{tech} + N_{az}^{wl} + N_{az}^{cl/d} + N_{az}^*$$

Equation 58

Technical risk has already been calculated in 4.2.8. Regarding the risk due to large height deviations, as it can be seen in Table 65, Table 66 and Table 67, in this case there are no reports due to large height deviations not involving whole numbers of flight levels and $N_{az}^* = 0$. On the other hand, as all the reported deviations are due to a coordination error between ATC units, the number of crossed levels needed to calculate the risk for climbing/descending aircraft is zero. The reason for this is that it is assumed that the level change, if any, took place in the transferring UIR following appropriate clearances, and when the aircraft enters the new UIR, it is already established on the incorrect flight level. Thus, $N_{az}^{cl/d} = 0$.

Therefore, the only term to be calculated is the risk due to aircraft levelling off at a wrong level. To do this, it is necessary to know the time spent at the incorrect flight level. As it can be seen in Table 65, Table 66 and Table 67, this information is only provided by Recife, and some hypothesis would be required to estimate it in the case of SAL and Dakar. For this reason, collision risk has been calculated first in Recife.

From Table 67, the total time spent at an incorrect flight level is 3.672 h (between FL290 and FL410). The deviation of the 26th April has not been considered in the assessment, as not enough information is provided. It is important to remark that all deviations correspond to flight levels with traffic in the same direction and, consequently, the term due to occupancy in the opposite direction will be zero.

The total flight time in Atlantic-Recife during the period of time for which height deviation reports have been received (i.e. from July 07 to April 08 and from June 08



to July 08) is 26501h. The total flight time in the whole Corridor for the same period of time is 123985 h. Then:

$$P_z^{wl}(S_z)_{same} = P_z^{wl}(S_z) = \frac{P_z(0) \times t_{same}^{wl}}{T} = \frac{0.57 * 3.672}{26501} = 7.898 \times 10^{-5}$$

$$P_z^{wl}(S_z)_{opp} = 0$$

With these results and the ones obtained for the rest of the parameters of Equation 52 in the analysis of the technical vertical, the vertical risk due to large height deviations in Atlantic-Recife UIR would be 1.0535×10^{-6} and its contribution to the risk in the whole Corridor would be 2.252×10^{-7} . These results are much higher than the TLS.

It must be taken into account that these values are obtained assuming that the probability of lateral overlap is $P_y(0) = 0.2881$, as it was explained in 4.2.3. This large value was obtained assuming that all aircraft are flying using GNSS, and it may be too conservative. However, if $P_y(0) = 0.059$ (the value adopted by the RGCSP, based on lateral path-keeping errors with a standard deviation of 0.3NM) is used, the risk due to large height deviations in Atlantic-Recife would be 2.2010×10^{-7} and its contribution to the total risk in the Corridor 4.7000×10^{-8} , which are still much higher than the $TLS = 5 \times 10^{-9}$

As the TLS is already exceeded considering the deviations reported by Atlantic-Recife, the contribution of those reported by SAL and Dakar, for which some hypothesis would be needed, is not calculated.

4.3.3.1. Considerations on the results



The total vertical risk calculated using the deviations reported by Atlantic-Recife is already much higher than the TLS. Therefore, when considering the deviations reported by Dakar and SAL, the risk would be even higher.

Nevertheless, it is important to remark that all the deviations received were due to a coordination error, and they are not related to RVSM operations. If these coordination errors were not taken into account, the total vertical risk would comply with the TLS, since it would be equal to the technical vertical risk.

It must also be taken into account that, despite these large values for total vertical risk, the deviation reports received indicated that there was not any traffic in conflict.

Total vertical risk could not be calculated in the pre-implementation safety assessment as no data related to large height deviations were received for that study. Therefore, results before and after the change in the routing configuration can not be compared. Nevertheless, it is believed that the coordination errors are not related to this new route structure.

The same problem, the collision risk being higher than the TLS if coordination errors are taken into account, has also been identified in other Regions, such as CAR/SAM or Asia/Pacific. In any case, as the problem is clearly identified, the use of adequate corrective actions to reduce coordination errors in the Corridor will reduce the risk.

5. CONCLUSIONS

More traffic data and large height deviation reports have been received for this study than for the previous one. Nevertheless, some information was still missing and some inconsistencies have been detected. Therefore, some conservative assumptions had to be made regarding the modelling of probability densities and the extrapolation of traffic data.



Taking this into account, the following conclusions can be extracted from the analysis in the six different locations considered (the risk associated to the Corridor is considered to be the largest of the values calculated for each location):

- Lateral collision risk assessments

- The probability of lateral overlap increases as the separation between routes decreases, as it was expected. The value obtained for $S_y = 50\text{NM}$ is between $P_y(50) = 6.8262 \times 10^{-8}$ and $P_y(50) = 7.3074 \times 10^{-8}$, depending on the location, whilst the lateral overlap probability obtained for $S_y = 90\text{NM}$ is between $P_y(90) = 2.0712 \times 10^{-8}$ and $P_y(90) = 2.2172 \times 10^{-8}$.
- For current traffic levels, the lateral collision risk obtained is 2.451×10^{-9} , whilst the lateral collision risk estimated for 2018 with an annual traffic growth rate of 8% is 5.2915×10^{-9} . These values don't take into account traffic on the RANDOM route. Nevertheless, since traffic on this route only represents 2.5% of the traffic in the Corridor, it is considered that the collision risk due to this route will not make the collision risk go above the TLS and the system is considered to be laterally safe until 2017.
- These results are higher than the ones obtained for the pre-implementation safety assessment, [Ref. 15], due to the traffic growth in the Corridor (higher than expected) and the different distribution of traffic on the flight levels of unidirectional routes.

- Vertical risk assessments

- Vertical risk is split into two parts, one for the technical vertical risk and the second one for the vertical risk due to all causes. The same collision risk model is used for

both. The differences are the value of the vertical overlap probability and the relative vertical speed to use in each one.

- The probability of vertical overlap due to technical causes was based on the probability distribution of Total Vertical Error (TVE). This was obtained by convoluting probability distributions of Altimetry System Errors (ASE) and typical Assigned Altitude Deviation (AAD). In the absence of any direct monitoring data from the EUR/SAM Corridor, height-keeping data and models from the EUR airspace have been used.
- The value of the vertical overlap probability obtained for $S_z=1000\text{ft}$ is $P_z(1000) = 4 \times 10^{-9}$.
- The vertical overlap probability obtained, $P_z(1000) = 4 \times 10^{-9}$, meets the global system specification that requires the probability of vertical overlap not to exceed a value of 1.7×10^{-8} .
- The global height-keeping performance specification also specifies bounds for the proportions of height-keeping deviations larger in magnitude than 300ft, 500ft, 650ft and between 950 and 1050ft. The results show that these criteria are met.
- The lateral overlap probability for aircraft nominally flying at adjacent flight levels of the same path, $P_y(0)$, has been obtained conservatively assuming that all aircraft are using GNSS and that their lateral path-keeping errors standard deviation is 0.0612NM. The value obtained is $P_y(0) = 0.2881$, much higher than the value assumed by the RGCSP, 0.059.
- The value of the vertical technical collision risk for the current traffic levels is estimated to be 0.2725×10^{-9} . The technical vertical collision risk estimated for

2018 with an annual traffic growth rate of 8% is 0.5883×10^{-9} . Both values are below the TLS.

- The technical vertical risk obtained in this study is higher than the one obtained in the pre-implementation safety assessment. This is due to the traffic growth in the Corridor (higher than expected), the different distribution of traffic on the flight levels of unidirectional routes and the use of a much more conservative value for the probability of lateral overlap, $P_y(0)$.
- The vertical risk due to large height deviations has been calculated using the deviations reported by Atlantic-Recife, which included all the required information. As the contribution of these deviations to the total vertical risk in the Corridor, (4.7000×10^{-8} if the value 0.059 is taken for $P_y(0)$), greatly exceeds the TLS, the contribution to the risk of SAL and Dakar deviations has not been calculated.
- Nevertheless, it is important to remark that **all the deviations received were due to a coordination error**, and they are not related to RVSM operations. If these coordination errors were not taken into account, the total vertical risk would comply with the TLS, since it would be equal to the technical vertical risk.
- Despite these large values for total vertical risk, the deviation reports received indicated that there was not any traffic in conflict.
- Total vertical risk could not be calculated for the previous routing configuration. However, it is believed that the high vertical risk obtained now, due to coordination errors, is not related to the change in the routes configuration.

It can be concluded that lateral and technical vertical collision risks are below the TLS. Nevertheless, the validity of these results depends on the validity of the assumptions made. Specially, those assumptions regarding the traffic samples should be verified with additional data from SAL, Dakar and Atlantic-Recife.



Regarding the total vertical risk, if coordination errors are to be considered, the risk greatly exceeds the TLS even with current traffic levels. In any case, as the problem is clearly identified, the use of adequate corrective actions to reduce coordination errors in the Corridor will reduce the risk. These measures should be applied as soon as possible.

As the accuracy of the assessment greatly depends on the availability and accuracy of the data provided, it is recommended that for next assessments:

- accurate flight progress data from all FIR/UIRs be made available, including as much information as possible in the traffic samples, to facilitate the verification of traffic flows, distribution and passing frequencies used in the analysis.
- data on lateral and vertical deviations obtained from radar data and incident reports be provided in order to improve the estimation of overlap probabilities (a continuous monitoring process is required to obtain a representative data sample on deviations for future assessments).



6. ACRONYMS

AAD	ASSIGNED ALTITUDE DEVIATION
ADS	AUTOMATIC DEPENDENT SURVEILLANCE
ASE	ALTIMETRY SYSTEM ERROR
ATC	AIR TRAFFIC CONTROL
ATS	AIR TRAFFIC SERVICES
DE	DOUBLE EXPONENTIAL DISTRIBUTION
EUR/SAM	EUROPE/SOUTH AMERICA
FIR	FLIGHT INFORMATION REGION
FL	FLIGHT LEVEL
FMC	FLIGHT MANAGEMENT COMPUTER
FTE	FLIGHT TECHNICAL ERROR
G	GAUSSIAN DISTRIBUTION
GL	GENERALISED LAPLACE DISTRIBUTION
HFDL	HIGH FREQUENCY DATA LINK
HMU	HEIGHT MONITORING UNIT
fts	KNOTS
MASPS	MINIMUM AVIATION SYSTEM PERFORMANCE STANDARDS
MDG	MATHEMATICS DRAFTING GROUP (EUROCONTROL)
NAT	NORTH ATLANTIC
NM	NAUTICAL MILE
RGCSP	REVIEW OF THE GENERAL CONCEPT OF SEPARATION PANEL
RNP	REQUIRED NAVIGATION PERFORMANCE
RVSM	REDUCED VERTICAL SEPARATION MINIMUM
SAT	SOUTH ATLANTIC
SATCOM	SATELLITE COMMUNICATIONS
SATMA	SOUTH ATLANTIC MONITORING AGENCY
STATFOR	AIR TRAFFIC STATISTICS AND FORECASTS (EUROCONTROL)
TVE	TOTAL VERTICAL ERROR
UIR	UPPER FLIGHT INFORMATION REGION

7. REFERENCES

- [Ref. 1] Atlas South Atlantic Crossing 57C, 22 Dec 05. Air navigation Chart
- [Ref. 2] Risk Assessment of RNP10 and RVSM in the South Atlantic Flight Identification Regions Including an Assessment for Limited Implementation of RVSM on RN741. (ARINC)
- [Ref. 3] AIP Spain. AIS. AIC 17/Jan/01



- [Ref. 4] Separation and Airspace Safety Panel. A New Parameter for Gross Lateral Errors (SASP-WG/A/2-WP/4, 21/10/01)
- [Ref. 5] Manual on airspace planning methodology for the determination of separation minima (ICAO Doc 9689-AN/953)
- [Ref. 6] Air Traffic Services Planning manual. Doc 9426 OACI
- [Ref. 7] ICAO Document 9574 (2nd edition). Manual on Implementation of a 300m (1000ft) Vertical Separation Minimum between FL290 and FL410 inclusive.
- [Ref. 8] RVSM Safety Assessment of the Australian Airspace for the period 1 Jan 2004 through 31 Dec 2004.- RASMAG/3-WP/16 06/06/2005. OACI
- [Ref. 9] Summary of the Airspace Safety Review for the RVSM Implementation in Asia Region.- RASMAG/4-WP11 25/10/2005. OACI
- [Ref. 10] The EUR RVSM Mathematical Supplement.-MDG/21 DP/01 August 2001.
- [Ref. 11] Hipótesis sobre el tráfico en rutas no publicadas en el Corredor EUR/SAM.- DNV-ADS-INF-020-0.1/06
- [Ref. 12] CAR/SAM-Course on Introduction to Safety Assessment. Lima, 19-23/06/06 (www.lima.icao.int)
- [Ref. 13] SAT/12-TF/1 Report. Appendix A to the Report on Agenda Item 2: An Update to the Summary of Reduced Vertical Separation Minimum (RVSM) Safety Assessment to Reflect the Operations Safety after the RVSM Implementation in CAR/SAM airspace in January 20th.- 5-9/09/06
- [Ref. 14] STATFOR. Eurocontrol Medium-Term Forecast. Flight Movements 2008-2014. Volumes 1 and 2.
- [Ref. 15] EUR/SAM Risk Assessments. DNV-ADS-INF-23-0.2/06. December 2006
- [Ref. 16] Revised Pre-Implementation Collision Risk Assessment for RVSM in the Africa Indian Ocean Region. NLR-CR-2007-637. February 2007
- [Ref. 17] Application of offset tracks. NLR. September 2007
- [Ref. 18] AIC NR 13/A/08GO 30 October 2008. Bureau NOTAM International de L'Ouest Africain. Pre-Operational Implementation of AFDP, FPASD, ADS and CPDLC within Dakar and Niamey FIRs.
- [Ref. 19] AIS-ESPAÑA. AIC 10 May 07. New route orientation on airways UN-741 and UN-866 (Corridor EUR/SAM)
- [Ref. 20] AIS-ESPAÑA. AIC 05 July 07. ADS/CPDLC Pre-operational phase of the SACCAN FANS 1/A System in the Canarias FIR/UIR
- [Ref. 21] Updated RMA Manual. SASP/13-WP/44. May 2008



ANNEX 1

METHODS FOR OCCUPANCY ESTIMATE



A1.1. DEFINITION

The occupancy concept is applicable for both vertical and lateral separation. In the case of lateral occupancy, the concept is applicable for aircraft flying in parallel routes at the same flight level, whilst in the vertical case, the concept is applicable to aircraft flying in the same route or in crossing routes at adjacent flight levels.

Same direction lateral occupancy for a parallel tracks system refers to the average number of aircraft which are, in relation to the typical aircraft:

- flying in the same direction as it;
- nominally flying on tracks one lateral separation standard away from it;
- nominally at the same flight level as it; and
- within a longitudinal segment centred on it.

The above definition has been expanded to include tracks that are separated by more than one lateral separation standard because there is a significant collision risk arising from the probability of overlap between non adjacent tracks.

A similar set of criteria can be used to define opposite direction occupancy, just replacing “flying in the same direction as it” by “flying in the opposite direction”.

The length of the longitudinal segment, $2S_x$, is considered to be the length equivalent to 20 minutes of flight at 480kts.



A1.2. METHODS FOR OCCUPANCY ESTIMATE

There are two methods to estimate lateral occupancy, called “Steady state flow model” and “Direct estimation from time at waypoint crossing”.

The first one is the only way of achieving an estimation of the occupancy when only records of daily traffic are available or if, in the direct estimation from time at waypoint crossing there are not big amounts of hourly information. The method of direct estimation provides more precise estimations and it is, generally, preferred.

For a given system, lateral occupancy, E_y , can be expressed as:

$$E_y = \frac{2T_y}{H}$$

Equation 59

Where:

- T_y represents the proximity time generated in the system, i.e. the total time spent by aircraft pairs on adjacent flight paths at the same flight level and within a longitudinal distance S_x of each other.
- H represents the total number of flight hours generated in the system during the considered period of time.

A1.2.1. STEADY STATE FLOW MODEL

This section is a transcription of sections 2.3, 3.1, 3.2 y 3.3 and appendix C of Chapter 4, Section 2, part II of [Ref. 6].



The occupancy E_y will be estimated for a parallel routes system in which it will be supposed that the flow of traffic towards the flight paths and along them is statistically stable during the considered period.

For a general system, the occupancy will be obtained as a weighted sum of the occupancy of all the subsystems “in stable state”, with respect to the number of flight hours generated in each one.

Tracks are numerated from 1 to t and flight levels from 1 to f . The traffic flow on track i , at flight level j (flight path ij) is m_{ij} , i.e. m_{ij} aircraft cross every point of the track every hour. The length of the track is L and it is assumed that all aircraft fly at the same speed V . T is the time during which the system is observed.

A1.2.1.1. Number of flight hours H

The time L/V is needed for an aircraft to fly through the system. So, in the flight path ij there are always $m_{ij} \cdot L/V$ aircraft and the number of aircraft in the whole system will be:

$$\sum_{i=1}^{i=t} \sum_{j=1}^{j=f} m_{ij} \cdot \frac{L}{V}$$

Equation 60

From this equation it is deduced that:

$$H = \frac{T \cdot L}{V} \sum_{\text{all trajectories } ij} m_{ij}$$

Equation 61



A1.2.1.2. Total proximity time T_y

Calculation of T_y is a little bit more complicated. Let’s consider an aircraft on the flight trajectory ij : the foreseen number of proximate aircraft on the adjacent flight trajectory $i-1$ is given by:

$$\frac{2 \cdot S_x}{V} \cdot m_{i-1,j}$$

Equation 62

So, during the L/V flight hours of this aircraft, the proximity time generated is:

$$\frac{2 \cdot S_x}{V} \cdot m_{i-1,j} \cdot \frac{L}{V}$$

Equation 63

During the T hours in which the system is observed, $m_{ij} \cdot T$ aircraft fly on the flight path ij , and the proximity time generated between trajectory ij and trajectory $i-1,j$ is:

$$\frac{2 \cdot S_x}{V} \cdot m_{i-1,j} \cdot \frac{L}{V} \cdot m_{ij} \cdot T$$

Equation 64

The total proximity time, T_y , is obtained adding all the previous pairs:

$$T_y = \sum_{i=1}^{i=t} \sum_{j=1}^{j=f} \frac{2 \cdot S_x}{V} m_{i-1,j} \cdot \frac{L}{V} \cdot m_{i,j} \cdot T$$

Equation 65

Or (simplifying notation):

$$T_y = \sum_{\substack{\text{all pairs} \\ \text{of tracks}}} m_{i-1,j} m_{i,j} \cdot \frac{2 \cdot S_x \cdot L \cdot T}{V^2}$$

Equation 66



A1.2.1.3. Occupancy

Substituting Equation 61 and Equation 66 into Equation 59, occupancy is finally given by:

$$E_y = \frac{2 \cdot T_y}{H} = \frac{2 \cdot \sum_{\substack{\text{all pairs} \\ \text{of tracks}}} m_{i-1,j} m_{i,j} \cdot \frac{2 \cdot S_x}{V}}{\sum m_{i,j}}$$

Equation 67

For same direction lateral overlap, aircraft flying on adjacent tracks in the same direction and at the same flight level must be considered. For opposite direction lateral overlap, aircraft flying on adjacent tracks in the opposite direction and at the same flight level must be considered.

If the system is not statistically stable, as it happens in the case in which traffic flows depend on the time, the occupancy value E_y should be calculated adding all the subsystems that are in a stable state. Thus, if there are r subsystems of this type:

$$E_y = \frac{2 \sum_{p=i}^{p=r} T_y^p}{\sum_{p=i}^{p=r} H^p} = \frac{\sum_{p=i}^{p=r} H^p E_y^p}{\sum_{p=i}^{p=r} H^p}$$

Equation 68

Where the subindex p indicates that the value corresponds to the subsystem p . T_j^p and H^p can be obtained for every subsystem p using the method described before.



A1.2.2. DIRECT ESTIMATION FROM TIME AT WAYPOINT PASSING

This has been the method used in this report.

It is based on the daily flight progress data of aircraft in the tracks system studied. The period of time of available flight progress data should be long enough, in order to be able to detect any important variation in the traffic flow.

Basically the method consists in examining the crossing time notified by all the aircraft of the system at a given waypoint.

The points utilized as reporting points must be approximately on a plane at right angles to the track system, in order to be able to compare passing times of aircraft on one route with passing times of aircraft on another route. That is why, in this study, times in SAL2 had to be corrected (extrapolated) to obtain crossing times in points that are at right angles to the route network.

The comparison of crossing times will give the number of proximate pairs. A proximate pair, between aircraft on adjacent routes and at the same flight level, is defined as the occurrence of two aircraft passing within a given longitudinal distance $2S_x$. If both aircraft fly in the same direction it will be a proximate pair in the same direction, whilst it will be an opposite direction proximate pair if they fly in opposite directions. As far as the distance S_x is concerned, it is often given by the time T_0 , being the time it takes an aircraft with an average speed of 480kts to fly that distance. In this study, S_x is 80NM and T_0 , 10 minutes.

If, for each and every flight level, passing times at the reporting point of all aircraft on one route are compared with the passing times of all aircraft on another route at the homologous reporting point, the number of proximate pairs between these two routes will be given by the number of cases in which the absolute value of the difference between both times is less than 10 minutes.



The same procedure must be followed with the remaining pairs of routes.

Considering all this, occupancy can be estimated using the following equation:

$$E_y = \frac{2n_y}{n}$$

Equation 69

where n_y is the total number of proximate pairs of aircraft and n is the total number of aircraft in the system.

A1.3. CROSSING OCCUPANCY

Crossing occupancy for a pair of routes with intersection angle θ is given by:

$$E_z(\theta) = \begin{cases} \frac{t_{sh}(\theta)}{t_F} \frac{2K(\theta)}{N}; & \text{for } t_{sh} < t_F \\ \frac{2K(\theta)}{N}; & \text{for } t_{sh} > t_F \end{cases}$$

Equation 70

Where:

- N is the number of aircraft in the system during the observation period
- $K(\theta_i)$ is the number of aircraft pairs in the crossing routes with angle θ_i
- t_{sh} is the average proximity time of pairs of aircraft in the crossing routes with angle θ
- t_F is the average flight time in the crossing routes



The “direct estimation from time at waypoint passing”, can also be used to estimate crossing occupancy. In this case, it is necessary to determine a time window so that the identification of the proximate pairs may be accomplished.

Lets consider two crossing routes, A and B, with angle θ , and aircraft flying at speeds V_A and V_B . This window depends on the crossing angle of the routes, the speeds of the aircraft and the horizontal distance, S_h . Pairs of aircraft for which separation is greater than S_h will not be considered as proximate events.

The time window can be obtained using the following expression:

$$\Delta t_{\max} = \sqrt{\frac{(V_A^2 + V_B^2 - 2V_A V_B \cos \theta) S_h^2}{V_A^2 V_B^2 \sin^2 \theta}}$$

Equation 71



ANNEX 2

ASE DISTRIBUTIONS FOR EUR/SAM CORRIDOR



A2.1. ASE DISTRIBUTIONS FOR EUR/SAM CORRIDOR

The overall ASE distribution for the EUR/SAM Corridor has been constructed from the ASE probability density functions obtained by Eurocontrol for the different aircraft monitoring groups found in the Corridor, weighted by the proportion of flights of each group, i.e.

$$f^{ASE}(a) = \sum_{i=1}^{n_{tg}} \beta_i f_i^{ASE}(a)$$

Equation 72

where n_{tg} denotes the number of different monitoring groups, β_i is the proportion of flights contributed by aircraft type group i and $f_i^{ASE}(a)$ is the probability density of the ASE of aircraft type group i , $i=1, \dots, n_{tg}$. Each monitoring group’s ASE probability density, $f_i^{ASE}(a)$, is the result of both within and between airframe ASE variability of all the airframes making up the group .

Each of the within or between airframe distributions can be mixtures of up to three Generalised Laplace probability densities, i.e:

$$\begin{aligned} f(x) = & \alpha_1 \frac{1}{2a_1 b_1 \Gamma(b_1)} \exp\left(-\left|\frac{x-\mu}{a_1}\right|^{1/b_1}\right) + \\ & + \alpha_2 \frac{1}{2a_2 b_2 \Gamma(b_2)} \exp\left(-\left|\frac{x-\mu}{a_2}\right|^{1/b_2}\right) + , \text{ with } \alpha_1 + \alpha_2 + \alpha_3 = 1 \\ & + \alpha_3 \frac{1}{2a_3 b_3 \Gamma(b_3)} \exp\left(-\left|\frac{x-\mu}{a_3}\right|^{1/b_3}\right) \end{aligned}$$

Equation 73

The parameters a_1 , a_2 and a_3 are usually referred to as scale parameters and the parameters b_1 , b_2 and b_3 as shape parameters and μ represents the mean of the random variable x , i.e. either within airframe ASE or between airframe ASE. $\Gamma(b)$

denotes de gamma function of b. All parameters are dependent on the monitoring group under consideration.

A generalised Laplace probability reduces to a Gaussian probability density when the scale parameter b is set to a value of 0.5, and it reduces to a Double Exponential probability density when the shape parameter is given a value of 1. A single probability density, be it Gaussian, Double Exponential or Generalised Laplace, is obtained by putting $\alpha_2=\alpha_3=0$ and a mixture of two probability densities may be obtained by putting $\alpha_3=0$.

Table A1. 1, shows the proportion of flights and the ASE probability density used for each of the monitoring groups found in the Canaries from 10th July 2007 to 10th July 2008.

The first column indicates the aircraft monitoring group, whilst the second one shows the proportion of flights per aircraft group. The third column indicates the pdf for the within and between airframe distributions used to obtain the ASE probability density for each monitoring group. The notation is: “between distribution_within distribution”. For each one, one, two or three terms may exist. G stands for Gaussian, DE, for Double Exponential and GL for Generaliced Laplace. The rest of the columns detail the parameters for each of the addends in Equation 73, for the between airframe distribution and for the within airframe distribution. There are three columns per addend, showing “a”, “b” and “ α ”. Parameters subscripts correspond to the position of the distribution in the type of pdf. As an example, columns of the first line indicate:

Type of pdf: G_G-DE		
Between distribution	Within distribution	
Gaussian (G)	Gaussian (G)	Double exponential (DE)
$a_1=44,617$	$a_2=41,019$	$a_3=48,269$
$b_1=0,5$	$b_2=0,5$	$b_3=1$
$\alpha_1=1$	$\alpha_2=0,81$	$\alpha_3=0,19$



Aircraft type	Proportion FT	Type of PDF	μ (ft)	a_1	b_1	α_1	a_2	b_2	α_2	a_3	b_3	α_3	a_4	b_4	α_4	a_5	b_5	α_5	a_6	b_6	α_6
A124	1,194E-4	G_G-DE	27,960	44,617	0,5	1	41,019	0,5	0,81	48,269	1	0,19									
A310-GE	3,190E-2	G_G-DE	-61,669	41,102	0,5	1	33,479	0,5	0,75	29,000	1	0,25									
A310-PW	1,030E-2	G_G-DE	3,698	38,233	0,5	1	24,244	0,5	0,68	31,512	1	0,32									
A318	2,687E-4	DE_G-DE	30,803	26,912	1	1	22,263	0,5	0,80	30,365	1	0,20									
A320	4,650E-2	G-DE_GL-GL-GL	27,210	39,542	0,5	0,74	34,268	1	0,26	55,188	0,54	0,18	31,272	0,55	0,82	200,362	0,15	0,00			
A330	2,828E-1	DE_G-G-DE	40,477	29,209	1	1	18,588	0,5	0,5	28,017	0,5	0,39	34,548	1	0,12						
A340	1,314E-1	G-DE_G-G-DE	-2,170	32,927	0,5	0,65	45,275	1	0,35	17,112	0,5	0,59	31,062	0,5	0,37	47,674	1	0,04			
A345	1,270E-2	G_G-DE	-1,967	27,726	0,5	1	21,777	0,5	0,89	40,010	1	0,11									
A346	6,100E-2	G-G-DE_G-G-DE	28,851	16,251	0,5	0,76	26,109	0,5	0,24	24,172	1	0,00	33,731	0,5	0,41	19,731	0,5	0,54	51,43	1	0,05
A380	8,960E-5	G-DE_G-DE	-0,772	54,227	0,5	0,99	117,804	1	0,01	25,182	0,5	0,65	33,817	1	0,35						
ASTR	2,400E-6	G-DE_G-DE	-0,772	54,227	0,5	0,99	117,804	1	0,01	25,182	0,5	0,65	33,817	1	0,35						
ASTR-1	9,400E-6	G_G	48,171	57,356	0,5	1	43,495	0,5	1												
ASTR-SPX	4,800E-5	G_G	49,692	48,918	0,5	1	32,934	0,5	1												
B701	4,186E-4	DE_G-DE	24,127	38,768	1	1	26,726	0,5	0,73	39,917	1	0,27									
B703	2,230E-4	G_G-DE	34,847	88,604	0,5	1	29,662	0,5	0,70	25,824	1	0,30									
B703NG	1,520E-5	G-DE_G-DE	-0,772	54,227	0,5	0,99	117,804	1	0,01	25,182	0,5	0,65	33,817	1	0,35						
B732	7,762E-4	DE_G-DE	-14,587	44,126	1	1	28,075	0,5	0,68	33,375	1	0,32									
B737C	7,578E-7	G_G-G-DE	-100,950	41,578	0,5	1	40,444	0,5	0,46	20,452	0,5	0,54	32,840	1	0,00						
B737CL	5,075E-4	G-DE_G-G-GL	-46,720	38,661	0,5	0,80	47,680	1	0,20	39,580	0,5	0,35	23,077	0,5	0,65	174,153	0,29	0,00			
B737NX	3,860E-2	G-DE_G-G-DE	-8,815	37,030	0,5	0,91	36,684	1	0,09	19,603	0,5	0,59	33,251	0,5	0,31	38,055	1	0,10			
B744-10	6,610E-2	G-DE_G-G-DE	-67,106	29,964	0,5	0,97	62,751	1	0,03	36,823	0,5	0,31	23,015	0,5	0,59	38,470	1	0,10			
B744-5	2,100E-2	G-G-DE_G-G-DE	-60,682	42,439	0,5	0,55	30,050	0,5	0,45	36,476	1	0,00	38,139	0,5	0,67	22,787	0,5	0,20	38,12	1	0,13
B747CL	4,600E-3	G-DE_G-G-DE	-41,599	44,343	0,5	0,98	84,614	1	0,02	31,921	0,5	0,64	46,278	0,5	0,31	47,833	1	0,05			
B747LCF	2,663E-4	G-DE_G-DE	-0,772	54,227	0,5	0,99	117,804	1	0,01	25,182	0,5	0,65	33,817	1	0,35						
B752	3,990E-2	G-G-DE_G-G-DE	-18,350	45,607	0,5	0,40	24,073	0,5	0,60	36,664	1	0,00	18,147	0,5	0,65	34,490	0,5	0,18	33,57	1	0,16
B753	2,090E-4	G_GL-GL-GL	-13,522	40,909	0,5	1	86,329	0,14	0,10	34,076	0,53	0,90	136,354	0,11	0,01						
B764	2,990E-5	G-DE_G-DE	-33,384	18,369	0,5	0,76	58,359	1	0,24	35,893	0,5	0,80	31,930	1	0,20						



Aircraft type	Proportion FT	Type of PDF	μ (ft)	a_1	b_1	α_1	a_2	b_2	α_2	a_3	b_3	α_3	a_4	b_4	α_4	a_5	b_5	α_5	a_6	b_6	α_6
B767	1,050E-1	G-G-DE_GL-GL-GL	-67,775	55,837	0,5	0,24	32,584	0,5	0,76	40,047	1	0,00	40,300	0,60	0,77	34,732	0,37	0,16	77,47	0,47	0,07
B772	6,110E-2	G_G-G-DE	28,280	28,018	0,5	1	18,123	0,5	0,49	29,031	0,5	0,31	34,960	1	0,20						
B773	1,110E-2	G-G-DE_G-G-DE	51,948	41,093	0,5	0,18	30,624	0,5	0,82	45,708	1	0,00	14,589	0,5	0,79	28,457	0,5	0,21	102,94	1	0,00
BD100	3,881E-4	G_G-G-DE	-3,274	32,983	0,5	1	26,929	0,5	0,78	26,105	0,5	0,00	37,665	1	0,22						
C17	1,200E-3	G_G-DE	-4,116	38,554	0,5	1	33,861	0,5	0,74	40,358	1	0,26									
C550-B	1,136E-4	G-G-DE_G-DE	31,830	39,689	0,5	0,58	22,032	0,5	0,42	30,099	1	0,00	25,428	0,5	0,75	35,526	1	0,25			
C550-II	3,030E-5	G_G-DE	4,384	45,913	0,5	1	26,328	0,5	0,96	74,510	1	0,04									
C550-IING	1,413E-7	G-DE_G-DE	-0,772	54,227	0,5	0,99	117,804	1	0,01	25,182	0,5	0,65	33,817	1	0,35						
C550-SII	5,300E-6	G_G-DE	-46,932	46,012	0,5	1	24,283	0,5	0,68	29,770	1	0,32									
C56X	1,493E-4	G-DE_G-G-DE	-33,414	27,939	0,5	0,85	40,975	1	0,15	20,388	0,5	0,66	32,952	0,5	0,29	42,880	1	0,06			
C650	1,194E-4	DE_G-DE	8,856	57,510	1	1	27,196	0,5	0,57	33,856	1	0,43									
C680	2,090E-4	G_G-DE	-28,441	28,959	0,5	1	20,453	0,5	0,66	21,630	1	0,34									
C750	5,374E-4	G-DE_G-DE	-3,253	48,187	0,5	0,94	92,491	1	0,06	29,844	0,5	0,65	25,649	1	0,35						
CL600	4,105E-4	G_G-DE	-10,982	41,929	0,5	1	30,170	0,5	0,53	29,102	1	0,47									
CL600-1	1,550E-5	G-DE_G-DE	-0,772	54,227	0,5	0,99	117,804	1	0,01	25,182	0,5	0,65	33,817	1	0,35						
CL604	1,100E-3	G_G-DE	15,381	38,693	0,5	1	24,334	0,5	0,60	30,778	1	0,40									
CL605	2,800E-6	G_G	47,117	35,473	0,5	1	28,451	0,5	1												
DC10	7,464E-4	G_G-G-DE	-5,022	47,402	0,5	1	46,488	0,5	0,40	30,567	0,5	0,60	135,263	1	0,00						
DC86-7	7,600E-5	G_G	-47,413	41,491	0,5	1	27,010	0,5	1												
DC86-7-1	4,410E-5	G_G	-28,278	53,856	0,5	1	29,466	0,5	1												
DC86-7NG	2,920E-5	G_G	6,985	46,425	0,5	1	22,830	0,5	1												
E135-145	2,700E-3	G_G-G-DE	11,076	66,610	0,5	1	43,204	0,5	0,12	26,846	0,5	0,85	51,724	1	0,03						
E170	9,255E-4	G-DE_G-DE	13,704	22,757	0,5	0,44	38,558	1	0,56	49,632	0,5	0,73	45,972	1	0,27						
F2TH	1,400E-3	G_G-DE	-20,195	56,943	0,5	1	33,881	0,5	0,77	34,655	1	0,23									
F900	4,200E-3	G_G-DE	21,586	53,543	0,5	1	34,637	0,5	0,82	43,131	1	0,18									
FA10	5,890E-5	DE_G-G-DE	10,550	42,664	1	1	35,029	0,5	0,58	20,260	0,5	0,30	42,464	1	0,12						
FA10NG	8,530E-7	G-DE_G-DE	-0,772	54,227	0,5	0,99	117,804	1	0,01	25,182	0,5	0,65	33,817	1	0,35						



Aircraft type	Proportion FT	Type of PDF	μ (ft)	a_1	b_1	α_1	a_2	b_2	α_2	a_3	b_3	α_3	a_4	b_4	α_4	a_5	b_5	α_5	a_6	b_6	α_6
FA20	8,960E-5	G-DE_G-DE	-15,269	52,646	0,5	0,76	22,518	1	0,24	35,829	0,5	0,33	36,886	1	0,67						
FA50	3,881E-4	G-G-DE_G-G-DE	28,533	45,952	0,5	0,44	61,232	0,5	0,56	61,324	1	0,00	39,950	0,5	0,65	21,877	0,5	0,31	80,301	1	0,04
FA7X	1,493E-4	G_G-DE	-17,538	33,278	0,5	1	31,060	0,5	0,40	20,372	1	0,60									
G150	2,990E-5	G_DE	54,320	41,470	0,5	1	23,888	1	1												
GALX	6,269E-4	G_G	-3,974	36,679	0,5	1	31,025	0,5	1												
GLEX	4,777E-4	G_G-DE	32,235	50,277	0,5	1	42,674	0,5	0,49	36,579	1	0,51									
GLF2	3,300E-6	G_DE	-29,231	74,515	0,5	1	33,139	1	1												
GLF2-3	1,350E-5	G_G	-89,489	77,131	0,5	1	42,693	0,5	1												
GLF2-G	5,200E-6	G_G	26,878	27,339	0,5	1	22,843	0,5	1												
GLF2B	5,800E-6	G_DE	22,285	40,170	0,5	1	42,111	1	1												
GLF2B-G	2,100E-6	G_G	44,286	32,570	0,5	1	23,070	0,5	1												
GLF3	2,990E-5	DE_G-DE	-46,049	57,791	1	1	30,477	0,5	0,44	30,981	1	0,56									
GLF4	1,500E-3	G_G-DE	-30,173	43,172	0,5	1	28,090	0,5	0,5	36,299	1	0,5									
GLF5	1,200E-3	G-DE_G-G-DE	15,628	63,531	0,5	0,98	157,118	1	0,02	35,153	0,5	0,60	16,884	0,5	0,15	44,934	1	0,25			
H25B-700	2,880E-5	G_G-DE	-25,724	71,965	0,5	1	27,778	0,5	0,43	53,980	1	0,57									
H25B-700-A	1,300E-6	G-DE_G-DE	-0,772	54,227	0,5	0,99	117,804	1	0,01	25,182	0,5	0,65	33,817	1	0,35						
H25B-700NG	7,500E-6	G_G-DE	-37,627	85,004	0,5	1	28,704	0,5	0,87	48,806	1	0,13									
H25B-800	8,663E-4	G-DE_G-DE	12,051	51,791	0,5	0,84	46,301	1	0,16	34,307	0,5	0,74	35,732	1	0,26						
H25B-800NG	2,160E-5	G_G	29,911	10,577	0,5	1	31,189	0,5	1												
IL62	1,194E-4	G_G	48,988	37,829	0,5	1	19,945	0,5	1												
IL76	1,791E-4	G_G-G-GL	62,730	64,354	0,5	1	29,413	0,5	0,00	28,087	0,5	0,57	12,990	1,48	0,43						
IL96	5,970E-5	G_G	37,578	21,942	0,5	1	23,969	0,5	1												
J328	5,970E-5	G_G-G-DE	62,277	32,606	0,5	1	20,655	0,5	0,89	41,535	0,5	0,10	74,198	1	0,01						
L101	1,100E-3	G-DE_G-DE	15,644	16,120	0,5	0,15	53,073	1	0,85	44,833	0,5	0,94	80,868	1	0,06						
LJ35/6	4,478E-4	G-DE_G-G-DE	70,547	36,164	0,5	0,70	38,209	1	0,30	39,204	0,5	0,49	24,387	0,5	0,49	86,688	1	0,02			
LJ40	5,970E-5	DE_G-DE	21,916	22,713	1	1	27,033	0,5	0,80	28,215	1	0,20									
LJ45	5,970E-5	G-DE_G-G-DE	38,354	20,050	0,5	0,73	68,172	1	0,27	49,431	0,5	0,13	25,382	0,5	0,87	51,222	1	0,00			



Aircraft type	Proportion FT	Type of PDF	μ (ft)	a_1	b_1	α_1	a_2	b_2	α_2	a_3	b_3	α_3	a_4	b_4	α_4	a_5	b_5	α_5	a_6	b_6	α_6
LJ55	1,493E-4	DE_G-DE	37,528	40,428	1	1	23,381	0,5	0,95	40,243	1	0,05									
LJ60	1,791E-4	G-DE_G-DE	54,226	31,896	0,5	0,83	41,071	1	0,17	24,777	0,5	0,62	29,113	1	0,38						
MD11	4,750E-2	G_GL-GL-GL	-11,469	45,442	0,5	1	38,884	0,64	0,54	36,202	0,39	0,33	51,878	0,62	0,14						
MD80	1,493E-4	G_G-G-DE	5,689	28,096	0,5	1	23,476	0,5	0,76	47,345	0,5	0,11	22,030	1	0,13						
PRM1	2,800E-3	G_G-G-DE	-5,174	24,525	0,5	1	27,181	0,5	0,69	15,125	0,5	0,17	38,929	1	0,13						
SBR1-65	2,990E-5	G_G	-68,966	18,711	0,5	1	32,930	0,5	1												
T154	5,970E-5	G-DE_G-DE	12,218	71,637	0,5	0,48	38,739	1	0,52	28,000	0,5	0,43	50,891	1	0,57						

Table A1. 1
Proportion of flight time and ASE distributions per aircraft type in the Canaries

